

# **The Cellular Process of Homologous Recombination and its Applications in Cancer Biology**

De celbiologische aspecten van homologe recombinitie en zijn  
toepassingen in de kanker biologie

~

**Berina Eppink**

ISBN: 978-94-90371-21-0

© 2010 Berina Eppink

No part of this book may be reproduced, stored in a retrieval system or transmitted in any form or by any means without permission of the author. The copyright of the publications remains with the author, unless otherwise stated.

The work presented in this thesis was performed at the department of Cell biology and Genetics at the ErasmusMC in Rotterdam.

The studies described in this thesis were supported by the Dutch Cancer Society (KWF)

Financial support by the Stichting Melanoom, the Dutch Cancer Society and the J.E. Jurriaanse Stichting for the publication of this thesis was gratefully acknowledged.

Cover design: Jasper van Dijke

Printing: Offpage

# **The Cellular Process of Homologous Recombination and its Applications in Cancer Biology**

De celbiologische aspecten van homologe recombinitie en zijn  
toepassingen in de kanker biologie

## **Proefschrift**

~

ter verkrijging van de graad van doctor aan de  
Erasmus Universiteit Rotterdam  
op gezag van de  
rector Magnificus

Prof.dr. H.G. Schmidt

en volgens besluit van het College voor Promoties.

De openbare verdediging zal plaatsvinden op:  
**vrijdag 11 juni 2010 om 13:30 uur**

door

~

**Berina Eppink**  
geboren te Winterswijk



## **Promotiecommissie:**

### **Promotoren:**

Prof.dr. R. Kanaar

Prof.dr. J.H.J. Hoeijmakers

### **Overige leden:**

Prof.dr. E.C. Zwarthoff

Dr. T.L.M ten Hagen

Dr. N. Goosen

### **Copromotor:**

Dr. J. Essers

# Contents

	page
<b>Chapter 1</b>	
Interplay and quality control of DNA damage repair mechanisms, a general introduction in DNA repair	7
<b>Chapter 2</b>	
Multiple interlinked mechanisms to circumvent DNA replication roadblocks recombination repair	35
<b>Chapter 3</b>	
Mono-ubiquitination of histone H2B by RNF20 at sites of DNA double strand breaks is required for timely homologous recombination repair	47
<b>Chapter 4</b>	
Repair of UV-induced DNA damage during S-phase involves multiple DNA repair pathways	61
<b>Chapter 5</b>	
ATP-dependent and ATP-independent <i>in vivo</i> roles of the Rad54 homologous recombination protein in nuclear foci kinetics	87
<b>Chapter 6</b>	
Mild hyperthermia inactivates BRCA2-mediated DNA repair	117
<b>Chapter 7</b>	
Prevention of thermotolerance after repetitive hyperthermia.	133
List of abbreviations	147
Nederlandse samenvatting	149
Curriculum Vitae	153
List of publications	154
PhD portfolio	155
Dankwoord	157



# Chapter 1

## **Interplay and quality control of DNA damage repair mechanisms**

A general introduction in DNA repair

**Berina Eppink<sup>1</sup>, Jeroen Essers<sup>1, 2, 3</sup> and Roland Kanaar<sup>1, 2</sup>**

<sup>1</sup>Department of Cell Biology & Genetics, Cancer Genomics Center, <sup>2</sup>Department of Radiation Oncology, <sup>3</sup>Department of Vascular Surgery, Erasmus Medical Center, Rotterdam, The Netherlands

## **Abstract**

The structure of DNA and subsequently the integrity of the genetic code are constantly threatened by numerous endogenous and exogenous DNA damaging agents. Restoration of proper DNA structure occurs through distinct and overlapping DNA damage repair pathways, depending on the specific lesion. Here, we review the classical DNA repair pathways as they were established from genetic and biochemical experiments. DNA repair pathways are often pictured to act in a precise machine-like manner. We discuss an alternative view that envisions DNA repair to arise from more unstable stochastic interactions between proteins and DNA substrates. Paradoxically, this more messy process makes DNA repair more robust and simultaneously provides the flexibility for quality control and pathway cross talk. Finally, we discuss how basic mechanistic insight in DNA repair mechanisms is currently being translated into anti-cancer therapies. We conclude with the scope of this thesis.

## 1. Introduction

Base pairing is an integral structural and functional feature of DNA. The prevalent structure of DNA is a right-handed double helix, consisting of two antiparallel single strands, each of which contains a linear sequence of deoxynucleotides with either adenine (A), cytosine (C), guanine (G) or thymine (T) bases. The base moieties point towards the center of the double helix, where they lie within hydrogen-bonding distance of each other. Canonical base pairing, also referred to as Watson-Crick pairing, follows a strict rule by which A pairs with T and G pairs with C, establishing two and three hydrogen bonds, respectively. Due to the nature of these interactions, both DNA strands contain the complementary sequence information as mirror images of each other. This ingenious structural template provides for endless and error-free duplication and maintenance of genetic information [1]. Important cellular transactions with DNA such as DNA replication, repair, recombination or gene expression make use of the template function of DNA, which in turn is based on a strict application of the Watson-Crick base pairing principle.

DNA is constantly threatened by plethora of DNA damage inducing agents, potentially damaging the integrity of the DNA structure and the genetic code. These DNA damaging agents can both be from endogenous as well as exogenous origin. Products of endogenous processes include reactive forms of oxygen, other by-products of cellular metabolism and even 'spontaneous' hydrolysis reactions. On the other hand, exogenous agents such as ionizing radiation (IR), ultraviolet (UV) radiation and genotoxic chemicals, also cause genomic alterations, including chemical adducts, intra- and interstrand crosslinks, single strand breaks (SSBs, also known as nicks) and double strand breaks (DSBs). These aberrations are repaired by what are generally considered to be distinct DNA repair pathways. The concept of a 'DNA repair pathway' is based on genetic and biochemical analyses and refers to a distinct set of proteins, which collectively and in a coordinated manner repair specific lesions. Given the importance of DNA integrity for survival and the great variety of structurally distinct DNA lesions, multiple DNA repair pathways have evolved that are highly conserved across organisms. The importance of accurate repair of DNA damage is reflected in the fact that defects in DNA repair pathways are associated with cancer predisposition and premature aging [2].

We review the classical DNA repair pathways and subsequently discuss an alternative view of DNA repair pathways that allows their functional interplay and provides a basis for quality control of DNA repair. Finally, we discuss how basic mechanistic insight in DNA repair mechanisms is currently making its translation into the development of anti-cancer therapies.

## 2. DNA repair pathways

The main mammalian DNA repair systems are base-excision repair (BER), nucleotide-excision repair (NER), translesion DNA synthesis (TLS), mismatch repair (MMR) and the DSB repair pathways non-homologous end joining (NHEJ) and homologous recombination (HR) [2]. Small chemical alterations of bases are targeted by BER. These

lesions may or may not impede transcription and replication, although they frequently miscode. BER is therefore particularly relevant for preventing mutagenesis. NER deals with the wide class of helix-distorting lesions that interfere with base pairing and generally obstruct transcription and replication. Most lesions processed by NER arise from exogenous sources, whereas BER is mostly, but not exclusively, concerned with damage of endogenous origin. Lesions for these two repair processes affect only one of the two DNA strands. These lesions are excised and the resulting single strand gap is filled in using the intact complementary strand as template. Despite these highly active DNA repair mechanisms, some SSBs may not be recognized and repaired, eventually leading to DSBs, for example due to DNA replication. DSBs are more problematic, as both strands are affected. Two major pathways, HR and NHEJ, repair DSBs. When DNA damage is present during replication, it threatens the integrity of the coding sequence. HR as well as MMR and TLS are involved in repair or bypass of lesions at sites of replication to ensure robust replication.

## **2.1 Base excision repair (BER)**

Endogenous base damage, including SSBs, are the most common DNA aberrations. Cells repair on average 10,000 such lesions every day. BER is the main multistep process that copes with this type of mostly endogenously inflicted DNA damage (Figure 1 A-I), as a result of reactive oxygen species, methylation and deamination, but it also deals with exogenously induced damage from environmental chemicals, tobacco smoke and radiation [3]. Misreplication of oxidized bases and abasic sites by replicative or TLS polymerases often give rise to point- and sometimes more complex mutations. Single nucleotide polymorphisms which are observed at a high frequency (1 in 300 bp) in mammalian genomes, likely result from such mutations. The origin of sporadic cancer is also very likely due to such spontaneous mutations in proto-oncogenes and tumor suppressor genes. BER facilitates the repair of base damage via two general pathways; short-patch (Figure 1 D-F) and long-patch repair (Figure 1 G-I). The short-patch BER pathway leads to a repair tract of a single nucleotide. The long-patch BER pathway produces a repair tract of at least two nucleotides. Both pathways involve four basic steps including damage detection, processing, gap filling and DNA ligation.

During the first step of BER, one of the earliest responses to DNA strand breakage is the induction of ADP-ribose polymer synthesis (PAR) by Poly-ADP-ribose polymerase-1 (PARP-1), covalently modifying itself and, to a lesser extent, other acceptor proteins with long chains of PAR [3, 4]. This step is required to recruit, stabilize or accumulate the scaffold protein XRCC1 to SSBs [3], which then mediates multiple interactions with enzymatic components of the repair process. The BER pathway consists of many glycosylases, each processing distinct DNA lesions (Figure 1B) [5]. These DNA glycosylases recognize the damaged base and hydrolyze the *N*-glycosyl bond between the damaged or incorrect base and the deoxyribose backbone, effectively removing the damaged base and creating an apurinic or apyrimidinic site (a-basic (AP) site), after which Ape1 (apurinic/

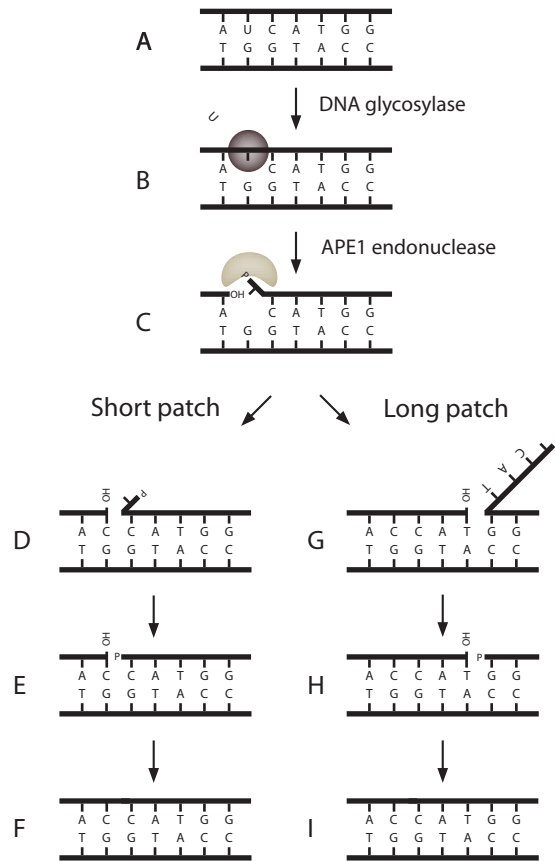


**Figure 1. Base excision repair**

(A-I) Shown is a general model for the short patch (left) and long patch (right) BER pathways. Short patch repair replaces the lesion with a single nucleotide; long patch repair replaces the lesion with approximately 2 to 10 nucleotides. In this example a cytosine is converted into a uracil, due to spontaneous deamination. (A, B) A DNA glycosylase recognizes the alteration and hydrolyzes the N-glycosyl bond between the damaged or incorrect base and the deoxyribose backbone. (C, D) Ape1 creates a nick 5' to the a-basic site, which is processed by its AP endonuclease activity, (E) creating a single-nucleotide gap in the DNA. (F) DNA polymerase  $\beta$  in complex with XRCC1 continues short patch repair by gap filling. DNA ligation is established completing the repair process and restoring the integrity of the helix by sealing the nick. (G) In long-patch repair DNA polymerases  $\delta/\epsilon$  synthesize 2-10 bases in a complex with PCNA, (H) after which the Fen1 removes the displaced DNA strand and (I) DNA ligase I closes the open end establishing an intact DNA strand.

apyrimidinic endonuclease) binds the AP site (Figure 1C) [5]. Ape1 initiates BER by a 5' incision (nick) in the DNA backbone, to remove the AP site (Figure 1D-E). The newly created nick is processed by its AP endonuclease activity, resulting in a single-nucleotide gap. Importantly, the gap contains a 3'-hydroxyl and a 5'-phosphate, substrates compatible with the downstream enzymatic reactions in BER. Following removal of the abasic site, DNA polymerase  $\beta$  proceeds the short patch repair by gap filling, in a complex with XRCC1. This scaffolding protein brings the DNA polymerase and ligase together [6]. DNA ligation by the XRCC1/ligase III complex completes the repair process and restores the integrity of the helix by sealing the nick (Figure 1F). The long-patch repair is not restricted to one damaged nucleotide, but synthesizes 2-10 nucleotides to fill the AP site. The sliding clamp PCNA (proliferating cell nuclear antigen) is loaded onto the DNA strand, aided by replication factor C (RFC), after which the polymerases are recruited. The replicative DNA polymerases  $\delta/\epsilon$  fill the gap by synthesizing 2-10 bases in a complex with PCNA (Figure 1G). After filling the gap the structure-specific Flap endonuclease-1 (Fen1) removes the displaced DNA flap (Figure 1H), and subsequently DNA ligase I can close the open end establishing an intact DNA strand (Figure 1I).

## 2.2 Nucleotide excision repair (NER)

NER repairs a wide variety of chemically and UV light-induced DNA lesions. Some carcinogenic agents covalently bind the DNA base, to form bulky adducts, other chemicals and UV irradiation are capable of covalently linking two bases within the same strand. Examples of such lesions include cyclobutyl pyrimidine dimers (CPDs) and pyrimidine (6-4) pyrimidone photoproducts. NER (Figure 2) can be divided in two sub-pathways; global genome repair (GG-NER), which operates genome wide and is able to identify helix-distorting lesions anywhere in the genome and transcription-coupled repair (TC-NER), which focuses on lesions that have been detected by RNA polymerase instead, thereby physically blocking the vital process of transcription [2]. The first step in DNA repair is the recognition of the damaged site. In the GG-NER pathway, the heterodimer XPC/hHR23B recognizes disrupted base pairing (Figure 2A) [7], while less DNA double-helix disrupting DNA lesions, such as CPDs, are recognized by the damaged DNA-binding proteins complex (DDB-complex), composed of DDB1 and DDB2 [8]. The persistence of this type of lesions may have major physiological consequences. Because of their slow repair these lesions are responsible for the vast majority of deleterious effects exerted by the UV component of sunlight, including mutagenesis and subsequent carcinogenesis, as well as acute sunburn and immuno suppression [9]. Recognition of lesions during transcription starts with the recruitment of CSA and CSB (Cockayne Syndrome proteins A and B) to DNA lesions, by the stalled RNA polymerase II, after which other NER proteins are assembled (Figure 2B-C).

Once the DNA lesion is recognized, the next step, common to both the GG-NER and TC-NER pathways, is the formation of a single-strand bubble around the lesion, by the transcription factor IIH (TFIIH) (Figure 2D). TFIIH consists of 10 subunits, of which XPB

and XPD are helicases responsible for unwinding the DNA around the lesion [10]. In TC-NER, the stalled RNA polymerase II has to be removed before repair can proceed. The RNA polymerase II is displaced by a complex, consisting of CSA, CSB, TFIIH and XPG [7, 11], whereas the XPC-complex is removed by XPA. XPA verifies and locates the damage and organizes the incision machinery around the damage by positioning the single-strand binding protein, replication protein A (RPA) to bind the non-damaged strand. Binding of RPA prevents re-annealing of the two single strands and may help stabilize NER reaction intermediates [12]. The final excision of a stretch of 24-32 nucleotides is completed by an incision by the ERCC1-XPF structure-specific endonuclease on the 5' end of the lesion, while the other end of the lesion is incised by XPG (Figure 2E) [12]. The excision of the damaged nucleotides and surrounding nucleotides leaves a small single-strand gap. Using the undamaged strand as a template, filling of the single-strand DNA (ssDNA) gap is performed by repair replication presumably using the regular DNA replication machinery, consisting of RPA, PCNA, RFC, and likely DNA polymerase  $\delta$  or  $\epsilon$  [13]. Finally, DNA ligase I ligates the remaining nick (Figure 2F).

Various hereditary diseases are associated with defects in NER, mainly recognized by their extreme sensitivity to UV-light. Xeroderma pigmentosum (XP) is a disorder that has its origin in mutations in at least one of the seven *XP*-genes (*XPA-XPG*). XP patients are hypersensitive for UV-induced skin cancer. In contrast, patients with mutations in the *CSA* or *CSB* genes, but also in *TFIIH* subunits, resulting in the Cockayne syndrome (CS), are not cancer-prone, since these mutations often lead to apoptosis. CS gives rise to a wide range of problems in patients, such as neurological development impairment, dwarfism, premature ageing and dysmyelination. Trichothiodystrophy (TTD), caused by mutations in subunits of *TFIIH* (*XPB*, *XPD*, *p8/TTDA*), shares many of the features of CS, with additional symptoms of brittle hair, nails and skin. It is remarkable that mutations in the *XPB* or *XPD* genes can cause all three diseases, probably because these *TFIIH* subunits play multiple functions in NER and transcription [2].

### 3. Repairing DSBs

There are multiple ways in which a cell can suffer DSBs, both from endogenous and exogenous sources. Endogenously they can arise accidentally as products of collapsed replication forks [14], but they can also occur as programmed events during immune-receptor gene rearrangements in lymphocytes and during meiotic recombination within germ cells [15]. Exogenous sources of DSBs are for instance the sun (UV-light) and multiple DSB-inducing agents such as IR and radio-mimetic drugs used in the clinic.

Two mechanistically distinct pathways have evolved to repair DSBs; HR and NHEJ. HR confines repair mostly to the S and G2 phase of the cell cycle when the DNA is replicated, which provides a perfect second copy of the sequence (sister chromatid) for aligning breaks and their accurate repair. In contrast, the less accurate NHEJ is most relevant in the G1 and G2 phase of the cell cycle [16], when a second allele is not available or not in close proximity. Since no template is used NHEJ can lead to loss or addition of a few bases [17].

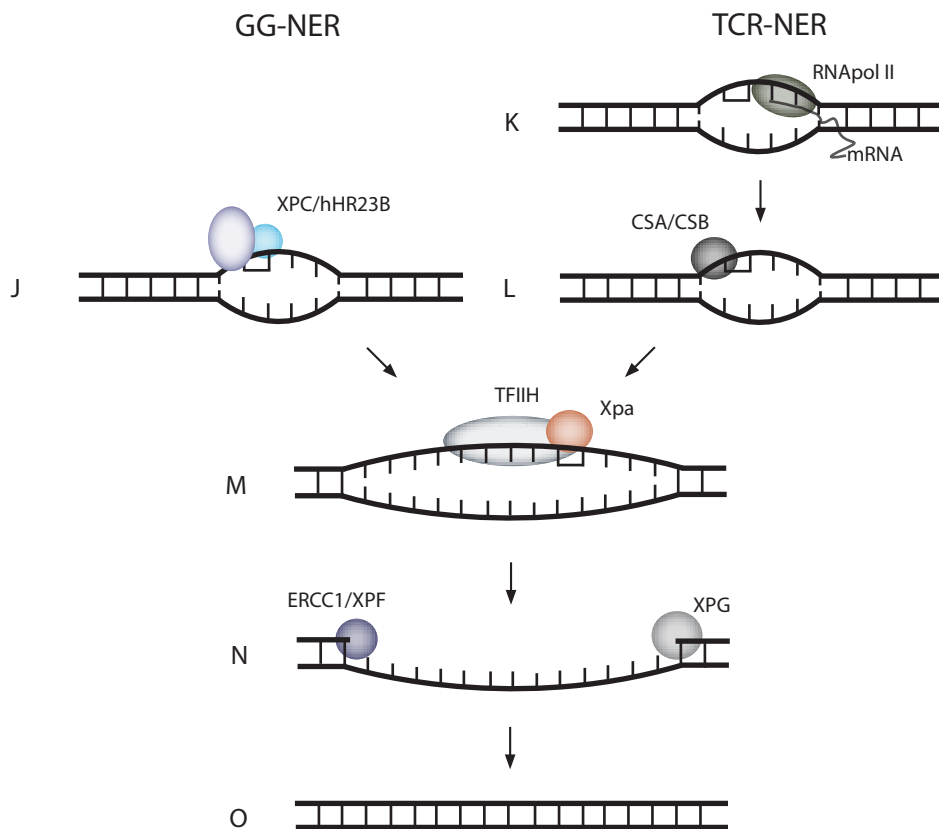


**Figure 2. Nucleotide excision repair**

(A-F) A simplified model for steps in NER is shown for repair of a UV-induced pyrimidine dimer. DNA damage recognition differs between global genome and transcription coupled NER (GG- and TC-NER, respectively). (A) After damage recognition by XPC/hHR23B, for some lesions facilitated by XPE-UV-DDB, (B) or by elongating RNA-PolII respectively (C) followed by CSA/CSB recruitment, (D-F) the GG-NER and TC-NER pathways utilize the common core NER reaction, which involves (D) recruitment of TFIIH and XPA followed by melting of the DNA around the lesion (E) and dual DNA strand excision by structure-specific endonucleases XPG at 3' and XPF/ERCC1 at the 5' side of the lesion respectively. (F) Finally, gap-filling and ligation by the replication machinery completes repair.

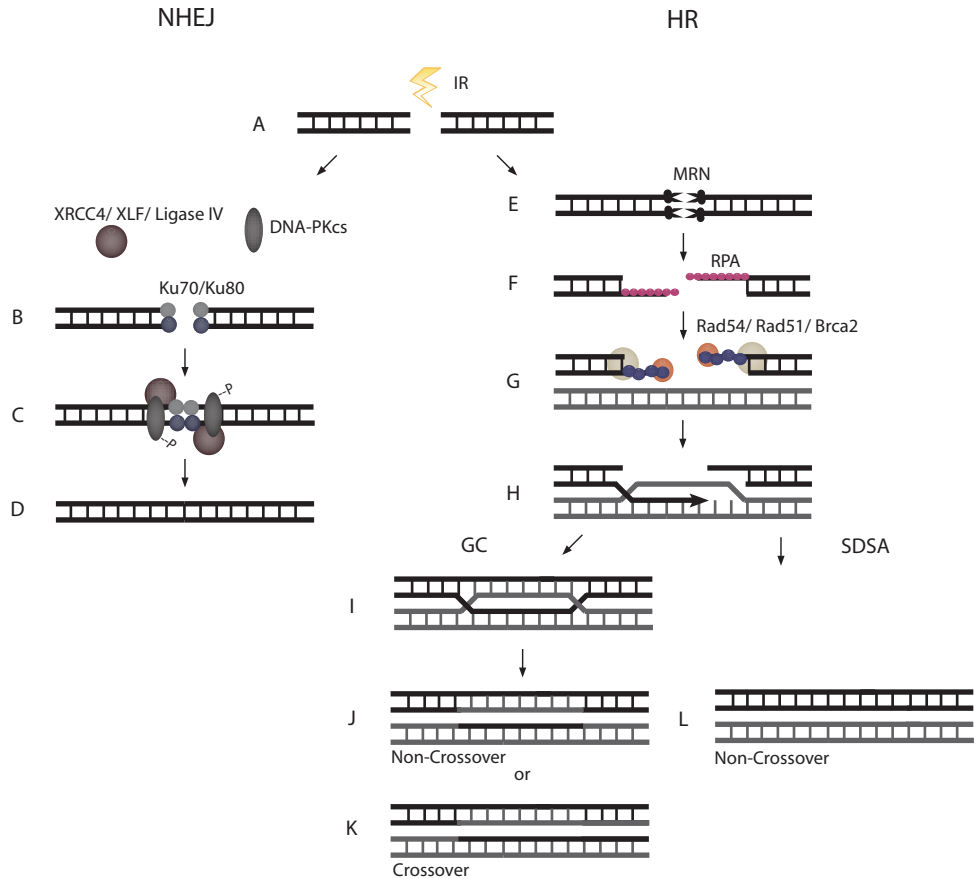


**Figure 3. Double strand break repair by NHEJ and HR**

(A) NHEJ and HR are two main pathways to repair a DSB. (B) During NHEJ recognition of the DSB is accomplished by binding of the KU heterodimer to a DNA end. (C) The two DNA ends are synapsed. DNA-PKcs is phosphorylated and the DNA ends are processed by a complex consisting of XLF, XRCC4 and DNA ligase IV. These ends often need modification by other factors such as Artemis. (D) The DNA ends are ligated by DNA ligase IV, and the DNA-repair factors dissociate. (E-K) HR provides an alternative pathway for repair of a DSB. (E) The DSB is recognized by MRN, a complex consisting of MRE11, RAD50 and NBS1. (F) The DNA ends are resected, allowing binding of RPA to the ssDNA tails, G, and subsequently RAD51 in reaction that can be assisted by RAD54 and BRCA2. (H) The ssDNA-protein filament recognizes a homologous region in an intact DNA duplex and initiates pairing, forming a D-loop. DNA synthesis occurs from the invading end of the damaged DNA, extending the repair region. (I) After strand invasion and synthesis, the second DSB end can be captured to form an intermediate with two Holliday junctions (HJs). (J, K) After gap-repair DNA synthesis and ligation, the structure is resolved at the HJs in a non-crossover or crossover mode. (H→L) Alternatively, the reaction can proceed via SDSA by strand displacement, annealing of the extended single-strand end to the ssDNA on the other break end, followed by gap-filling DNA synthesis and ligation.

### 3.1 Signaling the DSB

Once a DSB has occurred in the genome the global response to its formation starts with the actual detection of the break in the context of the chromosome. Ataxia–telangiectasia mutated (ATM) is a serine–threonine kinase that is rapidly activated when cells are exposed to DSBs [18]. Its full activation depends on autophosphorylation on Ser1981 and its interaction with the MRN complex [19]. The MRN complex, consisting of MRE11, RAD50 and NBS1, is the primary sensor of DSBs, holding the break together and responsible for attracting ATM [20]. ATM phosphorylates a number of proteins involved in cell cycle checkpoint control, apoptotic responses and DNA repair, including p53, CHK2, BRCA1, RPA, SMC1, FANCD2, RAD17, Artemis and NBS1 [18–20]. Phosphorylation of these and other proteins by ATM initiates cell-cycle arrest at G1/S, intra-S and G2/M checkpoints and also promotes DNA repair [21]. Mutations in the *ATM* gene are responsible for the rare autosomal recessive disorder ataxia–telangiectasia (AT), characterized by cerebellar degeneration, immunodeficiency and an increased risk of cancer. Cells from individuals with AT exhibit defects in DNA damage-induced checkpoint activation, radiation hypersensitivity and an increased frequency of chromosome breakage [22]. Upon DNA damage induction, ATM, ATR and DNA-PKcs, two other phosphoinositide 3-kinase-like kinases, phosphorylate the H2A histone variant H2Ax at its conserved serine residue (Ser139), after which it is called  $\gamma$ H2Ax [23]. H2Ax is phosphorylated over a mega base region of chromatin flanking the site of the unrepaired DSB. How  $\gamma$ H2Ax contributes to DSB repair is not yet fully understood, but it might help attracting other DNA damage mediators/sensors, such as NBS1, MDC1, ATM and 53BP1 to the break [18–20]. Recently, other chromatin modifications have been implicated in the general DSB response. RNF8, a RING-finger ubiquitin ligase, ubiquitinates H2A, H2B and H2AX upon DNA damage induction thereby providing a platform for DNA repair factors [24]. This ubiquitination signal is then amplified and stabilized by RNF168 [25], maybe to promote downstream events of DSB repair. In addition to the activation of ATM, a DSB can also be detected by the KU heterodimer involved in NHEJ, which is described below.

### 3.2 Non-homologous end-joining (NHEJ)

In human somatic cells NHEJ is an important repair pathway for DSBs (Figure 3). NHEJ works by joining the ends of a two-ended DSB thereby providing a mechanism to fix a break without the need for a second copy of the broken chromosome. NHEJ can be divided in three steps; DSB sensing, recruitment of the repair proteins to the break and assembly of these proteins to perform functional end-joining. The first step of NHEJ, the recognition of the DSB is done by binding of the Ku heterodimer to a DNA end for which it has a high affinity [26] (Figure 3B). The ring-shaped heterodimer consists of the Ku70 and Ku80 proteins [27]. It provides a scaffold to which other NHEJ proteins can bind. DNA end-bound Ku70/80 attracts the catalytic subunit of the DNA-dependent protein kinase (DNA-PKcs) and activates its kinase activity (Figure 3C) [26]. Although many different targets have been identified, the major function for this phosphorylation activity appears to be

regulation of NHEJ by DNA-PKcs autophosphorylation [26]. This reaction takes place after juxtaposition of DNA ends and is required for proper regulation of DNA end accessibility for other NHEJ proteins [28]. Compatible DNA ends can now be joined directly by the DNA ligase IV/XRCC4 complex (Figure 3C-D). This reaction is stimulated by XLF/Cernunnos, which interacts with XRCC4 [29, 30]. However, in many circumstances the DNA ends are not compatible. IR, for example, creates a large number of ends that contain damaged bases and/or DNA backbone sugars that need processing before ligation. Therefore, NHEJ can accommodate nucleases, such as Artemis and the MRN complex, DNA polymerases, kinases and other enzymes that render such ends ligatable by the ligase IV/XRCC4 complex [31, 32]. In many such cases the break is sealed when ssDNA overhangs anneal at regions in which micro homology exists, resulting in error-prone repair of the DSB [33].

### 3.3 Homologous recombination

HR is very important in preserving genome integrity, since it accurately maintains the coding DNA sequence and prevents deletions of sequences by using the homologous sister chromatid as a repair template (Figure 3). HR-mediated DSB repair can be divided in three stages [34]; pre-synapsis, in which recognition and processing of the DNA ends occurs; synapsis, where a joint molecule between the damaged DNA and its homologous template is formed and finally post-synapsis and resolution, where the joint molecule are further processed leading to final resolution of the joint molecule resulting in two repaired homologous DNAs. The creation of a DSB in DNA is not always an accidental and problematic event. A large number of DSBs are deliberately created in the DNA of germ-line cells undergoing meiosis, where they serve as sites for the initiation of genetic recombination between parental chromosomes [35]. Whereas in meiotic recombination HR occurs between the parental homologous chromosomes, HR-dependent DSB repair in somatic cells mainly uses the intact sister chromatid for repair.

The pre-synapsis stage of HR is initiated by resection of the 5' DNA end by the MRN complex and CtIP leading to a 3' single strand overhang (Figure 3E) [36]. After resection the overhang is bound by replication protein A (RPA) (Figure 3F). Coating of resected DSBs with RPA results in the activation of the ATR-mediated checkpoint [37]. RPA is subsequently replaced by the recombinase RAD51, the central protein of HR that promotes homology recognition, joint molecule formation and DNA strand exchange via the formation of a nucleoprotein filament (Figure 3G) [31]. The interaction of RAD51 with DNA can be influenced by BRCA2 and the RAD51 paralogs (RAD51B, RAD51C, RAD51D XRCC2 and XRCC3) [38]. BRCA2 can affects loading of RAD51 on DNA and promote the synthesis dependent strand annealing (SDSA) route of HR rather than gene conversion [39-42]. The RAD51-DNA nucleoprotein filament initiates invasion of homologous DNA, linking the broken end to an undamaged DNA duplex in a junction called a displacement-loop (D-loop), where the invading 3'-end primes DNA synthesis (Figure 3H) [43]. This step of HR as well as the disassembly of the RAD51 filaments and chromatin remodeling can be

promoted by the multi-functional double strand DNA (dsDNA) dependent ATPase RAD54 [44, 45]. Once the joint molecule between the nucleoprotein filament and target duplex is formed, the information lost during end processing can be restored by DNA polymerases and remaining nicks are sealed by a DNA ligase. At this stage the recombined DNA molecules can be physically joined in a structure with four dsDNA arms, often referred to as a Holliday junction (Figure 3I). To complete recombination this junction needs to be resolved for which multiple possibilities exist. In the final post-synapsis step the Holliday junction can move along the DNA by a process called branch migration before it is resolved by a resolvase, such as GEN1, into two separate duplexes [46]. This DSB repair route, referred to as gene conversion (Figure 3I-K), predicts that the other end of the break is captured by the displaced strand from the donor duplex (D-loop) and is used to prime a second round of leading strand DNA synthesis. A double Holliday junction (dHJ) intermediate is formed that can be resolved to form either crossover or non-crossover products. Most DSB repair events occur by a non-crossover mechanism, limiting loss of heterozygosity. Dissolution of the dHJ via BLM-TopoIII $\alpha$ -Rmi1 gives rise to non-crossover products, whereas resolution via GEN1 can lead to either crossover or non-crossover products [47]. Alternatively, during SDSA (Figure 3L), the invading strand that has been extended by DNA synthesis is displaced and anneals to complementary sequences exposed by 5'-3' resection of the other side of the breaks. The remaining gaps can be fixed by DNA synthesis and ligation. The SDSA model forms only non-crossover products, and there is no alteration to the donor duplex during this mode of repair.

## **4. Repair during replication**

Faithful DNA duplication during S-phase requires an extremely precise and efficient replication machinery. DNA replication is a more fragile process than expected from the high processivity of replicative DNA polymerases. One culprit is damage in the template DNA, such as AP sites and CPDs [48, 49]. Most lesions, which can easily be repaired when present in duplex DNA, can cause gaps and breaks when they are encountered during replication [14]. Due to the nature of the replication complex at the progressing fork, optimized for accuracy with high-fidelity polymerases, there is limited tolerance for structural aberrations in the DNA template. Therefore, replication forks are prone to inactivation and/or stalling, which can lead to incomplete replication and chromosomal rearrangements. This, in turn, can result in aneuploidy, activation of proto-oncogenes, or inactivation of tumor suppressor genes with diverse outcomes including cell transformation, loss of cell function, or cell death [17, 50]. The main repair processes involved in replication associated repair are MMR, HR and TLS.

### **4.1 Mismatch repair (MMR)**

Contrary to the other DNA repair mechanisms, the main role of MMR is not in the repair of DNA lesions due to endogenous or environmental agents. Instead, MMR corrects errors of DNA polymerases during S-phase that escape 3'  $\rightarrow$  5' exonucleolytic proofreading

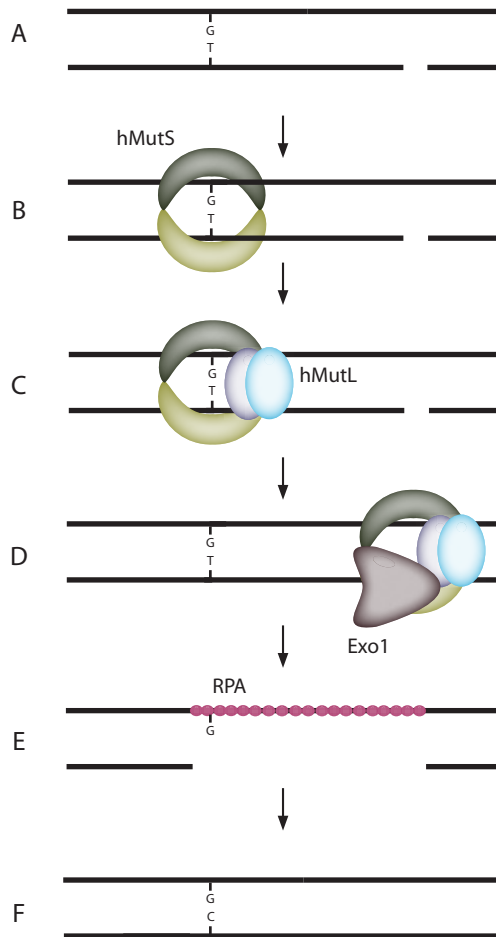


**Figure 4. Mismatch repair**

(A-F) Schematic representation of postreplicative mismatch repair in human cells. (A) In this example, misincorporation of thymidine opposite guanosine during DNA replication gave rise to a G/T mismatch, which has to be corrected to G/C. (B) The MMR process starts by recognition of the mismatch by the hMSH2/hMSH6 heterodimer (C) which undergoes an ATP-driven conformational change and recruits the hMLH1/hPMS2 heterodimer. This ternary complex can move in either direction along the DNA contour. (D) When it encounters a strand discontinuity loading of an exonucleases (EXO1) initiates degradation of the nicked strand towards the mismatch. (E) The single-stranded gap will be stabilized by RPA until the mismatch is removed. (F) The RPA-stabilized single-stranded gap can now be filled in by the replicative polymerase and the remaining nick can be sealed by DNA ligase.

activity or arise during HR [51, 52]. The MMR system repairs base-base mismatches that can give rise to point mutations and insertion/deletion loops that can give rise to frame shift mutations. Mismatches can be identified in DNA because they fail to form Watson–Crick base pairs. However, because neither nucleotide is damaged or modified, it is not obvious which strand carries the correct genetic information. Therefore, MMR cannot be accomplished by a mechanism such as BER or NER, which simply excises the damaged base or a short DNA fragment containing the damage, respectively. Unlike BER and NER, postreplicative MMR has to be targeted exclusively to the newly synthesized strand, which carries the erroneous genetic information.

In human cells, mismatch recognition is mediated predominantly by the heterodimer of hMSH2 and hMSH6, also referred to as hMutS $\alpha$  (Figure 4B)[53]. The mismatch-bound hMutS $\alpha$  undergoes an ATP-dependent conformational change, which converts it to a sliding clamp capable of moving along the DNA backbone [53]. The hMutS $\alpha$ -ATP-DNA complex is bound by a second heterodimer, composed of hMLH1 and either hPMS1 (hMutL $\alpha$ ) (Figure 4C) or hPMS2 (hMutL $\beta$ ) [51, 54]. This complex can slide in either direction, in search of a strand discontinuity. MMR must be directed to the newly synthesized strand, which in eukaryotes can be distinguished from the template strand solely by the presence of gaps between Okazaki fragments on the lagging strand, or by the 3'-terminus on the leading strand. When the hMutL $\alpha$  complex encounters a strand discontinuity loading of an exonuclease (EXO1) 5' of the mismatch initiates degradation of the nicked strand towards the mismatch (Figure 4D) [54]. If the strand discontinuity is located 3' from the mismatch, the hMutL $\alpha$  endonuclease creates an additional nick 5' from the mismatch, which then serves as the entry point for the 5' to 3' EXO1-mediated degradation of the daughter strand towards the mismatch [54]. The resulting gap will be stabilized by RPA (Figure 4E). Loading of the second hMutS $\alpha$  hMutL $\alpha$  complex at the mismatch will stimulate a second round of exonuclease degradation. The process continues until the mismatch is reached and no more loading of exonuclease occurs. The RPA-stabilized gap is an ideal substrate for the filling-in step, in which the replicative polymerase(s) can resynthesize the degraded region to leave a nick that can be sealed by a DNA ligase (Figure 4F).

The clinical implications of genome stabilization by MMR are illustrated by the fact that genetic defects in the human MMR pathway confer a strong predisposition to hereditary nonpolyposis colorectal cancer, characterized by instability of multiple microsatellite loci throughout the genome. Moreover, epigenetic silencing of key MMR genes may contribute to the development of 5% to 15% of sporadic cancers that have a microsatellite instability phenotype, including colorectal, gastric, endometrial, cervical, ovarian, breast, lung, and bladder cancers as well as high grade gliomas, leukemias, and lymphomas [55].

## 4.2 HR repair during replication

During replication different types of lesions and breaks can arise in the template DNA disturbing the processive replicative polymerase, often resulting in substrates for HR (Figure 5). In the case of a lesion, HR often only bypasses the lesions leaving the damage to be repaired by other pathways. In case of a break, HR repairs the damage and contributes to the restoration of the replication fork [14]. Stalling of a replication fork at a lesion in the DNA template uncouples the polymerase from the helicase activity, which results in continued unwinding of the DNA in the absence of DNA synthesis. Often, DNA synthesis is re-initiated downstream of the lesion at another fork or Okazaki fragment, leaving a large single-stranded area behind [56]. This gap can be repaired by a HR-mediated process called strand switching, resembling the conventional SDSA. Instead of having a two-ended DSB, there is a lesion forcing the HR machinery to pair with the newly synthesized strand, forming a D-loop (Figure 5B-D). Branch migration of the D-loop allows bypass of the lesion and results in a DNA structure from which an active replication fork can be assembled. The same procedure can be used to fill ssDNA gaps at the replication fork. But the ssDNA gap can also be filled by the combined action of a TLS polymerase, which inserts nucleotides opposite the lesion, and a replicative polymerase, which extends the DNA fragment (Figure 5E-F). Another possibility is that the stalled replication fork at the lesion regresses backwards to form a four-way junction often referred to as a 'chicken foot' (Figure 5G-H). This is generally assumed to be the result of the relaxation of supercoils by topoisomerases further along the DNA [57]. As a result, the lesion is returned into dsDNA context and can be repaired by other repair mechanisms. After the damage is removed and the nascent strand re-anneals with its original template strand, the active replication fork can be restored. The chicken foot structure also allows the nascent DNA strand, synthesized at the other site of the stalled fork, to serve as an alternative template for the strand whose synthesis was blocked by the lesion. If the replicated DNA fragment is long enough, it will cover the lesion site once the fork adapts its original conformation. This will result in an error-free damage bypass. Alternatively, the chicken foot can be cut by one of a series of structure-specific endonucleases, such as MUS81/EME1 or SLX1/SLX4, to generate a one-ended DSB [58]. One-ended DSBs can also arise from collapsed replication forks or by erosion of uncapped telomeres [59, 60]. They can be repaired by strand invasion into a homologous duplex DNA followed by replication in a process known as break induced replication (Figure 5I-J) [59]. At the molecular level, the broken DNA end is processed and a D-loop is created upon joint molecule formation with the homologous duplex DNA. The 3' end from the broken end is used to prime leading strand DNA synthesis templated by the donor duplex. During this process, a processive replication fork is established, requiring leading as well as lagging strand DNA synthesis, in contrast to SDSA that only requires leading strand DNA synthesis [61].

A particularly problematic lesion during DNA replication is a DNA interstrand crosslink (ICL). HR is instrumental the replication-associated repair of this lesion [62]. An ICL covalently connects the two complementary strands of the DNA helix, thereby blocking unwinding of the two DNA strands, interfering with processes such as replication and

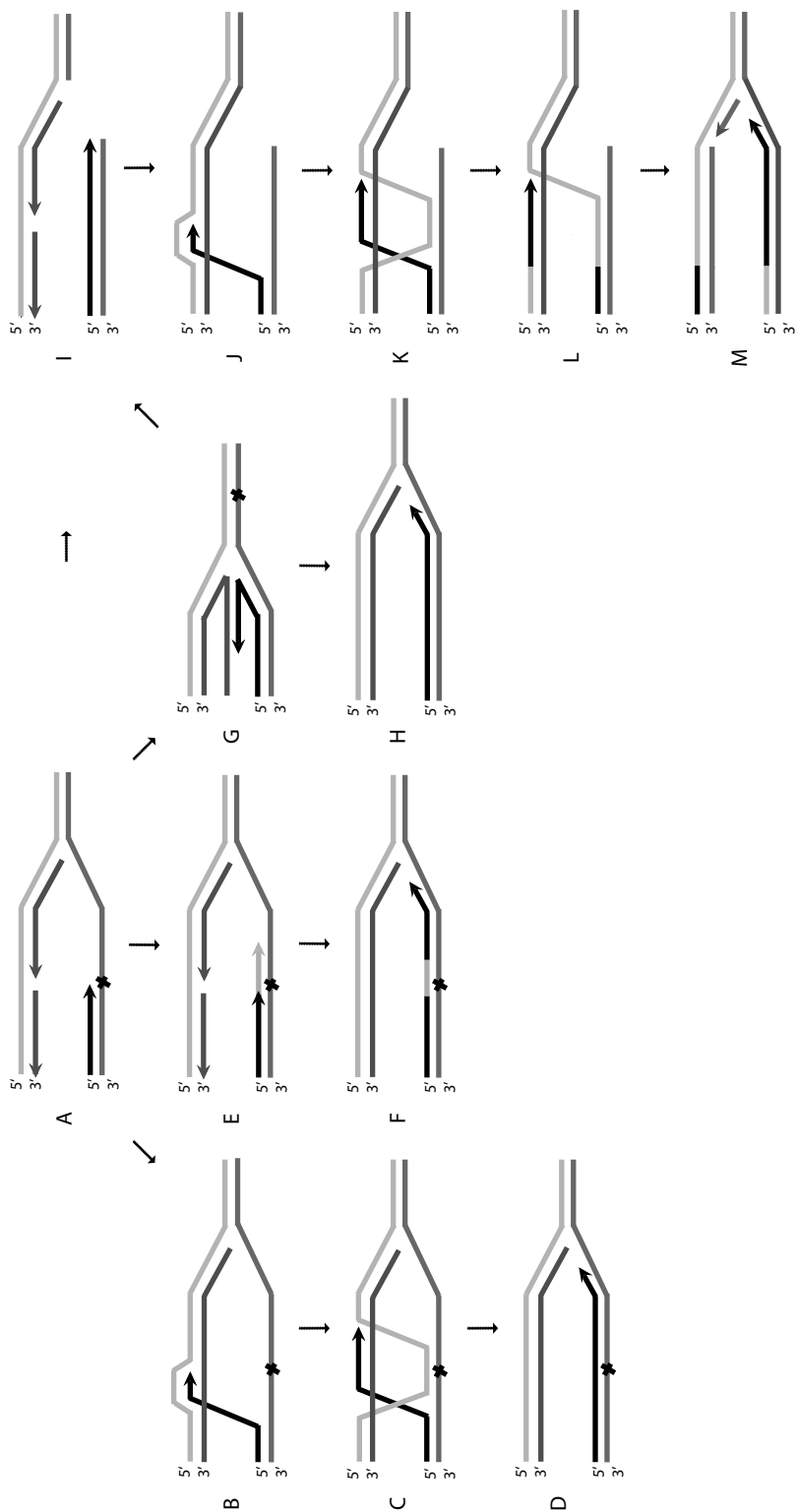


**Figure 5. Possible models for replication restart by HR.**

(A) A DNA replication fork encounters a lesion blocking active replication. (B) Uncoupling of DNA polymerases at the stalled fork results in either a single-stranded gap containing the lesion on the leading strand template or (I) in a DSB. Restart of replication is depicted in three ways. (B-D) First, the template strand lesion can be bypassed through recombinational repair as shown. (B) The blocked nascent strand can invade the homologous sister chromatid, forming a D-loop. (C) D-loop extension, formation of a Holliday junction and branch migration allows bypass of the lesion and (D) results in a DNA structure from which an active replication fork can be assembled. (E) Second, replication can be continued by a TLS polymerase, which temporarily replaces the replicative polymerase. (F) After incorporation of a few nucleotides the replicative polymerase is switched back and resumes replication. (G) Third, the stalled fork regresses backwards and forms a four-way junction. As a result, the lesion is returned into dsDNA context and can be repaired by other repair mechanisms. (H) After the damage is removed and the nascent strand re-anneals with their original template strand, the active replication fork can be restored. (I) Alternatively, the four-way junction can be cut by structure-specific endonucleases resulting in an one-ended DSB. (J) The one-ended DSB needs to be resected and can invade the homologous sister chromatid, forming a D-loop. (K) D-loop extension, which may require a TLS polymerase, can lead to a Holliday junction when the displaced lagging strand template strand pairs with the leading strand template strand. (L) The Holliday junction needs to be resolved (M) in order to be able to restore an intact replication fork.

---

transcription. In contrast to BER, NER and MMR lesions, the initial recognition of ICL is not through specific DNA damage recognition proteins, but rather indirectly by stalled replication. ICLs present a unique challenge to cells because they cannot be repaired by a simple excision and re-synthesis mechanism. Instead, ICL repair in S phase involves a group of proteins, called the Fanconi anemia proteins that appear to link stalled replication, structure-specific endonucleases and HR [63, 64]. A number of evolutionary related structure-specific endonucleases, including ERCC1/XPF, MUS81/EME1 and SLX1/SLX4, process branched DNA structures whose generation from stalled replication forks might require HR, thereby producing substrates, including DSBs, for both HR and TLS [58, 62]. In a possible scenario MUS81/EME1 cuts 3' of the lesion generating a one-ended DSB, while ERCC1/XPF incises on the other side of the crosslink [65]. TLS polymerases fill the gap formed by the unhooking step, while HR is used to restore the DNA break and finally the cross-linked adduct is removed by NER or other repair mechanisms.

### **4.3 Translesion DNA synthesis (TLS)**

TLS is a damage tolerance mechanism that supports replication past template lesions that stop or stall high-fidelity polymerases. TLS employs a specialized set of polymerases to replicate past damaged DNA. Mammalian cells express a number of these TLS polymerases, having different properties and substrate preferences. The Y-family of polymerases is the main family of TLS polymerases and consists of polymerase  $\eta$  (eta),  $\iota$  (iota),  $\kappa$  (kappa) and REV1. The B-family of polymerases represents another class, with polymerase  $\zeta$  (zeta) as its most prominent member. The main characteristic of TLS polymerases is their open active

sites and lack of proofreading activity, which allows them to bind and bypass modified DNA structures that arise due to the damage [66, 67]. The cost for this promiscuity is loss of fidelity; TLS polymerases tend to be error-prone than replicative polymerases. Initiating TLS in mammalian cells involves a series of steps, including the polymerase switch. TLS can be initiated when the replicative polymerase stalling exposes ssDNA at the site of the block. RING finger containing E3-ligase RAD18 binds to the ssDNA and together with the E2-conjugating enzyme RAD6 catalyzes binding of a single ubiquitin to the conserved K164 of PCNA, which is central in both replication and repair. PCNA encircles dsDNA as a trimer forming a sliding clamp that tethers proteins such as polymerases to DNA [68]. Mono-ubiquitination of PCNA is the signal to switch from replication to TLS [69, 70]. In contrast, poly-ubiquitination promotes recombination to rescue stalled replication forks [71]. Both mono-ubiquitinated PCNA and RAD18 interact with TLS polymerases and recruit them to the site of the blocked fork. The increased affinity for the TLS polymerase brings about the polymerase switch. The TLS polymerase can copy past the damaged template, frequently introducing mutations and thus must be rigorously controlled to prevent unwanted mutations.

## **5. Interplay and quality control during DNA damage repair**

Genetic analyses in numerous organisms formed the basis for delineating DNA repair pathways [72]. Screens for mutants sensitive to specific classes of DNA damaging agents coupled with epistasis analysis has resulted in the DNA repair pathways discussed above. Subsequent biochemical analyses revealed molecular mechanisms of DNA repair by placing many of the different gene products at specific steps of repair. However, early on it was clear that boundaries between DNA repair pathways might not be sharp. One indication came from cross sensitivities to DNA damaging agents. For example, mammalian cells mutant for the NER structure-specific endonuclease ERCC1/XPF are not only hypersensitive to UV light, but they are even more hypersensitive to ICL-inducing agents. This contrasts with other mammalian NER mutants, which are hardly hypersensitive to these agents. Since ICL repair is also strongly dependent on HR, it is an example of a composite DNA repair pathway requiring the functional interaction between components from what are considered elements of distinct DNA repair pathways. Another example of a composite DNA repair pathway is the interplay between HR and MMR, which is very important for inhibiting DNA rearrangements between slightly diverged sequences [51]. MMR aborts HR between divergent (homologous) sequences, for example between two alleles of the same gene. In higher eukaryotes, this anti-recombination is thought to protect the genome from recombination events between diverged repeats.

A mechanistic basis for the interplay between DNA repair pathways has been provided by cell biological experiments. Many DNA repair proteins accumulate at a high local concentration at the DNA damage in structures referred to as DNA damaged-induced foci [73]. Live cell experiments, in combination with photo-bleaching experiments have demonstrated that foci are dynamic structures in which the proteins actively turn over [73].

Since the different DNA repair proteins reversibly interact with the foci, repair of a specific lesion would be achieved by selection, through relative association affinities and stability of the resulting molecular complexes, of whichever component can act at a particular repair step of the lesion in question. The biological significance of pathway cross talk is to increase the diversity of repairable DNA lesions.

The dynamic nature of the accumulation of DNA repair proteins at sites of DNA damage not only provides a mechanism for cross talk between DNA repair pathways, but it also provides a means for quality control during DNA repair. The dynamic instability of the molecular interactions involved DNA repair allows constructive and destructive processes to occur in competition. Thus, there will be a constant building up and tearing down of inappropriate as well as appropriate reaction steps. Quality control can then be established by factors that slightly shift the equilibrium to eventually favor appropriate events [74]. Thus, paradoxically, messy unstable stochastic interactions, rather than machine-like precision may ensure that genome maintenance becomes a robust process that at the same time is flexible enough to allow pathway cross talk.

In the context of the view presented above, a general scenario for repair of a lesion would be for components involved in DNA lesion recognition to associate with lesions based on their relative selectivity for specific lesions. Additional components will interact reversibly and after surviving quality control, engage if their substrates and partners are present thereby pushing repair to the next intermediate. Subsequently, the cycle starts over with the next components that are able to act on the previously generated intermediate, eventually leading to repair. This, repair through these multiple, connected and overlapping interactions forms a web of molecular interactions from which a non-predetermined path to repair of a lesion will eventually emerge. Thus, the concept of distinct 'DNA repair pathways' based on genetic and biochemical analyses is still valid and useful, but their observed endpoints might not be reached in a predetermined organized manner [31].

## **6. Applications of mechanistic insight in DNA repair in anti-cancer treatment**

Genomic instability is a universal hallmark of cancer and is a double-edged sword with regard to its development and treatment. Understanding how cells maintain their genome might not just provide insight into how cancer cells arose in the first place, but could also reveal a way to kill them in a selective and ideally potentially harmless manner. Many common chemotherapeutic drugs are based on the principle of increasing the DNA damage load within tumor cells forcing them to go into cell cycle arrest and induce apoptosis. One class of drugs are topoisomerase inhibitors, such as etoposide and synthetic derivatives of camptothecin [75]. DNA topoisomerases resolve topological problems by means of transient DNA strand breakage and religation. By inhibiting or fixing the topoisomerase-DNA complex potentially lethal DNA damage can be introduced [76]. Another group of chemotherapeutics can introduce ICLs, such as cisplatin [77]. Although effective in damaging DNA, the major disadvantage of the chemotherapeutics is their lack of specificity

for cancer cells. A new generation of chemotherapeutic drugs is being developed based on knowledge obtained in the field of DNA repair. These drugs make use of the concept of synthetic lethality or synthetic sickness between DNA repair mechanisms and the fact that in tumor cells DNA repair is often compromised. The first promising results, representing the proof-of-principle of this approach, is the highly selective killing of BRCA-defective cells by inhibitors of PARP-1 [78-80]. The rationale behind these experiments is based on the fact that *BRCA* mutations convey a severe defect in HR. By inhibiting another DNA repair mechanism controlled by PARP, in this case BER, an overload of lesions is created that are deleterious in the context of defective HR. The efficacy of this type of approach in the treatment of cancer is now being tested in clinical trials with patients that are heterozygous for *BRCA* mutations [80]. Tumor cells, but not the normal cells, of these patients are HR deficient due to loss of the only functional *BRCA* allele. The tumor-specific HR deficiency should be the Achilles heel of the tumors cells when the patients are treated with inhibitors of PARP. Given that the DNA damage response is very complex, this example likely represents the tip of the iceberg and many more cases of synthetic lethality or sickness might be discovered. Not only does this approach allow highly selective targeting of tumor versus normal cells, but it also opens an avenue for more tailor made treatments of individual cancer patients.

## 7. Thesis scope

Double-stranded breaks are among the most dangerous type of DNA lesions because when not or inaccurately repaired these DSBs lead to DNA aberrations, resulting in incomplete replication, chromosomal aberrations and subsequently loss of cell function and cell death. The importance of accurate DSB repair is reflected in the fact that defects are associated with cancer predisposition. The main subject of this thesis is the DSB repair pathway homologous recombination. We will describe mechanistic insights in its role during replication and its regulation at the chromatin level. Furthermore we focus on one of its main players the ATPase RAD54. Finally we finish with the discovery that a commonly used anti-cancer therapy, elevated temperatures, also called hyperthermia, suppresses the process of homologous recombination.

In **chapter 2** we extend this introduction with a review on DNA replication fork stalling. In this chapter we highlight the relationship among three mechanisms involved in bypassing replication fork stalling; homologous recombination, translesion DNA synthesis (TLS) and *de novo* reinitiation of DNA synthesis. In **chapter 3** we focus on the chromatin context of DSB repair through analyzing histone H2B mono-ubiquitination, a highly dynamic chromatin modification carried out by the E3 ubiquitin ligase RNF20. We show that in the absence of RNF20 the timely accumulation of homologous recombination proteins at sites of DSBs is affected, functionally suppressing homologous recombination activity. These data indicate a role upstream of homologous recombination for RNF20 possible via the chromatin modification mono-ubiquitination of H2B. In **chapter 4** we further focus on the role of homologous recombination during UV-induced replication

problems. We show that in the absence of nucleotide excision repair, the homologous recombination proteins RAD51 and RAD54 colocalize in UV-induced foci at sites of replication. This localization is functional because, as measured at the level of single replication forks, *Rad54* deficient cells are less effective in continuing replication upon UV irradiation. Furthermore, homologous recombination deficiency under these conditions leads to an increase of DSBs, as well as chromosome gaps and breaks. Finally, our experiments reveal RAD54-dependent and -independent contributions of homologous recombination to cellular UV sensitivity and show that problems due to the absence of TLS Pol $\eta$  can be overcome by the action of RAD54. Thereby revealing that the lack of UV sensitivity in Pol $\eta$ -deficient cells is due to RAD54-dependent homologous recombination. In **chapter 5** the ATPase function of RAD54 in homologous recombination *in vivo* is further studied. For this purpose we compared knockin mouse embryonic stem cell lines that express GFP-tagged wild type RAD54 protein with cell lines expressing ATP hydrolysis defective RAD54 proteins. We show that the ATPase activity of RAD54 is essential for DSB repair by homologous recombination. Furthermore the ATPase activity of Rad54 is not required for timely accumulation of the main homologous recombination protein RAD51 at the site of DSBs into foci. On the contrary its ATPase activity affects disassembly of foci, indicating an essential role for RAD54 and its ATPase activity in homologous recombination.

Inhibitors of DSB repair are a relevant anti-cancer therapy since they sensitize cells to various DSB-inducing agents. Hyperthermia is one of the oldest clinically applied anti-cancer therapies and was suspected to inhibit DNA repair, but its primary mode of action remained elusive. In **chapter 6** we show that mild (41 - 42.5°C) hyperthermia inhibits the homologous recombination, induces degradation of BRCA2 and that this effect can be significantly enhanced by the addition of a heat shock protein (HSP) inhibitor. Mammalian tumor cells deficient in homologous recombination are sensitive to the inhibition of PARP-1. We demonstrate that hyperthermia can be used to sensitize innately homologous recombination-proficient tumor cells to PARP-1 inhibition, enabling design of novel therapeutic strategies involving localized induction of homologous recombination deficiency. One major culprit of treatment with hyperthermia is adaptation to hyperthermia also called thermo tolerance. In **chapter 7** we show the relationship between BRCA2 protein expression and thermotolerance. Thermotolerance reduces the effectiveness of hyperthermia treatment and correlates with BRCA2 status.

## References

1. Watson, J.D. and F.H. Crick, *Genetical implications of the structure of deoxyribonucleic acid*. Nature, 1953. **171**(4361): p. 964-7.
2. Hoeijmakers, J.H., *Genome maintenance mechanisms for preventing cancer*. Nature, 2001. **411**(6835): p. 366-74.
3. Barnes, D.E. and T. Lindahl, *Repair and genetic consequences of endogenous DNA base damage in mammalian cells*. Annu Rev Genet, 2004. **38**: p. 445-76.
4. D'Amours, D., et al., *Poly(ADP-ribosyl)ation reactions in the regulation of nuclear functions*. Biochem J, 1999. **342** ( Pt 2): p. 249-68.
5. Lindahl, T. and R.D. Wood, *Quality control by DNA repair*. Science, 1999. **286**(5446): p. 1897-905.
6. Sokhansanj, B.A., et al., *A quantitative model of human DNA base excision repair. I. Mechanistic insights*. Nucleic Acids Res, 2002. **30**(8): p. 1817-25.
7. Sugawara, K., et al., *Xeroderma pigmentosum group C protein complex is the initiator of global genome nucleotide excision repair*. Mol Cell, 1998. **2**(2): p. 223-32.
8. Tang, J. and G. Chu, *Xeroderma pigmentosum complementation group E and UV-damaged DNA-binding protein*. DNA Repair (Amst), 2002. **1**(8): p. 601-16.
9. Jans, J., et al., *Powerful skin cancer protection by a CPD-photolyase transgene*. Curr Biol, 2005. **15**(2): p. 105-15.
10. Oksenyk, V. and F. Coin, *The long unwinding road: XPB and XPD helicases in damaged DNA opening*. Cell Cycle. **9**(1): p. 90-6.
11. Foustieri, M., et al., *Cockayne syndrome A and B proteins differentially regulate recruitment of chromatin remodeling and repair factors to stalled RNA polymerase II in vivo*. Mol Cell, 2006. **23**(4): p. 471-82.
12. Nouspikel, T., *DNA repair in mammalian cells : Nucleotide excision repair: variations on versatility*. Cell Mol Life Sci, 2009. **66**(6): p. 994-1009.
13. Andressoo, J.O., J.H. Hoeijmakers, and H. de Waard, *Nucleotide excision repair and its connection with cancer and ageing*. Adv Exp Med Biol, 2005. **570**: p. 45-83.
14. Cox, M.M., et al., *The importance of repairing stalled replication forks*. Nature, 2000. **404**(6773): p. 37-41.
15. Bassing, C.H. and F.W. Alt, *The cellular response to general and programmed DNA double strand breaks*. DNA Repair (Amst), 2004. **3**(8-9): p. 781-96.
16. Beucher, A., et al., *ATM and Artemis promote homologous recombination of radiation-induced DNA double-strand breaks in G2*. Embo J, 2009. **28**(21): p. 3413-27.
17. van Gent, D.C., J.H. Hoeijmakers, and R. Kanaar, *Chromosomal stability and the DNA double-stranded break connection*. Nat Rev Genet, 2001. **2**(3): p. 196-206.
18. Shiloh, Y., *The ATM-mediated DNA-damage response: taking shape*. Trends Biochem Sci, 2006. **31**(7): p. 402-10.
19. Lee, J.H. and T.T. Paull, *Activation and regulation of ATM kinase activity in response to DNA double-strand breaks*. Oncogene, 2007. **26**(56): p. 7741-8.

20. Lavin, M.F., *ATM and the Mre11 complex combine to recognize and signal DNA double-strand breaks*. *Oncogene*, 2007. **26**(56): p. 7749-58.
21. Lobrich, M. and P.A. Jeggo, *The two edges of the ATM sword: co-operation between repair and checkpoint functions*. *Radiother Oncol*, 2005. **76**(2): p. 112-8.
22. Petrini, J.H., *The Mre11 complex and ATM: collaborating to navigate S phase*. *Curr Opin Cell Biol*, 2000. **12**(3): p. 293-6.
23. Rogakou, E.P., et al., *DNA double-stranded breaks induce histone H2AX phosphorylation on serine 139*. *J Biol Chem*, 1998. **273**(10): p. 5858-68.
24. Mailand, N., et al., *RNF8 ubiquitylates histones at DNA double-strand breaks and promotes assembly of repair proteins*. *Cell*, 2007. **131**(5): p. 887-900.
25. van Attikum, H. and S.M. Gasser, *Crosstalk between histone modifications during the DNA damage response*. *Trends Cell Biol*, 2009. **19**(5): p. 207-17.
26. Weterings, E. and D.J. Chen, *The endless tale of non-homologous end-joining*. *Cell Res*, 2008. **18**(1): p. 114-24.
27. Walker, J.R., R.A. Corpina, and J. Goldberg, *Structure of the Ku heterodimer bound to DNA and its implications for double-strand break repair*. *Nature*, 2001. **412**(6847): p. 607-14.
28. Meek, K., et al., *trans Autophosphorylation at DNA-dependent protein kinase's two major autophosphorylation site clusters facilitates end processing but not end joining*. *Mol Cell Biol*, 2007. **27**(10): p. 3881-90.
29. Ahnesorg, P., P. Smith, and S.P. Jackson, *XLFI interacts with the XRCC4-DNA ligase IV complex to promote DNA nonhomologous end-joining*. *Cell*, 2006. **124**(2): p. 301-13.
30. Buck, D., et al., *Cernunnos, a novel nonhomologous end-joining factor, is mutated in human immunodeficiency with microcephaly*. *Cell*, 2006. **124**(2): p. 287-99.
31. Wyman, C. and R. Kanaar, *DNA double-strand break repair: all's well that ends well*. *Annu Rev Genet*, 2006. **40**: p. 363-83.
32. Covo, S., et al., *Translesion DNA synthesis-assisted non-homologous end-joining of complex double-strand breaks prevents loss of DNA sequences in mammalian cells*. *Nucleic Acids Res*, 2009. **37**(20): p. 6737-45.
33. McVey, M. and S.E. Lee, *MMEJ repair of double-strand breaks (director's cut): deleted sequences and alternative endings*. *Trends Genet*, 2008. **24**(11): p. 529-38.
34. Wyman, C., D. Ristic, and R. Kanaar, *Homologous recombination-mediated double-strand break repair*. *DNA Repair (Amst)*, 2004. **3**(8-9): p. 827-33.
35. Neale, M.J. and S. Keeney, *Clarifying the mechanics of DNA strand exchange in meiotic recombination*. *Nature*, 2006. **442**(7099): p. 153-8.
36. Mimitou, E.P. and L.S. Symington, *DNA end resection: many nucleases make light work*. *DNA Repair (Amst)*, 2009. **8**(9): p. 983-95.
37. Zou, L., D. Liu, and S.J. Elledge, *Replication protein A-mediated recruitment and activation of Rad17 complexes*. *Proc Natl Acad Sci U S A*, 2003. **100**(24): p. 13827-32.
38. Sung, P. and H. Klein, *Mechanism of homologous recombination: mediators and helicases take on regulatory functions*. *Nat Rev Mol Cell Biol*, 2006. **7**(10): p. 739-50.

39. Carreira, A., et al., *The BRC repeats of BRCA2 modulate the DNA-binding selectivity of RAD51*. Cell, 2009. **136**(6): p. 1032-43.
40. Yang, H., et al., *The BRCA2 homologue Brh2 nucleates RAD51 filament formation at a dsDNA-ssDNA junction*. Nature, 2005. **433**(7026): p. 653-7.
41. Mazloum, N. and W.K. Holloman, *Brh2 promotes a template-switching reaction enabling recombinational bypass of lesions during DNA synthesis*. Mol Cell, 2009. **36**(4): p. 620-30.
42. Mazloum, N. and W.K. Holloman, *Second-end capture in DNA double-strand break repair promoted by Brh2 protein of Ustilago maydis*. Mol Cell, 2009. **33**(2): p. 160-70.
43. Lovett, S.T., *Connecting replication and recombination*. Mol Cell, 2003. **11**(3): p. 554-6.
44. Heyer, W.D., et al., *Rad54: the Swiss Army knife of homologous recombination?* Nucleic Acids Res, 2006. **34**(15): p. 4115-25.
45. Mazin, A.V., et al., *Rad54, the motor of homologous recombination*. DNA Repair (Amst). **9**(3): p. 286-302.
46. Ip, S.C., et al., *Identification of Holliday junction resolvases from humans and yeast*. Nature, 2008. **456**(7220): p. 357-61.
47. Wu, L. and I.D. Hickson, *The Bloom's syndrome helicase suppresses crossing over during homologous recombination*. Nature, 2003. **426**(6968): p. 870-4.
48. Michel, B., et al., *Multiple pathways process stalled replication forks*. Proc Natl Acad Sci U S A, 2004. **101**(35): p. 12783-8.
49. Branzei, D. and M. Foiani, *The DNA damage response during DNA replication*. Curr Opin Cell Biol, 2005. **17**(6): p. 568-75.
50. Flores-Rozas, H. and R.D. Kolodner, *Links between replication, recombination and genome instability in eukaryotes*. Trends Biochem Sci, 2000. **25**(4): p. 196-200.
51. Jiricny, J., *The multifaceted mismatch-repair system*. Nat Rev Mol Cell Biol, 2006. **7**(5): p. 335-46.
52. de Wind, N., et al., *HNPCC-like cancer predisposition in mice through simultaneous loss of Msh3 and Msh6 mismatch-repair protein functions*. Nat Genet, 1999. **23**(3): p. 359-62.
53. Kunkel, T.A. and D.A. Erie, *DNA mismatch repair*. Annu Rev Biochem, 2005. **74**: p. 681-710.
54. Modrich, P., *Mechanisms in eukaryotic mismatch repair*. J Biol Chem, 2006. **281**(41): p. 30305-9.
55. Peltomaki, P., *Role of DNA mismatch repair defects in the pathogenesis of human cancer*. J Clin Oncol, 2003. **21**(6): p. 1174-9.
56. Lopes, M., M. Foiani, and J.M. Sogo, *Multiple mechanisms control chromosome integrity after replication fork uncoupling and restart at irreparable UV lesions*. Mol Cell, 2006. **21**(1): p. 15-27.
57. Postow, L., et al., *Topological challenges to DNA replication: conformations at the fork*. Proc Natl Acad Sci U S A, 2001. **98**(15): p. 8219-26.

58. Klein, H.L. and L.S. Symington, *Breaking up just got easier to do*. Cell, 2009. **138**(1): p. 20-2.
59. Llorente, B., C.E. Smith, and L.S. Symington, *Break-induced replication: what is it and what is it for?* Cell Cycle, 2008. **7**(7): p. 859-64.
60. Royle, N.J., et al., *Telomere length maintenance--an ALternative mechanism*. Cytogenet Genome Res, 2008. **122**(3-4): p. 281-91.
61. Lydeard, J.R., et al., *Break-induced replication and telomerase-independent telomere maintenance require Pol32*. Nature, 2007. **448**(7155): p. 820-3.
62. Niedernhofer, L.J., A.S. Lalai, and J.H. Hoeijmakers, *Fanconi anemia (cross)linked to DNA repair*. Cell, 2005. **123**(7): p. 1191-8.
63. Moldovan, G.L. and A.D. D'Andrea, *How the fanconi anemia pathway guards the genome*. Annu Rev Genet, 2009. **43**: p. 223-49.
64. de Winter, J.P. and H. Joenje, *The genetic and molecular basis of Fanconi anemia*. Mutat Res, 2009. **668**(1-2): p. 11-9.
65. Hanada, K., et al., *The structure-specific endonuclease Mus81-Eme1 promotes conversion of interstrand DNA crosslinks into double-strands breaks*. Embo J, 2006. **25**(20): p. 4921-32.
66. Yang, W., *Damage repair DNA polymerases Y*. Curr Opin Struct Biol, 2003. **13**(1): p. 23-30.
67. Kunkel, T.A., Y.I. Pavlov, and K. Bebenek, *Functions of human DNA polymerases eta, kappa and iota suggested by their properties, including fidelity with undamaged DNA templates*. DNA Repair (Amst), 2003. **2**(2): p. 135-49.
68. Ellison, V. and B. Stillman, *Biochemical characterization of DNA damage checkpoint complexes: clamp loader and clamp complexes with specificity for 5' recessed DNA*. PLoS Biol, 2003. **1**(2): p. E33.
69. Kannouche, P.L., J. Wing, and A.R. Lehmann, *Interaction of human DNA polymerase eta with monoubiquitinated PCNA: a possible mechanism for the polymerase switch in response to DNA damage*. Mol Cell, 2004. **14**(4): p. 491-500.
70. Watanabe, K., et al., *Rad18 guides poleta to replication stalling sites through physical interaction and PCNA monoubiquitination*. Embo J, 2004. **23**(19): p. 3886-96.
71. Stelter, P. and H.D. Ulrich, *Control of spontaneous and damage-induced mutagenesis by SUMO and ubiquitin conjugation*. Nature, 2003. **425**(6954): p. 188-91.
72. Friedberg, E.C., et al., *DNA repair and mutagenesis*. second ed. 2005: ASM Press - American Society.
73. Essers, J., A.B. Houtsmuller, and R. Kanaar, *Analysis of DNA recombination and repair proteins in living cells by photobleaching microscopy*. Methods Enzymol, 2006. **408**: p. 463-85.
74. Kanaar, R., C. Wyman, and R. Rothstein, *Quality control of DNA break metabolism: in the 'end', it's a good thing*. Embo J, 2008. **27**(4): p. 581-8.
75. Basili, S. and S. Moro, *Novel camptothecin derivatives as topoisomerase I inhibitors*. Expert Opin Ther Pat, 2009. **19**(5): p. 555-74.

76. Koster, D.A., et al., *Antitumour drugs impede DNA uncoiling by topoisomerase I*. Nature, 2007. **448**(7150): p. 213-7.
77. Miyagawa, K., *Clinical relevance of the homologous recombination machinery in cancer therapy*. Cancer Sci, 2008. **99**(2): p. 187-94.
78. Farmer, H., et al., *Targeting the DNA repair defect in BRCA mutant cells as a therapeutic strategy*. Nature, 2005. **434**(7035): p. 917-21.
79. Bryant, H.E., et al., *Specific killing of BRCA2-deficient tumours with inhibitors of poly(ADP-ribose) polymerase*. Nature, 2005. **434**(7035): p. 913-7.
80. Fong, P.C., et al., *Inhibition of poly(ADP-ribose) polymerase in tumors from BRCA mutation carriers*. N Engl J Med, 2009. **361**(2): p. 123-34.





# Chapter 2

## **Multiple interlinked mechanisms to circumvent DNA replication roadblocks**

**Berina Eppink<sup>1</sup>, Claire Wyman<sup>1,2</sup> and Roland Kanaar<sup>1,2</sup>**

Published: Exp Cell Res. 2006 Aug 15;312 :2660-5.

<sup>1</sup>Department of Cell Biology & Genetics, <sup>2</sup>Department of Radiation Oncology, Erasmus MC,  
PO Box 1738, 3000 DR Rotterdam, The Netherlands

## Abstract

DNA replication is a fragile process, since unavoidable lesions in the template DNA cause replicative polymerases to stall, posing a serious threat to genome integrity. Homologous recombination, translesion DNA synthesis and *de novo* re-initiation of DNA synthesis ensure robust replication by navigating it passed damaged DNA. In this review we highlight the relationship between these three processes.

**Keywords:** Homologous recombination, DNA lesions, DNA replication, Translesion DNA synthesis, D-loops, Genome integrity, Replication re-start

## Introduction

A plethora of DNA damaging agents from multiple sources continuously assaults the integrity of DNA [1]. Examples include reactive oxygen species from normal metabolic processes in the cell and radiation or chemicals from the external environment. In turn each agent produces a wide spectrum of DNA lesions. To maintain DNA function as the carrier of instructions for cell growth and genetic information for the next generation, multiple DNA damage repair pathways have evolved. To initiate DNA damage repair, a number of these pathways depend on a protein or protein complex that specifically recognizes the aberration in DNA caused by certain classes of lesions. Either the damage recognition protein/complex repairs (or reverses) the damage directly or the DNA damage recognition entity serves as a platform for assembly of other proteins required for multi-step DNA repair. An alternative solution is to couple damage recognition to a process that scans DNA, such as transcription or replication. In principle, the scanning process allows a much larger variety of lesions to be detected compared to the direct recognition mode. A disadvantage of the scanning recognition mode, specifically when DNA damage recognition is piggy backing on DNA replication, is that it is limited to the S phase of the cell cycle. However, it is in this phase of the cell cycle that repairing DNA damage is of utmost importance [2].

In this review we highlight the relationship between DNA replication, homologous recombination and translesion DNA synthesis. Because of unavoidable lesions in the template, DNA replication is a fragile process [3]. Homologous recombination provides essential underpinning of DNA replication by navigating it passed DNA damage. In addition, the power of homologous recombination as a DNA repair pathway is that it can repair DNA lesions that affect both strands of the DNA double helix, which necessarily preclude the use of the complementary strand as a repair template. Instead, homologous recombination uses the undamaged sister chromatid as a repair template. This feature in turn confines repair by homologous recombination mostly to the S phase of the cell cycle.

## Augmentation of DNA replication to minimize genome instability

DNA replication turned out to be a much more fragile process than expected from the high processivity of replicative DNA polymerases. As indicated above, one culprit is damage in the template DNA. Most lesions, which can easily be repaired in duplex DNA, can cause gaps and double-strand breaks when they are encountered during replication [4]. Due to the nature of the replication complex at the progressing fork, optimized for accuracy with high-fidelity polymerases, there is limited tolerance for structural aberrations in the DNA template. Therefore, replication forks are prone to inactivation and/or stalling [4], which can lead to incomplete replication and chromosomal rearrangements. This, in turn, can result in aneuploidy, activation of oncogenes, or inactivation of tumor suppressor genes with diverse outcomes including cell transformation, loss of cell function, or cell death [5, 6].

Template lesions can be bypassed by translesion DNA polymerases, which insert nucleotides opposite damaged bases [7]. However, these enzymes lack the fidelity of normal

replicative polymerase, and TLS can increase mutation frequency. In addition, single- and double-stranded breaks are not easily bypassed by TLS. Alternatively, inactivated or stalled DNA replication can be repaired by homologous recombination whereby a stalled nascent strand is paired with its complement in the sister chromatid (Figure 2.1). The sister chromatid functions as a repair template allowing replication past the lesion [4, 8]. In addition to bypassing DNA lesions, homologous recombination provides an advantage over other DNA repair pathways because homologous DNA strand pairing keeps all strands associated to facilitate reassembly of a processive replication fork with coupled leading and lagging strand DNA synthesis.

### **Link between DNA replication, repair and recombination**

Originally DNA replication, repair and recombination were seen as separate processes accomplished by distinct sets of proteins. A number of pioneering studies suggested that the protein complex responsible for processive replication could disassociate upon encountering a barrier or block before completing replication [9, 10]. A potential solution to this problem was provided by the hypothesis that homologous recombination could be used to re-establish a replication fork [11]. This notion is conceptually similar to T4 bacteriophage replication which includes an origin independent but recombination dependent replication mode [12]. Recombination dependent replication is based on the 3' end of the phage DNA invading a homologous duplex to form the D-loop [13]. The invading end serves as a primer for DNA synthesis, which allows a replication fork to be established. This mechanistic connection between replication and recombination is also important for the host cell itself and turned out to be widely utilized among prokaryotes and eukaryotes, where lesions at the replication fork need to be repaired or bypassed [4].

### **Translesion DNA synthesis**

A relatively recently discovered class of polymerases, the TLS polymerases, form the basis of a completely different mechanism for bypassing aberrant structures at replication forks [7]. TLS is a damage tolerance mechanism that supports replication past template lesions that stop or stall high-fidelity polymerases. Initiating TLS in human cells involves a series of steps. First, stalling of the high-fidelity polymerase results in the exposure of single-stranded DNA at the site of the block. Then, in eukaryotes, fork-associated single-stranded DNA leads to recruitment of Rad18, an E3 ubiquitin ligase, which together with the E2 ubiquitin conjugase Rad6, bring about the mono-ubiquitination of PCNA, the DNA polymerase sliding clamp [14]. Mono-ubiquitination of PCNA is suggested to signal the switch from replication to repair function [15, 16]. Both the mono-ubiquitinated PCNA and Rad18 interact with a TLS polymerase (pol $\eta$ ) whereby it is localized to the site of the blocked fork. In mammals ten TLS polymerases have been identified, including pol $\eta$ , pol $\iota$  and Rev1 [17]. Prokaryotes such as *E. coli* possess three specialized TLS polymerases, Pol II, Pol IV and Pol V [18]. The specific circumstances requiring each TLS polymerase and mechanisms controlling their loading at primer templates may vary and are not all currently defined.

Furthermore, the details of their engagement will be different in prokaryotes and eukaryotes since bacteria do not contain ubiquitin. However, all TLS polymerases share features making them well suited for replicating damaged templates. Their reduced replication fidelity allows them to accommodate altered template bases in their active sites and thereby to carry out synthesis past such bases. Their low processivity causes them to dissociate after insertion of only a few bases. This is crucial because their low fidelity, required at damaged bases, would generate mutations with increased frequency when copying undamaged bases.

## Homologous recombination

Homologous recombination is a versatile mechanism capable of repairing a variety of DNA lesions encountered during replication (Fig. 1). The common feature of all homologous recombination mediated DNA repair reactions is exchange of DNA strands between homologous DNA sequences [19]. The process of homologous recombination can be divided into a number of basic steps. Early in recombination single-strand DNA is generated through a variety of ways depending on the context of the lesion to be repaired. The single-stranded DNA is bound by many protomers of a DNA strand exchange protein to form a nucleoprotein filament, which is catalytically active in strand exchange. The central role of the nucleoprotein filament in recombination is underscored by its conservation. Of all proteins involved in recombination, the DNA strand exchange proteins including RecA in *E. coli* and Rad51 in eukaryotes, are the most highly conserved in structure and function [20, 21]. The nucleoprotein filament mediates homology recognition and exchange of DNA strands. These recombination activities are controlled at the stage of loading the recombinase, which depends on the structure of the DNA. For example, in *E. coli*, recombination involving DNA ends requires the RecBCD helicase/nuclease for DNA processing and recombinase loading [19]. At single-stranded gaps, that arise for instance at stalled replication forks, the RecF, RecO and RecR proteins are involved in loading the recombinase [3, 4, 22, 23]. In eukaryotes BRCA2 has a role in controlling the activity of the Rad51 recombinase [24]. *In vitro* data indicates this involves loading Rad51 onto single-stranded DNA and at single-strand/double-strand junctions [25, 26]. However, the molecular details for establishing a recombinase filament on distinct DNA substrates in eukaryotes are not yet clearly defined. Once formed, the nucleoprotein filament initiates invasion of homologous DNA, linking the single-stranded DNA to an undamaged duplex in a junction called a D-loop [22]. In the case of DNA double-strand break repair the invaded 3' end can serve as a primer for DNA synthesis. *In vitro* the RecA protein is efficient in strand invasion and D-loop formation, while the eukaryotic Rad51 proteins require stimulation by accessory proteins such as Rad54 [27]. The final stage of recombination involves resolution of the joined DNA molecules. After priming DNA synthesis, the invaded strand in the D-loop can be ejected as proposed in synthesis dependent DNA strand annealing models [28]. Alternatively, D-loop intermediates can be converted to Holliday junctions (Fig. 1), structures with four double-stranded DNA arms, from which the crossover point can move along DNA by branch migration [29]. As an

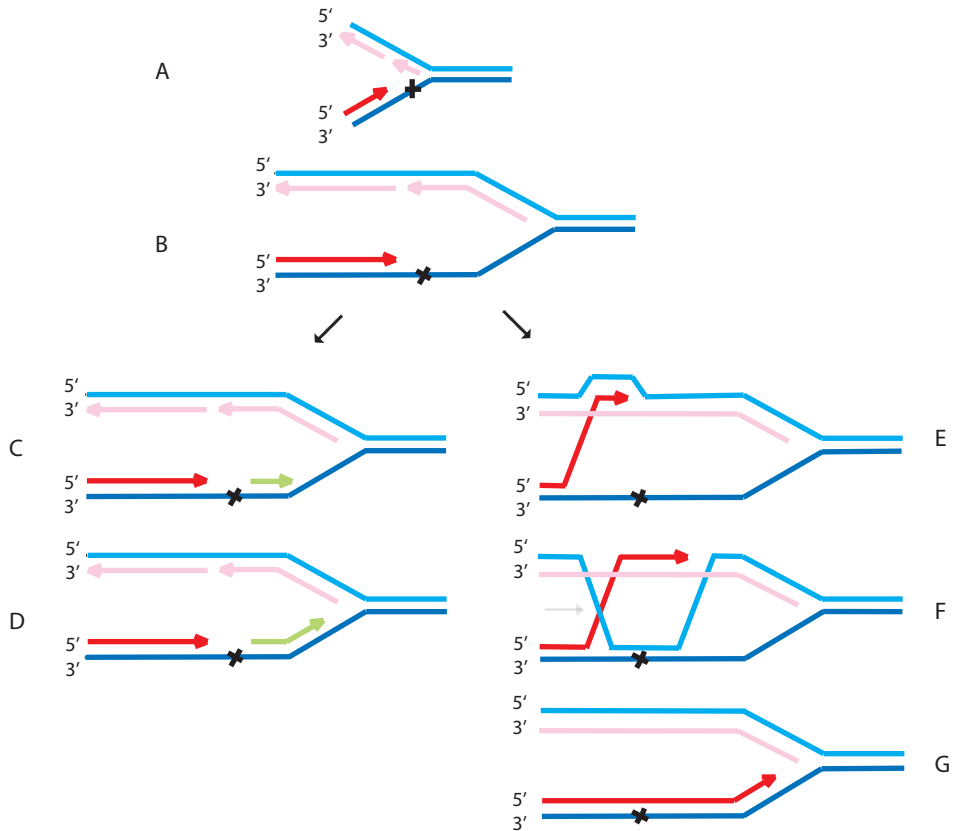


**Figure 1. Recombination versus *de novo* DNA synthesis initiation to bypass DNA damage in the leading strand template.** A DNA replication fork encounters a lesion in the leading strand template in A. Uncoupling of DNA polymerases at the stalled fork results in continued lagging strand synthesis creating a single-strand region on the leading strand template as indicated in B. Restart of replication is depicted in two ways. First, in C, replication can be restarted by *de novo* synthesis of a primer (green) on the leading strand template downstream of the lesion. Elongation from this primer leaves the lesion in a single-stranded gap (D), requiring either homologous recombination, TLS, or their combination for repair. Second, the template strand lesion can be bypassed through recombinational repair as shown in E-G. The blocked nascent strand can invade the homologous sister chromatid, forming a D-loop (E). D-loop extension, which may require a TLS polymerase, can lead to a Holliday junction when the displaced lagging strand template strand pairs with the leading strand template strand (F). Branch migration of the Holliday junction (in the direction indicated by the grey arrow pointing to the crossed strands) allows bypass of the lesion and results in a DNA structure from which an active replication fork can be assembled (G).

additional possibility, the D-loop junction need not mature into a fully double-stranded Holliday junction [30]. In either case, the junctions require structure-specific endonucleases for resolution of the recombination partners [31].

### **Re-initiation of DNA synthesis on damaged DNA templates**

As mentioned above, during homologous recombination mediated DNA repair, DNA synthesis can be primed off the 3' end of the invaded strand of the D-loop (Fig. 1). However, a D-loop is not a canonical primer-template junction and this raises the question which DNA polymerase would be able to extend the invaded strand. Recent biochemical fractionation experiments using human cell extract revealed that, in contrast to the replicative pol $\delta$ , the TLS polymerase pol $\eta$  can efficiently prime DNA synthesis from D-loop structures [32]. This is not a general property of TLS polymerases because pol $\iota$  is inactive on D-loops and extracts from Xeroderma pigmentosum Variant cell lines, which lack pol $\eta$  activity, are impaired in D-loop extension. How pol $\eta$  is targeted to the D-loop is not clear, but there might be a role for the Rad51 homologous recombination protein at this stage. Upon UV-light irradiation Rad51 and pol $\eta$  relocates into colocalizing foci [33]. Furthermore, both proteins can be co-immunoprecipitated and pre-incubation of D-loop substrates with Rad51 protein stimulates the activity of pol $\eta$ . A physical interaction between a TLS polymerase and a recombinase protein is not unprecedented, because the *E. coli* RecA protein interacts with pol V [34]. The requirement for pol $\eta$  is likely to be generally in homologous recombination, as suggested by genetic experiments in chicken DT40 cell lines. Pol $\eta$ -deficient DT40 cells are deficient in homologous recombination as measured by both immunoglobulin gene conversion and homologous gene targeting [35]. Thus, there might be a dual function of pol $\eta$ , in general TLS of UV light-induced lesions and in the re-initiation of DNA synthesis during some forms of homologous recombination repair.

While priming DNA synthesis from D-loop structures generated by homologous recombination is a convenient initial step to re-establish an active DNA replication fork, recently an interesting alternative has been suggested [36]. Restarting replication that has been blocked by a DNA lesion in the leading strand template is particularly challenging. As oppose the lagging strand DNA synthesis, leading strand DNA synthesis normally depends on only a single priming event at the DNA replication origin. A block in leading strand synthesis will uncouple the polymerases at the fork, results in a large single-stranded gap on the leading strand template (Fig. 1), due to continued lagging strand synthesis [37]. Recent experiments revealed that *E. coli* replication forks can be reprimed even on the leading strand [36]. This *de novo* priming, requiring the DnaB replicative DNA helicase and the DnaG primase, is dependent on either the PriA or PriC origin independent DNA synthesis re-start proteins. A number of models for the restart of replication forks blocked by DNA lesions in the leading strand template have been proposed, including fork regression to produce a Holliday junction coupled to template switch recombination to restart the fork or cleavage of the Holliday junction followed by homologous recombination mediated D-loop

formation [4]. In contrast to the newly discovered *de novo* priming reaction, none of the previous models satisfactorily explain the presence of gaps in the nascent leading strands that have long been known to occur upon UV-light irradiation [38]. Rather than obviate the need for replication-associated repair, the *de novo* priming reaction actually underscores the close connections between replication, repair and TLS. Completing replication requires that the resulting leading strand gaps are repaired by either a pol V dependent fill-in reaction, homologous recombination or both. Indeed, under conditions in which the PriC system is the only available restart pathway, RecFOR-mediated single-strand gap recombinational repair is essential [39].

## Future directions

As is often the case, the information discussed here concerning how recombination and replication are coupled raises more questions than it answers. For instance, identifying a TLS polymerase as important for homologous recombination in eukaryotic cells immediately raises the question of how the Rad51 protein stimulates pol $\eta$ . The generation of D-loop structures requires a Rad51 nucleoprotein filament. However, is this the active Rad51 moiety required to stimulate pol $\eta$ ? In at least one similar situation in *E. coli*, this is not the case. RecA physically interacts with the TLS polymerase pol V and is required for pol V-mediated TLS [18]. Yet, TLS is inhibited by the RecA nucleoprotein filament and the active TLS polymerase is apparently pol V associated with a RecA monomer [34]. If a similar situation exists in eukaryotic cells, this suggests that mechanisms that actively disrupt Rad51 nucleoprotein filaments might be important for TLS. A candidate protein in this regard would be Rad54, which has been implicated in removing Rad51 from DNA [40, 41].

DNA replication is a tightly controlled process, particularly in mammalian cells, to assure that all DNA is replicated once and only once every cell cycle to prevent aneuploidy. For this reason replication is highly controlled at the step of initiation. Replication initiation occurs only at specific regions called origins of replication that are controlled in strict coordination with cell cycle progression. However, specific sites for initiating replication poses a challenge in the context of replication restart at stalled forks. Because DNA lesions are distributed throughout the genome, fork reactivation must be independent of replication origins but random initiation of DNA synthesis must also be avoided. To this end bacteria such as *E. coli* have specialized systems, such as the PriA and PriC that facilitate loading the replisome onto (recombination) intermediates to restart replication [22]. Similar mechanisms must be operational in eukaryotes, but the molecular components and their mode of action have not yet been elucidated.

The links between replication and recombination in eukaryotes are largely unexplored. Most ideas in this area have come from research on bacteria and their phages where well-developed genetics and biochemistry allow critical testing of many possible models. Technically it is now becoming feasible to start asking questions about how mammalian cells are solving similar problems. There is no doubt that themes familiar from

prokaryotes will show up, but we should not be surprised if the increased complexity of the mammalian genome has necessitated the development of some interesting twists to coping with the replication restart problem.

## Acknowledgements

Work in the CW and RK laboratories is supported by grants from the Dutch Cancer Society (KWF), the Netherlands Organization for Scientific Research (NWO), the Association for International Cancer Research (AICR) and the European Commission.

## References

1. Hoeijmakers, J.H., *Genome maintenance mechanisms for preventing cancer*. Nature, 2001. **411**(6835): p. 366-74.
2. Branzei, D. and M. Foiani, *The DNA damage response during DNA replication*. Curr Opin Cell Biol, 2005. **17**(6): p. 568-75.
3. Kowalczykowski, S.C., *Initiation of genetic recombination and recombination-dependent replication*. Trends Biochem Sci, 2000. **25**(4): p. 156-65.
4. Cox, M.M., et al., *The importance of repairing stalled replication forks*. Nature, 2000. **404**(6773): p. 37-41.
5. van Gent, D.C., J.H. Hoeijmakers, and R. Kanaar, *Chromosomal stability and the DNA double-stranded break connection*. Nat Rev Genet, 2001. **2**(3): p. 196-206.
6. Flores-Rozas, H. and R.D. Kolodner, *Links between replication, recombination and genome instability in eukaryotes*. Trends Biochem Sci, 2000. **25**(4): p. 196-200.
7. Lehmann, A.R., *Replication of damaged DNA*. Cell Cycle, 2003. **2**(4): p. 300-2.
8. Michel, B., et al., *Multiple pathways process stalled replication forks*. Proc Natl Acad Sci U S A, 2004. **101**(35): p. 12783-8.
9. Hanawalt, P.C., *The U.V. sensitivity of bacteria: its relation to the DNA replication cycle*. Photochem Photobiol, 1966. **5**(1): p. 1-12.
10. Strauss, B.S., in *DNA-repair mechanisms*, H. Altmann, Editor. 1972, Schattauer F.K.: Stuttgart. p. 421-432.
11. Skalka, A., *A replicator's view of recombination (and repair)*, in *Mechanisms in Recombination*, R.F. Grell, Editor. 1974, Plenum Press: New York. p. 421-432.
12. Luder, A. and G. Mosig, *Two alternative mechanisms for initiation of DNA replication forks in bacteriophage T4: priming by RNA polymerase and by recombination*. Proc Natl Acad Sci U S A, 1982. **79**(4): p. 1101-5.
13. Kreuzer, K.N., *Recombination-dependent DNA replication in phage T4*. Trends Biochem Sci, 2000. **25**(4): p. 165-73.
14. Ulrich, H.D., *How to activate a damage-tolerant polymerase: consequences of PCNA modifications by ubiquitin and SUMO*. Cell Cycle, 2004. **3**(1): p. 15-8.
15. Hoege, C., et al., *RAD6-dependent DNA repair is linked to modification of PCNA by ubiquitin and SUMO*. Nature, 2002. **419**(6903): p. 135-41.

16. Kannouche, P.L., J. Wing, and A.R. Lehmann, *Interaction of human DNA polymerase  $\eta$  with monoubiquitinated PCNA: a possible mechanism for the polymerase switch in response to DNA damage*. Mol Cell, 2004. **14**(4): p. 491-500.
17. Friedberg, E.C., A.R. Lehmann, and R.P. Fuchs, *Trading places: how do DNA polymerases switch during translesion DNA synthesis?* Mol Cell, 2005. **18**(5): p. 499-505.
18. Goodman, M.F., *Error-prone repair DNA polymerases in prokaryotes and eukaryotes*. Annu Rev Biochem, 2002. **71**: p. 17-50.
19. Wyman, C., D. Ristic, and R. Kanaar, *Homologous recombination-mediated double-strand break repair*. DNA Repair (Amst), 2004. **3**(8-9): p. 827-33.
20. Yu, X., et al., *What is the structure of the RecA-DNA filament?* Curr Protein Pept Sci, 2004. **5**(2): p. 73-9.
21. Wyman, C. and R. Kanaar, *Homologous recombination: down to the wire*. Curr Biol, 2004. **14**(15): p. R629-31.
22. Lovett, S.T., *Connecting replication and recombination*. Mol Cell, 2003. **11**(3): p. 554-6.
23. Morimatsu, K. and S.C. Kowalczykowski, *RecFOR proteins load RecA protein onto gapped DNA to accelerate DNA strand exchange: a universal step of recombinational repair*. Mol Cell, 2003. **11**(5): p. 1337-47.
24. Shivji, M.K. and A.R. Venkataraman, *DNA recombination, chromosomal stability and carcinogenesis: insights into the role of BRCA2*. DNA Repair (Amst), 2004. **3**(8-9): p. 835-43.
25. Yang, H., et al., *BRCA2 function in DNA binding and recombination from a BRCA2-DSS1-ssDNA structure*. Science, 2002. **297**(5588): p. 1837-48.
26. San Filippo, J., et al., *Recombination mediator and Rad51 targeting activities of a human BRCA2 polypeptide*. J Biol Chem, 2006. **281**(17): p. 11649-57.
27. Petukhova, G., S. Stratton, and P. Sung, *Catalysis of homologous DNA pairing by yeast Rad51 and Rad54 proteins*. Nature, 1998. **393**(6680): p. 91-4.
28. Krogh, B.O. and L.S. Symington, *Recombination proteins in yeast*. Annu Rev Genet, 2004. **38**: p. 233-71.
29. West, S.C., *Molecular views of recombination proteins and their control*. Nat Rev Mol Cell Biol, 2003. **4**(6): p. 435-45.
30. Osman, F., et al., *Generating crossovers by resolution of nicked Holliday junctions: a role for Mus81-Eme1 in meiosis*. Mol Cell, 2003. **12**(3): p. 761-74.
31. Heyer, W.D., *Recombination: Holliday junction resolution and crossover formation*. Curr Biol, 2004. **14**(2): p. R56-8.
32. McIlwraith, M.J., et al., *Human DNA polymerase  $\eta$  promotes DNA synthesis from strand invasion intermediates of homologous recombination*. Mol Cell, 2005. **20**(5): p. 783-92.
33. Kannouche, P., et al., *Domain structure, localization, and function of DNA polymerase  $\eta$ , defective in xeroderma pigmentosum variant cells*. Genes Dev, 2001. **15**(2): p. 158-72.

34. Schlacher, K., et al., *DNA polymerase V and RecA protein, a minimal mutasome*. Mol Cell, 2005. **17**(4): p. 561-72.
35. Kawamoto, T., et al., *Dual roles for DNA polymerase eta in homologous DNA recombination and translesion DNA synthesis*. Mol Cell, 2005. **20**(5): p. 793-9.
36. Heller, R.C. and K.J. Mariani, *Replication fork reactivation downstream of a blocked nascent leading strand*. Nature, 2006. **439**(7076): p. 557-62.
37. Lopes, M., M. Foiani, and J.M. Sogo, *Multiple mechanisms control chromosome integrity after replication fork uncoupling and restart at irreparable UV lesions*. Mol Cell, 2006. **21**(1): p. 15-27.
38. Bridges, B.A. and S.G. Sedgwick, *Effect of photoreactivation on the filling of gaps in deoxyribonucleic acid synthesized after exposure of Escherichia coli to ultraviolet light*. J Bacteriol, 1974. **117**(3): p. 1077-81.
39. Grompone, G., et al., *Requirement for RecFOR-mediated recombination in priA mutant*. Mol Microbiol, 2004. **52**(2): p. 551-62.
40. Solinger, J.A., K. Kiianitsa, and W.D. Heyer, *Rad54, a Swi2/Snf2-like recombinational repair protein, disassembles Rad51:dsDNA filaments*. Mol Cell, 2002. **10**(5): p. 1175-88.
41. Tan, T.L., R. Kanaar, and C. Wyman, *Rad54, a Jack of all trades in homologous recombination*. DNA Repair (Amst), 2003. **2**(7): p. 787-94.



# Chapter 3

**Mono-ubiquitination of histone H2B by RNF20  
at sites of DNA double strand breaks is required  
for timely homologous recombination repair**

**Berina Eppink, Nicole van Vliet and Roland Kanaar**

Modified from manuscript in preparation

## Abstract

Genome stability is maintained through the DNA damage response (DDR) – a complex network of pathways that responds to DNA damage by activating DNA repair and cell-cycle checkpoints and modulating many signaling pathways. The DDR is activated by DNA double strand breaks (DSBs), which are among the most cytotoxic lesion induced by ionizing radiation. Optimal processing and repair of DSBs require chromatin reorganization at damaged sites. Chromatin reorganization associated with DNA transactions such as transcription is coupled to alterations in post-translational modifications (PTMs) of the histone proteins that constitute the basic chromatin fiber. Here we focus on histone H2B mono-ubiquitination, a highly dynamic PTM carried out by the E3 ubiquitin ligase RNF20. We present novel insight in the molecular mechanism of the role of RNF20 upon DSB induction. Specifically we show that in the absence of RNF20 the timely accumulation of homologous recombination (HR) proteins at DSBs is affected, functionally suppressing HR activity. Furthermore we show that timely accumulation of HR proteins is dependent on mono-ubiquitination of human histone H2B (mUbH2B), a modification previously associated with transcription-coupled nucleosome dynamics. These data indicate a role upstream of HR for RNF20 possible via the chromatin modification mono-ubiquitination of H2B.

## Introduction

The integrity of the DNA sequence is constantly threatened by a plethora of DNA damage inducing agents, potentially damaging the integrity of the DNA structure and the genetic code. DSBs are among the most life-threatening type of DNA lesions because when unrepaired or inaccurately repaired they can lead to DNA aberrations, resulting in incomplete replication, chromosomal aberrations (including aneuploidy), and subsequently loss of cell function and cell death. Two major pathways, homologous recombination (HR) and non-homologous end joining (NHEJ), have evolved to repair DSBs. NHEJ works by sealing the ends of a two-ended broken DNA strands together, mediated by the KU70/80 heterodimer, DNA-PKcs, DNA ligase IV and XRCC4 [1]. HR makes use of the pristine second copy of the sequence (sister chromatid) for aligning the breaks and is mediated by the MRN (MRE11, RAD50 and NBS1) complex, the DNA strand exchange protein RAD51 and the mediators BRCA2, RPA, RAD54 and XRCC3 [2]. A specific cellular characteristic of HR associated proteins is their accumulation at a high local concentration at sites of DNA damage in subnuclear structures referred to as foci [3, 4].

Optimal processing and repair of DSBs require chromatin reorganization at damaged sites [5]. Chromatin reorganization associated with DNA transactions such as transcription is coupled to alterations in post-translational modifications (PTMs) of the histone proteins that constitute the basic chromatin fiber [6, 7]. The rich repertoire of histone PTMs form a histone code, whose dynamics plays a major role in chromatin reorganization associated with DNA transactions [8]. However it is not clear which sensors are responsible for the signaling during DSB repair.

Here we focus on histone H2B mono-ubiquitination, a highly dynamic PTM previously known to be associated with transcribed chromatin. Mono-ubiquitination of histone H2B in humans is carried out by the E3 ubiquitin ligase complex RNF20/40 and knockdown of RNF20 but not RNF40 significantly reduced levels of mono-ubiquitination of H2B [9, 10]. Human RNF20 and RNF40 are orthologs of the budding yeast protein BRE1, an E3 ubiquitin ligase in mono-ubiquitination of yeast histone H2B on lysine 123 [11]. Absence of yeast protein BRE1 leads to X-ray sensitivity [12], similarly the absence of RNF20 and as a consequence RNF40 renders cells sensitive to the DSB inducing agent neocarzinostatin (Y. Shiloh unpublished data). Additionally RNF20 and RNF40 are present in an ATM associated complex. Taken together these data suggest a role for RNF20 in DSB repair, likely via histone H2B mono-ubiquitination. To investigate whether RNF20 and thereby the mono-ubiquitination of H2B influences DSB repair we focused on the effect of RNF20 on HR.

## Results

### **The absence of RNF20 delays localization of HR proteins to DSBs.**

To investigate the influence of RNF20 on DSB repair and in particularly HR, we monitored the localization of RAD51, BRCA2 and RPA to sites of local DNA damage either in the presence or absence of RNF20. Depletion of RNF20 was induced by siRNA treatment of

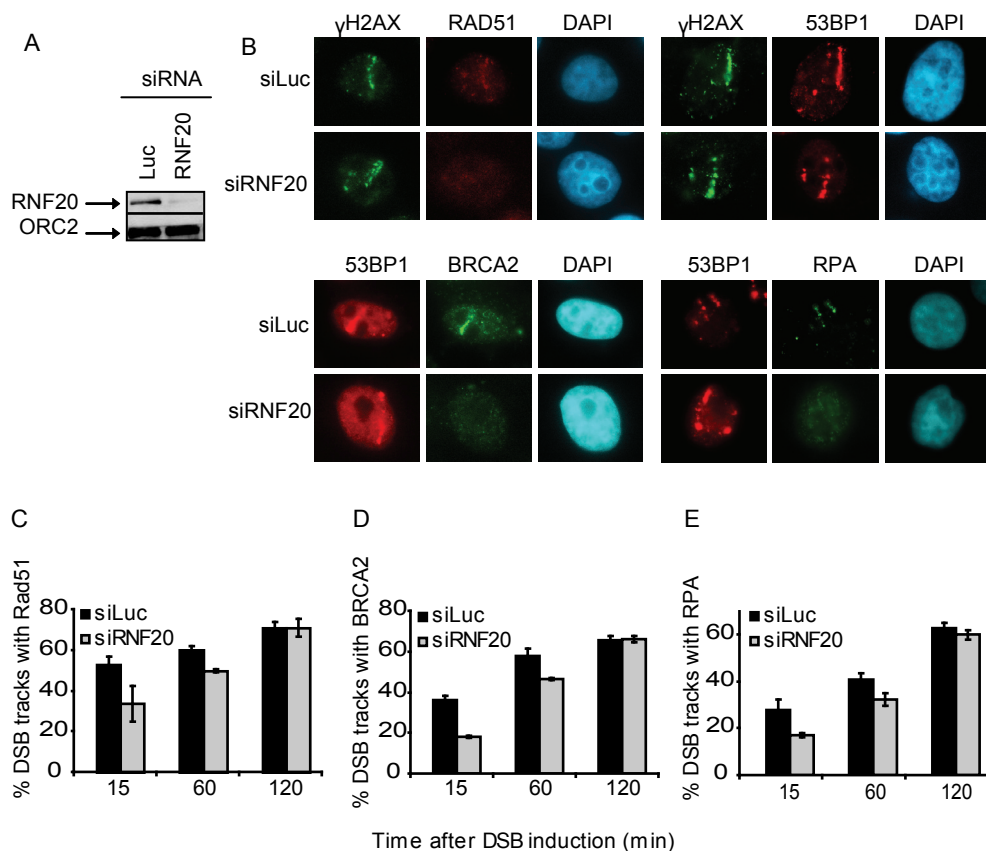


**Figure 1. The absence of RNF20 reduces localization of HR proteins to DSBs.** HeLa cells were transfected with siRNA against luciferase or RNF20 for 48 hrs. (A) Down regulation was monitored by probing for RNF20. Equal sample loading was verified by probing for hORC2. (B) Confocal images of accumulation of repair proteins at DSB sites in the presence or absence of RNF20. HeLa cells were transfected with siRNA against luciferase (siLuc) or RNF20 (siRNF20) for 48h and were stained for DNA (DAPI),  $\gamma$ H2AX (green) or 53BP1 (red), which were used as markers of the DSBs induced by  $\alpha$ -particles, and either of the following proteins: RPA34 (green), BRCA2 (green) or RAD51 (red). (C) Quantification of accumulation of BRCA2 at DSB sites after 15, 60 and 120 minutes in the presence or absence of RNF20. HeLa cells were stained for DNA (DAPI) 53BP1 (marker) and BRCA2. Graphs represent average percentage of BRCA2 positive tracks per 53BP1 track. 100 cells containing damage induced by  $\alpha$ -particles were scored per experiment. Error bars represent the range of percentages obtained from 3 independent experiments. (D) Quantification of accumulation of RAD51 at DSB sites similar to C with  $\gamma$ H2AX as a marker. (E) Quantification of accumulation of RPA at DSB sites after 30, 60 and 120 minutes similar to C.

HeLa cells for 48 hrs with siRNA against luciferase serving as a control. Down regulation was monitored by western blotting (Figure 1A). After sufficient down regulation was achieved, HeLa cells were irradiated with an Americium<sup>241</sup> source emitting alpha particles [13, 14] in a setup that results in the formation of linear tracks of DSBs in the cells. Cells were subsequently fixed and stained for the main HR proteins RAD51, BRCA2 and replication protein A (RPA) at 15 or 30, 60 and 120 minutes after irradiation (Figure 1 B-E). To indicate the site of DSBs the cells were also probed for either phosphorylated H2AX ( $\gamma$ H2AX) or 53BP1, both early responders to DSBs and forming nuclear foci at the sites of the DSBs [15]. Both the accumulation  $\gamma$ H2AX and 53BP1 into nuclear foci was not affected upon RNF20 depletion (Y. Shiloh unpublished results) and were therefore suitable as markers. In luciferase treated HeLa cells RAD51, BRCA2 and RPA all localized to the site of damage and the percentage of positive tracks in a cell population was determined relative to either 53BP1 or  $\gamma$ H2AX positive tracks (Figure 1A). Over time there is an increasing percentage of localization of these proteins to the sites of damage (Figure 1C-E). Upon RNF20 depletion we observed a transient, but considerable delay in the recruitment of RAD51, BRCA2 and RPA to DSBs. These data indicate a role for RNF20 in the cellular response upon DSB induction thereby influencing the accumulation of HR proteins.

### No delay in cell cycle progression in the absence of RNF20

Recruitment of HR players to DSBs occurs mainly at the S and G2 phases of the cell cycle, since the HR mechanism is functional when sister DNA molecules are available for recombination and the levels of these proteins are low at G1 [16]. To exclude the possibility that synchronization effects or stalling of the cells in G1 caused the delay in accumulation of HR proteins, the cell cycle status was analyzed after RNF20 depletion. HeLa cells were treated with siRNA for 48 hrs and subsequently fixed and stained for PI (whole DNA content) and BrdU (sites of replication). Depletion of RNF20 did not lead to any changes in cell cycle distribution (Figure 2), indicating that the effect of delayed localization of HR proteins is not caused by changes in cell cycle progression.

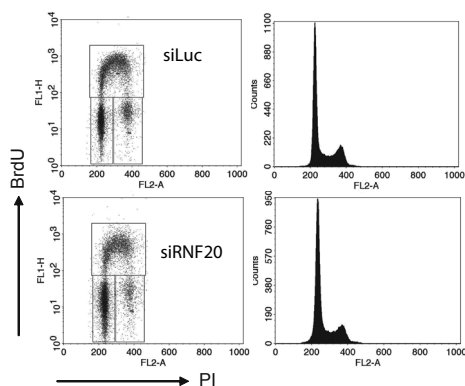
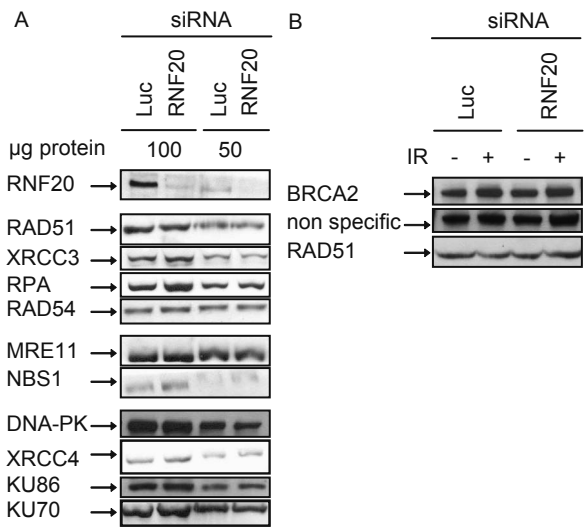


**Figure 2. No delay in cell cycle progression in the absence of RNF20.** HeLa cells were transfected with siRNA against luciferase or RNF20 for 48 hrs. After 48 hrs they were pulse labeled with BrdU and fixed. Their DNA content was determined by staining with propidium iodide (PI) and their replication status was assessed by staining with anti-BrdU antibodies. Shown are PI profiles in the panels on the right and BrdU incorporation (y-axis) versus PI-staining (x-axis) plots in the left panels.

**Depletion of RNF20 does not result in altered DSB repair protein levels**

In mammalian cells the first role shown for RNF20 is the mono-ubiquitination of H2B, a modification associated with transcription-coupled nucleosome dynamics [10, 17]. To sort out whether the effect of RNF20 on DSB repair is simply caused by reduced levels of repair proteins which could potentially result from abrogation of transcription due to reduced mUbH2B by RNF20 we checked the protein levels of main NHEJ and HR proteins. We measured the levels of the NHEJ proteins DNA-PKcs, XRCC4, KU86 and KU70 and of the HR proteins BRCA2, RAD51, XRCC3, RPA, RAD54, MRE11 and NBS1 (Figure 3A). All protein levels did not change in the absence of RNF20. In addition, BRCA2 and RAD51 protein levels also did not change upon irradiation (Figure 3B). NHEJ and HR proteins are present in normal levels in these RNF20 depleted cells, indicating that the reduced levels of RNF20 did not lead to altered protein levels as a result of disturbed transcription.

**Figure 3. Depletion of RNF20 does not result in altered DSB repair protein levels.** HeLa cells were transfected with siRNA against luciferase or RNF20 for 48 hrs. **(A)** The levels of main NHEJ and HR proteins after downregulation of RNF20 were analyzed by immunoblotting. Shown here are: the NHEJ proteins: DNA-PKcs, XRCC4, KU86 and KU70 and the HR proteins: BRCA2, RAD51, XRCC3, RPA, RAD54, MRE11 and NBS1. **(B)** The levels of RAD51 and BRCA2 after RNF20 downregulation and irradiation were analyzed by immunoblotting with antibodies against hRAD51 and hBRCA2. Equal sample loading was shown by a non specific band.



**Strong reduction of HR mediated gene conversion in the absence of RNF20**

The delay in accumulation of HR proteins in absence of RNF20, prompted us to analyze the efficiency of HR. We used a reporter system in U2OS cells to measure HR efficiency. In this system, an 18 bp sequence recognized by the site-rare restriction endonuclease I-SceI is placed between tandem mutant copies of the gene encoding GFP [18]. Because of the

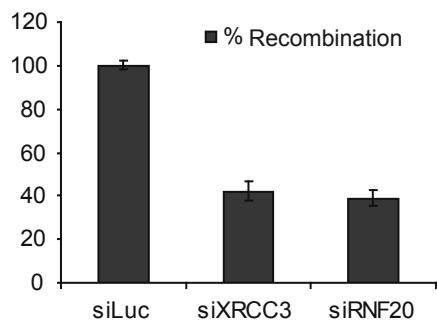


**Figure 4. Strong reduction of HR mediated gene conversion in the absence of RNF20** U2Os #18 cells were transfected with siRNA against luciferase (luc), XRCC3 or RNF20 for 48hrs after which I-Sce-I was expressed for 24hrs. Quantification of percentage of recombination events. The luciferase control is normalized to 100. Error bars represent the standard error of the mean, Figure is representative for 3 independent experiments.

orientation of the GFP direct repeats, HR between these two copies generates a wild-type GFP gene, which can be detected by FACS analysis. As shown in Figure 4 depletion of RNF20 reduced the efficiency of I-SceI-induced HR by around 60% similar as for XRCC3, a known HR factor. These data indicate that RNF20 has a major effect on DSB-induced HR activity.

#### Effect of RNF20 depletion on localization of HR proteins dependent on mUbH2B

To investigate whether the effect of RNF20 on localization of HR proteins is mediated via the mono-ubiquitination of H2B we analyzed the accumulation of RAD51 on alpha tracks in the presence of a wild type or mutant (K120R/K125R) mCherryH2B.

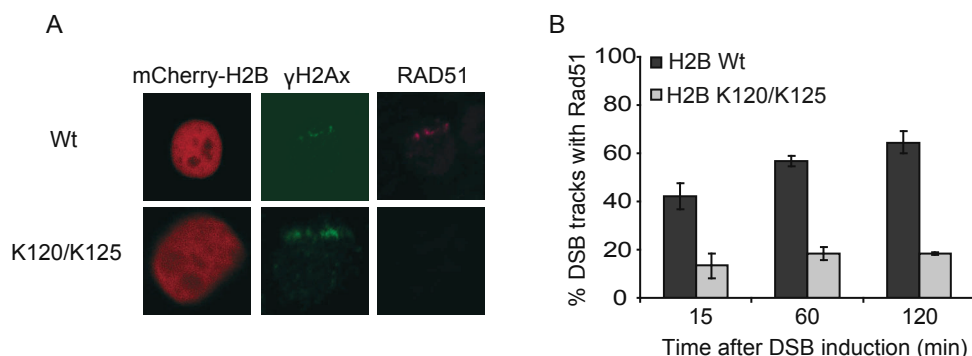


**Figure 5. Effect of RNF20 depletion on localization of HR proteins dependent on mUbH2B** (A) Visualization of accumulation of RAD51 at DSB sites after transient expression of wild type or mutant K120R/K125R mCherry-H2B. Hela cells were stained for  $\gamma$ H2AX (green) mCherry-H2B (red) and RAD51 (purple). (B) Quantification of accumulation of RAD51 at DSB sites after 15, 60 and 120 minutes in the presence of wild type or mutant mCherry-H2B. Graphs represent average percentage of Rad51 positive tracks per  $\gamma$ H2AX track. 50-100 cells containing damage induced by  $\alpha$ -particles were scored per experiment. Error bars represent the range of percentages obtained from 3 independent experiments.

RNF20 was implicated in mono-ubiquitination of human H2B on lysine 120 [9]. The K120R substitution prevents mono-ubiquitination at this position; the K125R substitution does not allow a secondary mono-ubiquitination, which may take place in the absence of the primary mono-ubiquitination site at K120 [19]. In the absence of a functional mono-ubiquitination site on H2B, Rad51 did not accumulate to the same extent as in the case of wild type H2B (Figure 5A). Contrary to the transient effect of RNF20 depletion on the recruitment of HR proteins, expression of the K120R/K125R histone H2B led to a profound, sustained effect (Figure 5B). A possible explanation for this is that the mutated H2B completely blocks H2B mono-ubiquitination while for the knock-down the efficiency may vary. In conclusion these data indicate that timely accumulation of HR proteins at sites of DSBs is dependent on H2B mono-ubiquitination most likely via RNF20.

## Discussion/conclusion

In this study we present novel insight in the molecular mechanism of the role of the E3 ubiquitin ligase RNF20 upon DSB induction. Specifically we show that in the absence of RNF20 the timely accumulation of HR proteins at DSBs is affected, functionally suppressing HR activity. Furthermore we show that timely accumulation of HR proteins is dependent on mono-ubiquitination of human histone H2B (mUbH2B), a modification previously associated with transcription-coupled nucleosome dynamics [20, 21]. These data indicate a role for RNF20 upstream of HR via the chromatin modification mono-ubiquitination of H2B.

First we have shown that RNF20 delays accumulation of HR proteins RAD51, BRCA2 and RPA at sites of DSBs (Figure 1). Accumulation in foci is a specific cellular characteristic of HR associated proteins [3, 4]. RAD51 [22] BRCA2 and RPA accumulate and colocalize in foci after IR [3, 22, 23]. IR induced foci correlate with functional recombination, since absence of one of the RAD51 paralogs or BRCA2 abrogates foci formation of RAD51 [23], implying that IR-induced foci are a functional marker for HR. The accumulation of RAD51 and BRCA2 correspond to joint molecule formation during HR and RPA corresponds to resection. Our data (Figure 1) show that resection as well as joint molecule formation is delayed. These data indicate that absence of RNF20 leads to impaired HR. Indeed the efficiency of recombination in the absence of RNF20 is affected to the same extent as XRCC3 one of the RAD51 paralogs (Figure 4).

Furthermore our data show that depletion of RNF20 does not alter NHEJ and HR protein levels (Figure 3). RNF20 affects transcription [19], although not as severely as expected. RNF20 depletion produces a significant reduction in the cellular pool of ubH2B, but only a modest fraction of the total transcriptome was affected and cell viability was not compromised [19]. One explanation can be although ubH2B is present on most active genes in humans, only a subset of the genes actually requires ubH2B for expression [19, 24]. These data together with our finding suggest that the effect of RNF20 on DSB repair is not via altered transcription levels.

Absence of RNF20 leads to a delay in accumulation of HR proteins functionally interfering with HR. These data imply a role for RNF20 upstream of HR, comparable to its yeast ortholog BRE1. From yeast experiments we know that mono-ubiquitination of histone H2B by BRE1 is necessary to facilitate the di- and tri-methylation of histone H3 [25], otherwise conferring X-ray sensitivity. It is likely that RNF20 facilitates similar processes influencing the DSB response. Indeed our experiments confirmed that also in mammals the absence of mono-ubiquitination of H2B leads to reduced levels of DSB repair (Figure 5). This general effect on HR suggests that lack of mUbH2B might diminish the access of HR proteins to the damaged sites, which would be reflected in the extent of their accumulation at these sites.

Mono-ubiquitination of H2B by RNF20 appears not the only histone modification necessary for timely DSB repair. Indeed, an analogous pathway to mUbH2B formation is the recently reported recruitment to DSB sites of RNF8, an ubiquitin ligase for histone H2A mono-ubiquitination found to be required for proper DSB response [26-29] and damage-induced mono-ubiquitination of histone H4 by the BBAP E3 ligase [30]. It was recently suggested that RNF8 is involved in histone H2B mono-ubiquitination as well [31]. Our and other [19] data suggest that RNF20 is the major E3 ligase in the induction of mUbH2B. However RNF8 could perhaps in response to DSBs play a role up- or downstream of RNF20. In conclusion we have shown a new role for RNF20, it influences timely repair of DSBs via HR likely via mono-ubiquitination of histone H2B.

## Materials and methods

**Antibodies.** Following antibodies were used for western blotting: mouse anti-BRCA2 (Ab-1, Calbiochem), Mouse anti-RNF20, Rabbit anti-Rad51 [32], Rabbit anti-Mre11 [33], Rabbit anti-Orc2 (#559266, BD Pharmingen), Rabbit anti-XRCC3 (ab6494, Abcam), Rabbit anti-Rad54 [34], Mouse anti-RPA34 (Ab-2, Oncogene), Goat anti-NBS1 (sc-8580, Santa Cruz biotechnology), Rabbit anti-XRCC4 (ab-58464, Abcam), Goat anti-Ku86 (sc-1484, Santa Cruz biotechnology), Goat anti-Ku70 (sc-1486, Santa Cruz biotechnology) Rabbit anti-DNApK [35], rabbit anti-ORC2 (#559266, BD Pharmingen) and relevant horseradish peroxidase-conjugated secondary antibodies (Jackson ImmunoResearch). Following antibodies were used for immunofluorescence: mouse anti-BRCA2 (Ab-1, Calbiochem), mouse anti-RPA34 (Ab-2, Oncogene), mouse anti- $\gamma$ H2AX (05-636, Millipore), rabbit anti-RAD51 [32], rabbit anti-53BP1 (NB100-304, Novus biologicals) and relevant Alexa flour secondary antibodies (Molecular probes).

**Cell lysis and immunoblotting.** Cells were lysed in SDS sample buffer (2% SDS, 10% glycerol, 60 mM Tris-HCl pH 6.8) and incubated for 5 min at 95°C. Protein concentration was determined by the Lowry protein assay, extracts were supplemented with 0.5%  $\beta$ -mercaptoethanol and 0.02% bromophenol blue. After fractionation by SDS-PAGE, proteins were transferred to a PVDF membrane and probed with the relevant antibodies. For immunoblotting of BRCA2, a 3-8% Tris-acetate gel system was used.

**Irradiation and immunofluorescence.** Cells were irradiated by  $\alpha$ -particles as described previously [14]. Shortly, HeLa cells were transfected with siRNA against luciferase (CGUACGCGGAAUACUUCGAdTdT) or RNF20 (smartpool Dharmacon) for 48 hrs, after 24 hrs cells were plated on a 1.8  $\mu$ m-thick polyester membrane and transfection was repeated. Cells were irradiated with  $\alpha$ -particles and subsequently fixed and stained for immuno-fluorescence at indicated time points as previously described [13].

**Recombination assay.** Site specific recombination after I-Sce-I DSB induction was measured as described before [18]. As a control U2Os #18 cells treated with siRNA against XRCC3 (GGACCUGAAUCCCAGAAUUUU) were taken.

## References

1. Weterings, E. and D.J. Chen, *The endless tale of non-homologous end-joining*. Cell Res, 2008. **18**(1): p. 114-24.
2. San Filippo, J., P. Sung, and H. Klein, *Mechanism of eukaryotic homologous recombination*. Annu Rev Biochem, 2008. **77**: p. 229-57.
3. Essers, J., et al., *Nuclear dynamics of RAD52 group homologous recombination proteins in response to DNA damage*. Embo J, 2002. **21**(8): p. 2030-7.
4. Tashiro, S., et al., *Rad51 accumulation at sites of DNA damage and in postreplicative chromatin*. J Cell Biol, 2000. **150**(2): p. 283-91.
5. Downs, J.A., M.C. Nussenzweig, and A. Nussenzweig, *Chromatin dynamics and the preservation of genetic information*. Nature, 2007. **447**(7147): p. 951-8.
6. Osley, M.A., A.B. Fleming, and C.F. Kao, *Histone ubiquitylation and the regulation of transcription*. Results Probl Cell Differ, 2006. **41**: p. 47-75.
7. Berger, S.L., *The complex language of chromatin regulation during transcription*. Nature, 2007. **447**(7143): p. 407-12.
8. Escargueil, A.E., et al., *What histone code for DNA repair?* Mutat Res, 2008. **658**(3): p. 259-70.
9. Kim, J., S.B. Hake, and R.G. Roeder, *The human homolog of yeast BRE1 functions as a transcriptional coactivator through direct activator interactions*. Mol Cell, 2005. **20**(5): p. 759-70.
10. Zhu, B., et al., *Monoubiquitination of human histone H2B: the factors involved and their roles in HOX gene regulation*. Mol Cell, 2005. **20**(4): p. 601-11.
11. Hwang, W.W., et al., *A conserved RING finger protein required for histone H2B monoubiquitination and cell size control*. Mol Cell, 2003. **11**(1): p. 261-6.
12. Game, J.C., et al., *The RAD6/BRE1 histone modification pathway in Saccharomyces confers radiation resistance through a RAD51-dependent process that is independent of RAD18*. Genetics, 2006. **173**(4): p. 1951-68.
13. Aten, J.A., et al., *Dynamics of DNA double-strand breaks revealed by clustering of damaged chromosome domains*. Science, 2004. **303**(5654): p. 92-5.

14. Stap, J., et al., *Induction of linear tracks of DNA double-strand breaks by alpha-particle irradiation of cells*. Nat Methods, 2008. **5**(3): p. 261-6.
15. Bekker-Jensen, S., et al., *Spatial organization of the mammalian genome surveillance machinery in response to DNA strand breaks*. J Cell Biol, 2006. **173**(2): p. 195-206.
16. Wyman, C. and R. Kanaar, *DNA double-strand break repair: all's well that ends well*. Annu Rev Genet, 2006. **40**: p. 363-83.
17. Pavri, R., et al., *Histone H2B monoubiquitination functions cooperatively with FACT to regulate elongation by RNA polymerase II*. Cell, 2006. **125**(4): p. 703-17.
18. Puget, N., M. Knowlton, and R. Scully, *Molecular analysis of sister chromatid recombination in mammalian cells*. DNA Repair (Amst), 2005. **4**(2): p. 149-61.
19. Shema, E., et al., *The histone H2B-specific ubiquitin ligase RNF20/hBRE1 acts as a putative tumor suppressor through selective regulation of gene expression*. Genes Dev, 2008. **22**(19): p. 2664-76.
20. Weake, V.M. and J.L. Workman, *Histone ubiquitination: triggering gene activity*. Mol Cell, 2008. **29**(6): p. 653-63.
21. Fleming, A.B., et al., *H2B ubiquitylation plays a role in nucleosome dynamics during transcription elongation*. Mol Cell, 2008. **31**(1): p. 57-66.
22. Tan, T.L., et al., *Mouse Rad54 affects DNA conformation and DNA-damage-induced Rad51 foci formation*. Curr Biol, 1999. **9**(6): p. 325-8.
23. van Veelen, L.R., et al., *Ionizing radiation-induced foci formation of mammalian Rad51 and Rad54 depends on the Rad51 paralogs, but not on Rad52*. Mutat Res, 2005. **574**(1-2): p. 34-49.
24. Minsky, N., et al., *Monoubiquitinated H2B is associated with the transcribed region of highly expressed genes in human cells*. Nat Cell Biol, 2008. **10**(4): p. 483-8.
25. Giannattasio, M., et al., *The DNA damage checkpoint response requires histone H2B ubiquitination by Rad6-Bre1 and H3 methylation by Dot1*. J Biol Chem, 2005. **280**(11): p. 9879-86.
26. Wang, B. and S.J. Elledge, *Ubc13/Rnf8 ubiquitin ligases control foci formation of the Rap80/Abraxas/Brca1/Brcc36 complex in response to DNA damage*. Proc Natl Acad Sci U S A, 2007. **104**(52): p. 20759-63.
27. Kolas, N.K., et al., *Orchestration of the DNA-damage response by the RNF8 ubiquitin ligase*. Science, 2007. **318**(5856): p. 1637-40.
28. Huen, M.S., et al., *RNF8 transduces the DNA-damage signal via histone ubiquitylation and checkpoint protein assembly*. Cell, 2007. **131**(5): p. 901-14.
29. Mailand, N., et al., *RNF8 ubiquitylates histones at DNA double-strand breaks and promotes assembly of repair proteins*. Cell, 2007. **131**(5): p. 887-900.
30. Yan, Q., et al., *BBAP monoubiquitylates histone H4 at lysine 91 and selectively modulates the DNA damage response*. Mol Cell, 2009. **36**(1): p. 110-20.
31. Wu, J., et al., *Histone ubiquitination associates with BRCA1-dependent DNA damage response*. Mol Cell Biol, 2009. **29**(3): p. 849-60.

32. Essers, J., et al., *Analysis of mouse Rad54 expression and its implications for homologous recombination*. DNA Repair (Amst), 2002. **1**(10): p. 779-93.
33. de Jager, M., et al., *DNA-binding and strand-annealing activities of human Mre11: implications for its roles in DNA double-strand break repair pathways*. Nucleic Acids Res, 2001. **29**(6): p. 1317-25.
34. Essers, J., et al., *Disruption of mouse RAD54 reduces ionizing radiation resistance and homologous recombination*. Cell, 1997. **89**(2): p. 195-204.
35. van der Burg, M., et al., *A new type of radiosensitive T-B-NK+ severe combined immunodeficiency caused by a LIG4 mutation*. J Clin Invest, 2006. **116**(1): p. 137-45.





# Chapter 4

## Versatile DNA repair mechanisms to circumvent UV-induced replication problems

**Berina Eppink<sup>1,5</sup>, Agnieszka A. Tafel<sup>1,5</sup>, Katsuhiro Hanada<sup>1,4</sup>, Ellen van Drunen<sup>3</sup>, Ian D.  
Hickson<sup>4</sup>, Jeroen Essers<sup>1,2</sup> and Roland Kanaar<sup>1,2,\*</sup>**

Department of Cell Biology & Genetics<sup>1</sup>, Cancer Genomics Center, Department of Radiation Oncology<sup>2</sup>, Department of Clinical Genetics<sup>3</sup>, Erasmus MC, P.O. Box 2040, 3000 CA Rotterdam, The Netherlands; Weatherall Institute of Molecular Medicine, University of Oxford, John Radcliffe Hospital, Oxford OX3 9DS, UK<sup>4</sup>.

<sup>5</sup>These authors contributed equally to this work.

\*Correspondence: r.kanaar@erasmusmc.nl

## Abstract

Ultraviolet (UV) radiation-induced DNA lesions can be efficiently repaired by nucleotide excision repair (NER). However because NER relies on the complementary strand as a repair template, it is less effective during replication of UV-damaged chromosomes, since lesions are placed in a single-strand DNA context. In contrast, translesion DNA synthesis (TLS) and homologous recombination are capable of dealing with lesions in single-stranded DNA. Here we analyze the interplay between NER, TLS and homologous recombination in mammalian embryonic stem cells. In an environment where NER is deficient, we show that the homologous recombination proteins RAD51 and RAD54 colocalize in UV-induced foci at sites of replication. This localization is functional because, as measured at the level of single replication forks, *Rad54* deficient cells are less effective in continuing replication upon UV irradiation. Furthermore, homologous recombination deficiency under these conditions leads to an increase of double-stranded DNA breaks, as well as chromosome gaps and breaks. Finally, our experiments reveal RAD54-dependent and -independent contributions of homologous recombination to cellular UV sensitivity and show that problems due to the absence of TLS Pol $\eta$  can be overcome by the action of RAD54. Thereby revealing that the lack of UV sensitivity in Pol $\eta$ -deficient cells is due to RAD54-dependent homologous recombination.

## Introduction

Homologous recombination, the exchange of DNA strands between homologous DNA molecules, plays a pivotal role in genome duplication and in providing genome stability through DNA repair. For example, it is involved in repair of exogenously induced DNA damage such as double-stranded breaks (DSBs) [1]. Homologous recombination can restore DNA integrity in an error-free manner by using a homologous DNA molecule, usually the sister chromatid, as a repair template [2]. The core homologous recombination protein in mammalian cells is the strand exchange protein RAD51, which is essential for cell viability [3, 4]. During homologous recombination numerous accessory proteins, or mediators, influence and control the action of RAD51, with some of them functioning in different sub-pathways of homologous recombination [5].

RAD54, a double strand (ds) DNA-dependent ATPase, is an important component of the homologous recombination machinery [6-10] that physically interacts with RAD51 [9, 11-13]. The ATPase activity of RAD54 is required for its translocation along DNA [9, 14-16], which underlies many of the roles it can fulfill in homologous recombination [10, 17]. For example, biochemical experiments show that RAD54 can augment homologous pairing by RAD51, remodel nucleosomes, promote branch migration and displace RAD51 from dsDNA. [13, 18-24]. A specific cellular characteristic of homologous recombination-associated proteins is their accumulation at a high local concentration at sites of DNA damage in subnuclear structures referred to as foci [25, 26]. RAD51 and RAD54 accumulate and colocalize in foci after treatment of cells with ionizing radiation (IR) [9, 25, 27].

Nucleotide excision repair (NER) is a multi-step DNA repair pathway that removes bulky helix distorting DNA lesions, such as UV-induced intra-strand cyclobutylpyrimidine dimers and 6-4 photoproducts [28]. After damage recognition, involving among others the XPA protein, a ~25-30 nucleotide stretch around the lesion is excised and the intact complementary strand is used to direct accurate repair [29]. In addition to NER, translesion DNA synthesis (TLS) allows cells to navigate UV-induced DNA damage, particularly during S phase. TLS involves activities of specific TLS DNA polymerases that can synthesize short stretches of DNA through a template tract containing a lesion [30]. The importance of TLS is underscored by the severe skin cancer predisposition in xeroderma pigmentosum variant (XP-V) patients, in which the translesion polymerase (Pol)  $\eta$  gene is mutated [31, 32]. Cells derived from these patients, although proficient in NER, are impaired in lesion bypass associated with DNA replication on damaged templates [33]. Homologous recombination is most notable for its role in repair of DSBs, however, it also contributes to the repair of interstrand DNA crosslinks, single-strand gaps and stalled replication forks [34]. This versatility arises from the DNA strand exchange reaction, which, in contrast to NER, allows homologous recombination to assist in repair of lesions that are not in the context of intact dsDNA. Thus, during DNA replication homologous recombination and TLS can be a more suitable repair or tolerance pathways for UV lesions than NER.

During replication of damaged DNA replication forks can stall and/or collapse. Numerous mechanisms for how homologous recombination might be able to contribute to

re-starting replication have been proposed [35-37]. Evidence implicating homologous recombination in single-strand gap or one-ended DSB repair, such as would have to occur at stalled or collapsed replication forks has come from observations in *E. coli*, yeast and vertebrate cells [35, 36, 38-43]. In yeast cells, the level of break-induced replication, which represents one of the possible mechanisms of repair of a collapsed replication fork, is severely diminished in *rad51Δ* cells [44, 45]. Additionally, accumulation of unrepaired chromosomal breaks during S phase is observed in conditional *Rad51*<sup>-/-</sup> DT40 cells [46]. One of its roles could be in the formation of a DNA displacement loop at the perturbed replication fork to bypass the lesions as has been proposed for RecA, the bacterial RAD51 homolog [47]. RAD54 can augment this step *in vitro* [48-51]. Additional biochemical activities of RAD54 that might be beneficial in downstream steps are its ability to promote branch migration [15] and convert Rad51-promoted joint molecules into substrates for DNA polymerisation [18, 24, 52].

Here, we used the RAD54 protein as a cellular marker for the homologous recombination process to follow the cellular response of mammalian stem cells to UV irradiation. By genetically inactivating NER and homologous recombination through disruption of the *Xpa* and *Rad54* genes respectively, we demonstrated the contribution of homologous recombination to chromosomal integrity upon UV irradiation. Furthermore, our data reveal RAD54-dependent and -independent contributions of homologous recombination to the cellular sensitivity to UV-light and they uncover that RAD54 can compensate for the loss of TLS Polη with regard to UV-light sensitivity

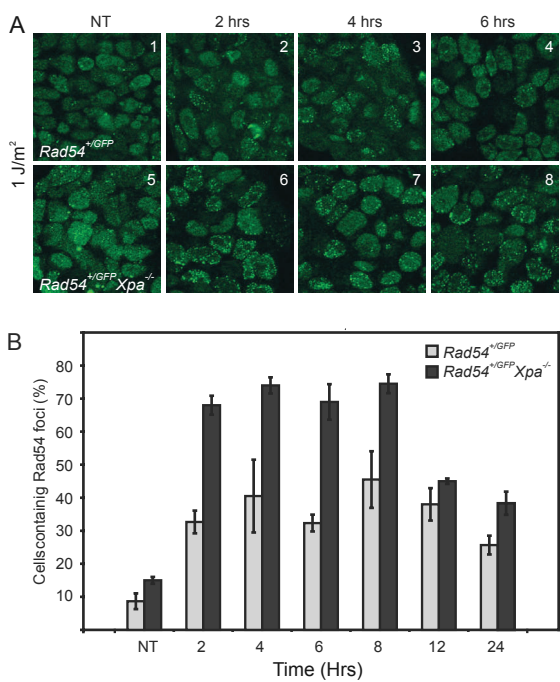


**Figure 1. More UV-induced RAD54 foci in the absence of NER.** (A) Confocal images of *Rad54*<sup>+/GFP</sup> and *Rad54*<sup>+/GFP</sup> *Xpa*<sup>-/-</sup> mouse ES cells after treatment with 1 J/m<sup>2</sup> of UV-light. Cells were fixed at the indicated times after irradiation. (B) Quantification of foci containing cells. Bars represent percentage of cells containing more than five RAD54 foci (light grey *Rad54*<sup>+/GFP</sup> cells; dark grey, *Rad54*<sup>+/GFP</sup> *Xpa*<sup>-/-</sup> cells). Error bars represent the standard error of mean (SEM). The time of analysis after treatment is indicated below the graph. At least 50 cells were analyzed for each cell line at each time point.

## Results

### Relocalization of RAD54 upon UV irradiation

To investigate homologous recombination in the context of the cellular response to UV-induced DNA damage in mammalian cells, we generated mouse embryonic stem (ES) cells carrying a *Rad54*<sup>GFP</sup> knockin allele that expresses biologically functional RAD54-GFP from the endogenous *Rad54* locus. The allele was integrated in wild-type ES cells as well as in NER deficient *Xpa*<sup>-/-</sup> ES cells (Supplemental Figure 1). *Xpa*<sup>-/-</sup> cells were used to increase the DNA damage load of unrepaired UV lesions. Next, we monitored the nuclear distribution of the RAD54 protein in *Rad54*<sup>+/GFP</sup> and *Rad54*<sup>+/GFP</sup> *Xpa*<sup>-/-</sup> cells upon UV irradiation. Most untreated *Rad54*<sup>+/GFP</sup> cells showed a relatively homogeneous nuclear distribution of RAD54-GFP with a small portion of the cells displaying a limited number of spontaneous foci, as reported previously [25] (Figure 1A). Interestingly, untreated *Rad54*<sup>+/GFP</sup> *Xpa*<sup>-/-</sup> cells already exhibited a significant increase in foci compared to *Rad54*<sup>+/GFP</sup> ES cells (Figure 1A and B). *Rad54*<sup>+/GFP</sup> *Xpa*<sup>-/-</sup> cells exposed to 1 J/m<sup>2</sup> UV-light showed a strong increase in RAD54 focus formation, but this induction was attenuated in *Rad54*<sup>+/GFP</sup> cells (Figure 1A and B).

We quantified differences in the RAD54-mediated response to UV-light between *Rad54*<sup>+/GFP</sup> and *Rad54*<sup>+/GFP</sup> *Xpa*<sup>-/-</sup> cell lines by determining the percentage of cells containing more than five RAD54 foci. In both cell lines the percentage of foci-positive cells increased after exposing cells to 1 J/m<sup>2</sup> of UV-light. However, induction of RAD54 foci by UV-light was on average 2-fold lower in NER-proficient cells than in NER-deficient cells (Figure 1B). This difference was sustained between 2 and 8 hrs following treatment. Twelve hrs after treatment, the number of RAD54 foci-positive cells began to decrease again. These results indicate that NER attenuates the requirement for homologous recombination in response to UV-induced DNA damage.

### The presence of homologous recombination proteins at sites of replication

RAD54 foci formed preferentially in *Rad54*<sup>+/GFP</sup> *Xpa*<sup>-/-</sup> ES cells compared to XPA-proficient cells upon irradiation with a low dose of UV-light, and were frequently located close to the periphery (Figure 2A). This particular pattern of foci is reminiscent of that of proliferating cell nuclear antigen (PCNA) during DNA replication. PCNA, which is a sliding clamp on DNA that confers processivity to replicative DNA polymerases, displays a homogenous nuclear staining in G1 and G2 cells and forms small foci throughout the nucleus in early S phase, foci near the nuclear periphery in mid-S phase and larger accumulations late in S phase, often near the nucleolus [53-58]. To confirm the UV-induced presence of RAD54 at sites of replication in a NER-deficient background colocalization experiments were performed. RAD54 colocalized not only with PCNA (Figure 2B), but also with sites of ongoing DNA replication as marked by incorporation of the nucleotide analog iododeoxyuridine (IdU) (Figure 2C). Like RAD54, the key homology recognition and DNA strand exchange protein RAD51 displayed the same response to UV-induced DNA lesions. In *Xpa*<sup>-/-</sup> cells a low dose of UV-light induced RAD51 foci that colocalized with RAD54 in a PCNA-like pattern (Figure 2D). We conclude that in the absence of active

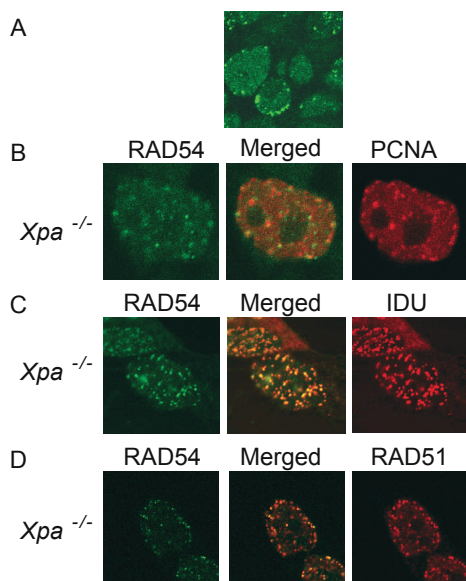


**Figure 2. Relocalization of RAD54 near sites of replication upon UV irradiation.** (A) Zoom of a confocal image from (A) of *Rad54<sup>+/GFP</sup> Xpa<sup>-/-</sup>* mouse ES cells after treatment with 1 J/m<sup>2</sup> of UV-light. (B) Confocal image of colocalization of RAD54-GFP with transiently expressed mCherry-PCNA 4 hrs after 1 J/m<sup>2</sup> UV irradiation in XPA-deficient cells. (C) Confocal image of colocalization of RAD54-GFP with immuno-stained IdU after 1 J/m<sup>2</sup> UV in an XPA-deficient cell. (D) Confocal image demonstrating colocalization of RAD54-GFP and immuno-stained RAD51 foci after 1 J/m<sup>2</sup> in XPA-deficient cells.

NER, very low doses of UV-light triggers localization of the homologous recombination proteins RAD54 and RAD51 to UV-induced DNA damage near sites of replication.

### The stability of replication forks is reduced in *Rad54<sup>-/-</sup> Xpa<sup>-/-</sup>* ES cells after UV-light treatment

To demonstrate the involvement of homologous recombination, through RAD54 activity, in assisting the recovery of replication forks stalled due to DNA damage, we analyzed the efficiency of replication recovery on individual chromosomal fibers [59-62]. Sites of active DNA replication were visualized using two differentially modified nucleotide analogs, IdU (detected in red; Figure 3A and B), which was added before the administration of DNA damage and chlorodeoxyuridine (CldU, detected in green; Figure 3A and B) which was added following UV exposure [63]. To visualize sites of DNA replication, we prepared chromosomal DNA fragments on glass slides and used IdU and CldU antibodies to detect the modified nucleotides that were incorporated into the chromosomal DNA. Tracks containing IdU represent all sites of DNA replication that were active before treatment with UV-light. Tracks containing CldU represent the sites where *de novo* replication started after UV-light treatment. If replication continued after UV-light exposure, CldU sites will colocalize with IdU sites resulting in yellow tracks (yellow in Figure 3A and B). The average number CldU (green), IdU (red) or two colored tracks (yellow) per 50  $\mu$ m fiber was determined for 30 individual fibers per genotype. To investigate the role of homologous recombination in replication restart, specifically when NER is absent, two independent *Rad54<sup>-/-</sup> Xpa<sup>-/-</sup>* clones (#C1 and #G2) were generated next to wild-type, *Rad54<sup>-/-</sup>* and *Xpa<sup>-/-</sup>*

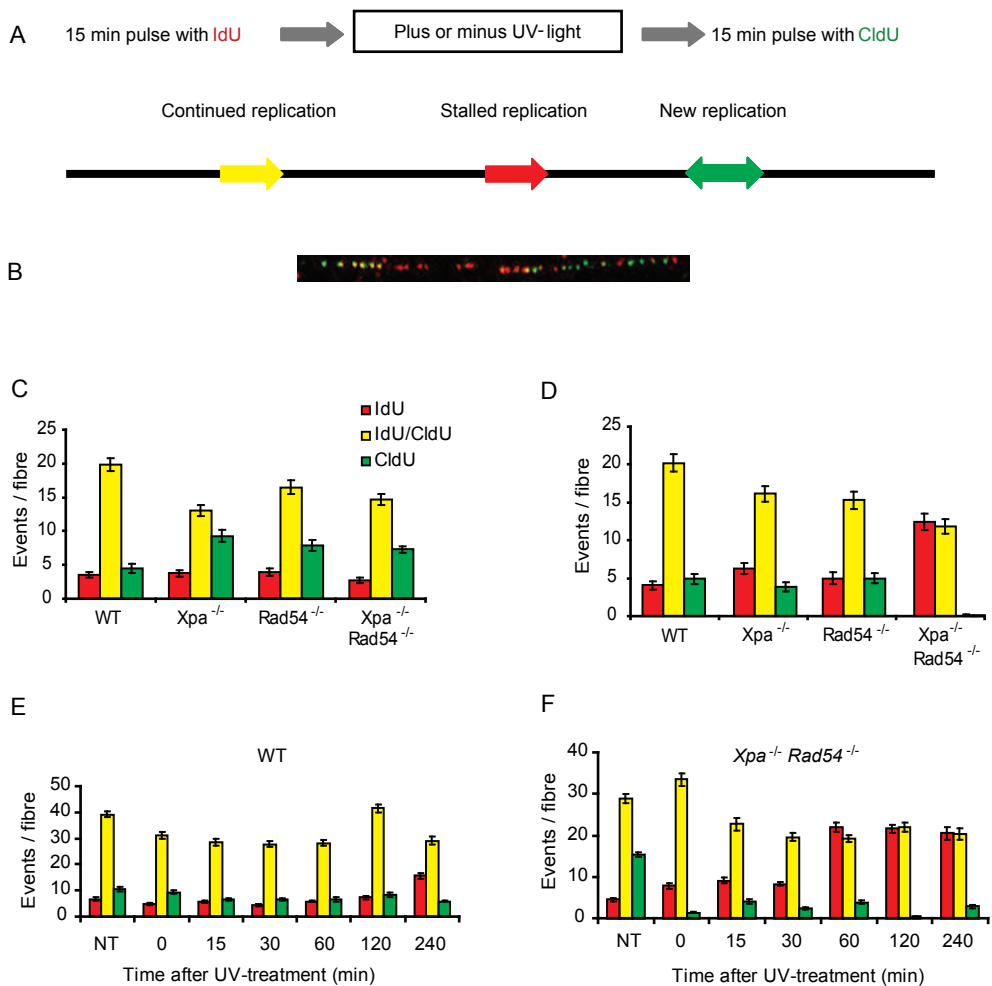


**Figure 3. RAD54-dependent recovery of stalled DNA replication.** DNA replication was analyzed using DNA fiber fish. Mouse ES cells, either wild-type, *Xpa*<sup>-/-</sup>, *Rad54*<sup>-/-</sup> or *Xpa*<sup>-/-</sup> *Rad54*<sup>-/-</sup>, were either non-treated or subjected to 80 J/m<sup>2</sup> UV-light and DNA fibers were prepared. (A) Schematic representation of labeled replication tracks. Red arrows (IdU) represent stalled replication forks. Yellow arrows (IdU/CldU) represent restarted replication forks upon UV irradiation. Events marked by green (CldU) only correspond to *de novo* DNA synthesis. (B) An example of a confocal image of fibers with labeled replication events. (C) The percentage of stalled replication forks (IdU), continued replication forks (IdU/CldU) and *de novo* replication forks (CldU) in untreated cells was quantified as the average number of forks per 50  $\mu$ M fiber. Error bars represents the standard error of the mean (n=30). (D) As in panel C, except the cells were treated with in 80 J/m<sup>2</sup> and analyzed after 2 hrs. (E) As in panel C, the percentage of stalled replication forks (IdU), continued replication forks (IdU/CldU) and *de novo* replication forks (CldU) in untreated and treated wild-type cells over time (NT, 0, 15, 30, 60, 120 and 240 minutes) per 50  $\mu$ M fiber. Error bars represents the SEM (n=30). (F) As in panel (E) except measured in *Xpa*<sup>-/-</sup> *Rad54*<sup>-/-</sup> mouse ES cells.

mouse ES cells [64, 65]. In non-treated wild-type cells the major fraction of replication forks was continuous ( $19.9 \pm 1.0$ ) and a similar amount of replication sites stalled ( $3.5 \pm 0.4$ ) or started *de novo* ( $4.5 \pm 0.6$ ) (Figure 3C). This pattern was similar in the non-treated mutant cells, most forks were continuous but the amount of *de novo* started forks varied. Cells were then exposed to a single dose of  $80 \text{ J/m}^2$  of UV-light and CldU was incorporated 2 hrs after the UV irradiation. Chromosomal fibers isolated from wild-type cells (Figure 3D) contained an average number of  $4.1 (\pm 0.5)$  stopped replication sites,  $20.2 (\pm 1.2)$  continuous replication sites, and  $4.9 (\pm 0.7)$  new replication sites. Single *Xpa*<sup>-/-</sup> and *Rad54*<sup>-/-</sup> mutant cells showed a similar distribution. In the double mutant *Xpa*<sup>-/-</sup> *Rad54*<sup>-/-</sup> cell line however replication was severely disturbed. There were fewer sites with continuous replication ( $11.9 \pm 1.0$ ) compared to both wild-type and single mutants. But the most striking differences were the total loss of new replication ( $0.2 \pm 0.1$ ) and the more than four-fold increase in stalled replication forks ( $12.4 \pm 1.1$ ).

To gain more insight in the dynamics of stalled replication forks under our experimental conditions we followed the status of replication over time and incorporated CldU 0, 15, 30, 60, 120 and 240 minutes after UV irradiation. Since both single *Rad54*<sup>-/-</sup> and *Xpa*<sup>-/-</sup> mutant cells did not display any obvious difference compared to wild-type ES cells we compared wild-type with *Xpa*<sup>-/-</sup> *Rad54*<sup>-/-</sup> ES cells. As expected in unperturbed wild-type cells no changes appeared in incorporation of IdU and CldU over time (Figure 3E). However, when we performed these time-course experiments in *Xpa*<sup>-/-</sup> *Rad54*<sup>-/-</sup> ES cells, we observed a UV-induced gradual increase in IdU-containing tracks. After 1 hr a maximum of IdU-containing tracks was observed, indicative of stalling of 50% of the replications forks (Figure 3F). These data indicate that RAD54-mediated homologous recombination has a role in continuation of replication, and that over time UV irradiation leads to the production of more substrates for homologous recombination during replication.

### **RAD54 suppresses UV-light induced DSBs in *Xpa*<sup>-/-</sup> ES cells**

A major role of homologous recombination is solving replication associated problems, for example those that can arise during replication of a damaged template [37]. In the absence of this protective effect of homologous recombination, replication forks can collapse and break. Therefore, we investigated whether lack of RAD54 resulted in an increase in UV-induced DSBs. Wild-type, *Rad54*<sup>-/-</sup>, *Xpa*<sup>-/-</sup> and the *Rad54*<sup>-/-</sup> *Xpa*<sup>-/-</sup> double mutant ES cells were either untreated or irradiated with  $10 \text{ J/m}^2$  and the integrity of their chromosomal DNA was assessed by pulsed field gel electrophoresis (PFGE) (Figure 4A). UV irradiation led to an increase in broken DNA in wild-type, *Rad54*<sup>-/-</sup> and *Xpa*<sup>-/-</sup> cells, confirming that UV-light can promote the formation of DSBs [66]. However, NER-deficient homologous recombination-defective *Rad54*<sup>-/-</sup> *Xpa*<sup>-/-</sup> double mutant cells displayed a two-fold higher increase in DSBs (Figure 4B). These results suggest that RAD54 and therefore homologous recombination are involved in the repair of DSBs after UV irradiation.

### ***Rad54*<sup>-/-</sup> *Xpa*<sup>-/-</sup> ES cells accumulate more structural chromosomal aberrations than *Xpa*<sup>-/-</sup> cells after UV-light treatment**

One of the hallmarks of an inability of a cell to restart blocked replication resulting in DSBs is the accumulation of structural chromosomal aberrations after challenging DNA replication [67]. To investigate whether chromosomal aberrations were increased in *Rad54*<sup>-/-</sup> *Xpa*<sup>-/-</sup> ES cells, we analyzed the accumulation of replication-associated chromosomal aberrations, chromatid gaps and chromosomal breaks, after challenging the cells with UV-light.

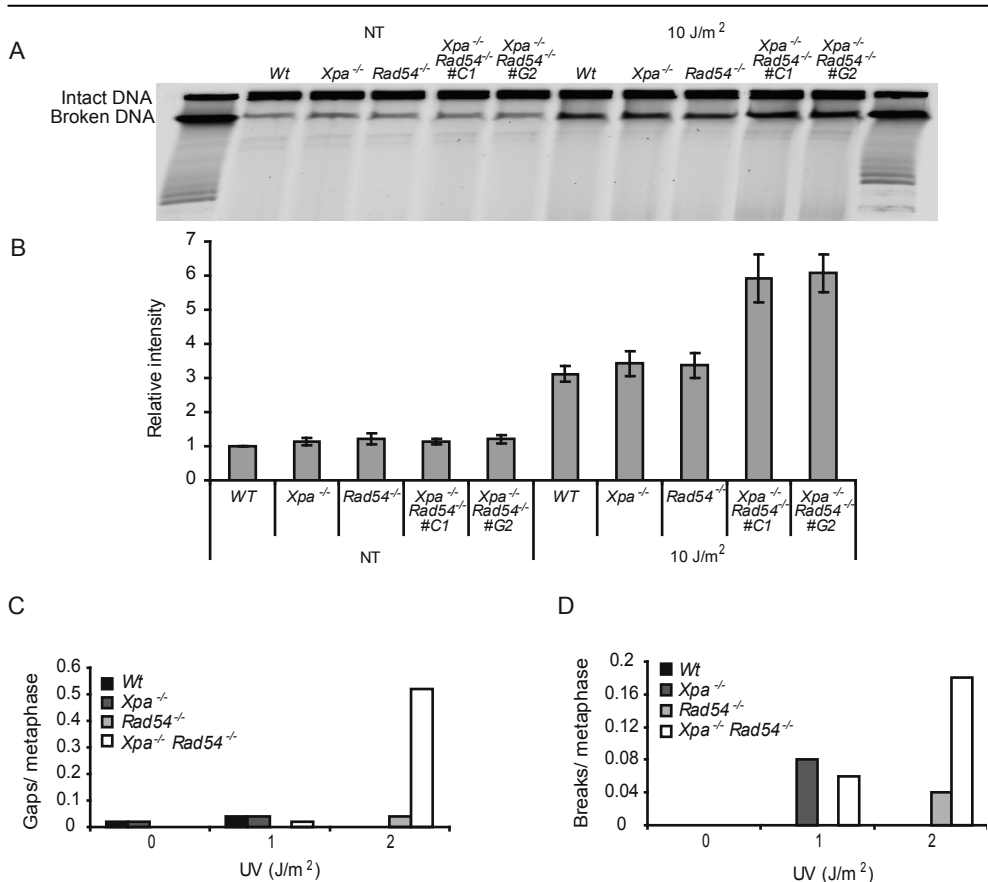


**Figure 4. The combination of NER and homologous recombination deficiency results in increased DSBs formation and chromosomal aberrations upon UV irradiation.** (A) DSB formation induced by 10 J/m<sup>2</sup> UV-light was analyzed using PFGE in wild-type, *Xpa*<sup>-/-</sup>, *Rad54*<sup>-/-</sup> and *Xpa*<sup>-/-</sup> *Rad54*<sup>-/-</sup> mouse ES cells. (B) Quantification of UV-induced formation of broken DNA. The amount of broken DNA was calculated as the intensity of DNA in the migrated fraction of the mutated samples over the wild type. Error bars represent the SEM. (C) Chromosomal aberrations detected in metaphase spreads of wild-type, *Xpa*<sup>-/-</sup>, *Rad54*<sup>-/-</sup> and *Xpa*<sup>-/-</sup> *Rad54*<sup>-/-</sup> ES cells. Quantification of the average number of gaps per metaphase spread after increasing doses of UV-light (0, 1 and 2 J/m<sup>2</sup>). (D) Quantification of the average number of breaks per metaphase spread after increasing doses of UV-light (0, 1 and 2 J/m<sup>2</sup>).

Chromatid gaps occurring in metaphase chromosomes result from a single-strand gap and chromosomal breaks arise from DSBs. Wild-type, *Rad54*<sup>-/-</sup> and *Xpa*<sup>-/-</sup> cells displayed background levels of gaps after treatment with low doses of UV-light (Figure 4C). However, irradiation of *Xpa*<sup>-/-</sup> *Rad54*<sup>-/-</sup> cells with 2 J/m<sup>2</sup> of UV-light resulted in a highly significant increase in the number of chromatid gaps. Similarly, the same dose of UV-light gave rise to a significantly ( $p = 0.0017$ ) elevated frequency of chromosomal breaks in *Xpa*<sup>-/-</sup> *Rad54*<sup>-/-</sup> cells (Figure 4D). Thus, in the absence of both NER and homologous recombination both single-strand gaps and DSBs remain unrepaired during replication and that these lesions are normally repaired by homologous recombination.

### **Contribution of homologous recombination to cell viability after UV-light treatment**

Increased RAD54 focus formation, problems during replication, and the increase in DSBs leading to chromosomal aberrations prompted us to analyze the UV-light sensitivity of cells impaired in both homologous recombination and NER. *Xpa*<sup>-/-</sup> ES cells are hypersensitive to UV irradiation while *Rad54*<sup>-/-</sup> ES cells are not [64, 68]. Two *Rad54*<sup>-/-</sup> *Xpa*<sup>-/-</sup> clones (#C1 and #G2), as well as *Rad54*<sup>-/-</sup>, *Xpa*<sup>-/-</sup> and wild-type control ES cells were analyzed for their ability to form colonies after treatment with increasing doses of UV-light (Figure 5A). As expected, both wild-type and *Rad54*<sup>-/-</sup> ES cells were not hypersensitive to UV-light. On the other hand *Rad54*<sup>-/-</sup> *Xpa*<sup>-/-</sup> cells were as hypersensitive to UV-light as *Xpa*<sup>-/-</sup> ES cells (Figure 5A). Similar results were obtained by using siRNA against XPA and RAD54 in the human osteosarcoma cell line U2Os (Figure 5B and D). Thus, the colony forming ability assay is not sensitive enough to detect a contribution of the RAD54-mediated sub-pathway of homologous recombination to cellular survival in response to UV irradiation. However, the core homologous recombination reaction does contribute to cell viability since just a mild down regulation of RAD51 using siRNA led to UV-light hypersensitivity of U2Os cells (Figure 5C and D), indicating a role of RAD51 and therefore homologous recombination in repair or bypass of UV-light induced lesions.

In addition to NER and homologous recombination, translesion DNA synthesis (TLS) provides a mechanism to navigate UV-induced DNA damage, particularly through the TLS DNA polymerase  $\eta$  (Pol $\eta$ ) [30]. To test the interplay between RAD54- and RAD51-mediated homologous recombination and Pol $\eta$ -mediated TLS in the cellular response to UV irradiation, U2Os cells were treated with siRNA against Pol $\eta$ , RAD51 or RAD54 and their combination, after which the clonogenic survival of the cells in response to UV-light was measured (Figure 5C and D). Both the absence of RAD54 and Pol $\eta$  did not lead to hypersensitivity to UV-light as reported earlier [69-73]. The combined lack of both RAD54 and Pol $\eta$  however led to an increased sensitivity for UV-light and the combination of both RAD51 and Pol $\eta$  led to an even further increase in sensitivity to UV-light (Figure 5C and D). Thus, our data reveal that in response to UV irradiation, cells employ both RAD54-dependent and -independent homologous recombination pathways and problems due to the absence TLS Pol $\eta$  that can lead to cell killing can be overcome by the action of RAD54 and RAD51.

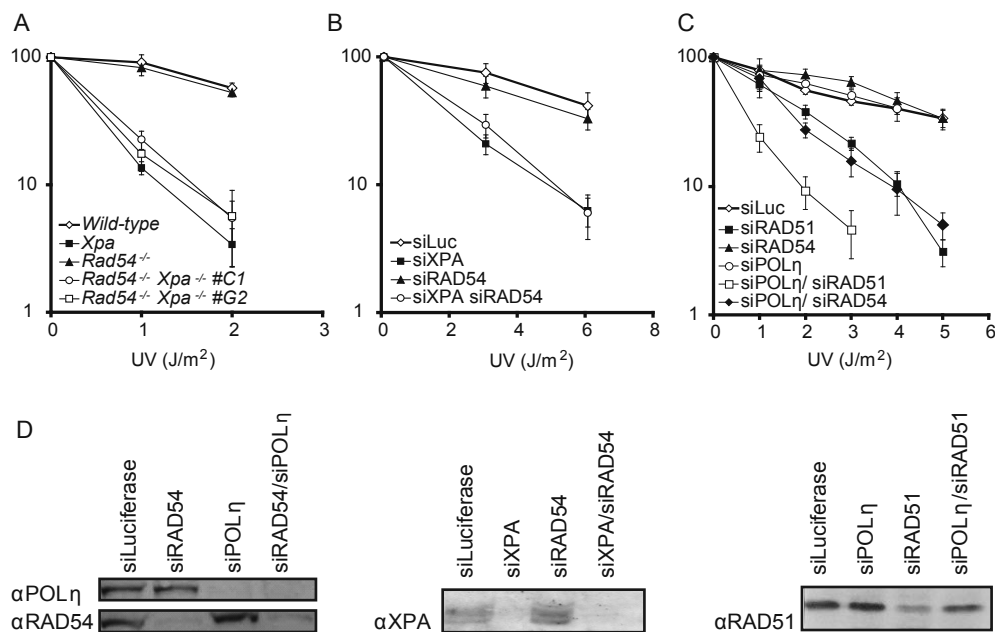


**Figure 5. Homologous recombination affects cell survival in response to UV-induced DNA damage.** (A) Relative cloning efficiency of wild-type (rhombus), Xpa<sup>-/-</sup> (filled square), Rad54<sup>-/-</sup> (filled triangle) and Xpa<sup>-/-</sup> Rad54<sup>-/-</sup> #C1 (open round) and #G2 (open square) mouse ES cell after irradiation with UV-light. (B) Relative cloning efficiency of U2Os cells transfected with siRNA directed against luciferase (rhombus), XPA (filled square), RAD54 (filled triangle), and both XPA and RAD54 (open round) and irradiated with the indicated dose of UV-light. (C) Relative cloning efficiency of U2Os cells transfected with siRNA directed against luciferase (open rhombus), RAD51 (closed square), RAD54 (closed triangle), Polη (open round), Polη and RAD51 (open square) or Polη and RAD54 (closed rhombus) and irradiated with the indicated dose of UV-light. Error bars represent the SEM. (D) shows the reduction of XPA, RAD54, RAD51 and Polη protein levels in U2Os cells transfected with siRNA directed against the corresponding protein as detected by immuno blotting.

## Discussion

It has been well established that the homologous recombination proteins RAD54 and RAD51 are important for the repair of IR-induced DSBs in mouse ES cells [46, 64]. In response to IR-, but not UV-induced DNA damage the majority of cells in a population accumulate RAD54 and RAD51 in foci at the sites of DNA damage [74]. Here we show that in the absence of NER, UV-light induces a vigorous response of the homologous recombination proteins resulting in their relocalization into foci near sites of replication in the majority of cells. We demonstrate at the replication fork level that homologous recombination activity is important in mammalian stem cells for the continuation of DNA

replication after induction of DNA damage by UV-light in NER-deficient cells. The attenuation of homologous recombination under these conditions results in an increase of DSBs correlating with an increase in chromosomal aberrations. Furthermore, our data reveal RAD54-dependent and -independent contributions of homologous recombination to the cellular sensitivity to UV-light and they uncover that RAD54 can compensate for the loss of TLS Pol $\eta$  with regard to UV-light sensitivity.

To monitor homologous recombination in response to UV-light at the cellular level we took advantage of a specific feature of many homologous recombination proteins; their accumulation into foci at sites of DNA damage [25, 26]. For example, RAD51 and RAD54 accumulate and colocalize in foci upon treatment of cells with IR [9, 25, 27]. These foci are biologically relevant because cell lines defective in RAD51 and RAD54 focus formation, such as BRCA2 or RAD51 paralog mutants, are defective in homologous recombination, show spontaneous chromosomal instability and increased sensitivity to IR and the interstrand DNA crosslinker mitomycin C [27, 75]. These features imply that DNA damage induced foci are functional markers for homologous recombination. To visualize RAD54 foci in live cells, we generated mouse ES cells containing a *Rad54*<sup>GFP</sup> knockin allele. This allele expresses a fully biologically active RAD54-GFP fusion protein at endogenous protein expression levels (Supplementary Figure 1) and enables monitoring of foci at a low DNA damage load. When NER is inactivated through the inactivation of XPA, the amount of RAD54 foci is substantially increased after a low dose of UV-light indicating the presence of substantially more DNA substrates for homologous recombination (Figure 1). The induced RAD54 foci colocalize with RAD51 (Figure 2D) and are frequently located close to the nuclear periphery, indicative of sites of DNA replication (Figure 2A). Indeed, the homologous recombination foci colocalize with active sites of replication, as marked by PCNA and nucleotide incorporation (Figure 2).

These observations prompted us to examine the effects of homologous recombination at replication forks in more detail. Analysis of individual sites of replication along single chromosomal fibers shows that homologous recombination activity is important for the continuation of DNA replication after induction of DNA damage by UV-light in NER-deficient mammalian cells (Figure 3). We find an increase of stalled replication sites on a continuous stretch of intact DNA fibers. This is an important result because this means that homologous recombination can act on a template lacking DSBs implicating a form of single-stranded gap recombination. This may be the mammalian analog of the RecFOR-mediated homologous recombination pathway in *E. coli*, which promotes template switching to bypass a lesion obstructing the replication fork and mediates restart of replication [36]. Our chromosomal aberration data are consistent with action of homologous recombination at sites other than DSBs, because they reveal a persistence of single-stranded gaps in metaphase chromosomes (Figure 4C). These single-stranded gaps can arise from stalling of replication and the continuous unwinding of the DNA helix by the replicative helicase, due to uncoupling of the replicative polymerase and helicase [76-78].

In addition to single-stranded gaps, RNA expression profiling experiments suggest that UV-light induced cyclobutylpyrimidine dimers in DNA trigger DSBs [66]. Indeed, our PFGE experiments reveal physical evidence for UV-light induced DSBs (Figure 4A and B). UV-light induces DSBs to similar levels in wild-type, NER-deficient (*Xpa*<sup>-/-</sup>) and homologous recombination-deficient (*Rad54*<sup>-/-</sup>) cells. However, in case of a higher damage load on the replication fork under NER deficient conditions the necessity for homologous recombination becomes clear, as significantly more DSBs arise in *Xpa*<sup>-/-</sup> *Rad54*<sup>-/-</sup> double mutant cells. Similarly, more chromosomal breaks can be observed in metaphase spreads from *Xpa*<sup>-/-</sup> *Rad54*<sup>-/-</sup> cells (Figure 4D). Taken together, these data reveal the functionality of RAD54 at sites of replication when cells are stressed by UV-light.

Even though the absence of RAD54 results in more UV-light induced gaps and breaks at chromosomal level when NER is defective (Figure 4C and D), this does not result in increased sensitivity to UV-light in clonogenic survival assays (Figure 5A and B). The observation that a mutation in a protein involved in metabolism of UV-induced DNA damage does not lead to UV sensitivity is not unprecedented, since cells from XP-V patients, defective in the TLS Polη, are not UV sensitive [71]. In case of RAD54, this might be caused by the fact that these aberrations are present at a very low level and RAD54 likely acts in a specific sub-pathway of homologous recombination that is not essential for cell viability [64]. In contrast, homologous recombination overall is essential for viability of mammalian cells because absence of RAD51, the core protein during DNA strand exchange, results in early embryonic lethality [3, 4]. Thus, even though RAD54 foci are a convenient marker for locations in the cell where homologous recombination is active, the RAD54 protein does not necessarily always functionally participate in it. Nevertheless, our data confirm the importance of RAD51-mediated homologous recombination, since mild RNAi induced reduction of RAD51 results in sensitivity to UV-light (Figure 5C), which therefore reveals the existence of a RAD54-independent homologous recombination sub-pathway.

The results described above suggest that there are at least two pathways involving homologous recombination that help the cell to successfully navigate UV-induced DNA damage, single-stranded gap and double-stranded break induced homologous recombination. This is not surprising because the flexibility of homologous recombination provides multiple ways to rearrange DNA strands at stalled DNA replication forks. Alternatively, although not mutually exclusive, UV-light might induce different DNA substrates that require different homologous recombination sub-pathways for their repair. Our data is consistent with both pathways being dependent on the core homologous recombination protein RAD51 and on RAD54. This correlates with the involvement of RAD54 in repair of DSBs that do not necessarily arise in the context of replication [79]. The contribution of RAD54-dependent homologous recombination to UV-lesion resistance is minor as its effect can be measured in some assays, such as DSB formation and chromosomal aberrations (Figure 4), but not in clonogenic survival in response to UV-light, an assay that does demonstrate the involvement of RAD51 (Figure 5).

We next considered whether TLS can be an alternative to the homologous recombination based pathways for tolerating UV-light induced DNA damage. Our data from siRNA experiments presented in Figure 5 support this notion. Down regulation of TLS Pol $\eta$  or RAD54 does not lead to UV-light sensitivity, while down regulation of RAD51 causes an intermediate sensitivity to UV-light. Interestingly, simultaneous down regulation of Pol $\eta$  and RAD54 results in an intermediate UV-light sensitivity, thus unmasking the contribution of both RAD54 and Pol $\eta$  to cellular survival to UV-light in a clonogenic survival assay. Down regulation of Pol $\eta$  and RAD51 triggers the greatest UV-light sensitivity. Taken together, our results are consistent with the existence of at least three routes through which the cells can tolerate UV-induced DNA damage; Pol $\eta$ -dependent TLS and RAD54-dependent and -independent RAD51-mediated homologous recombination.

The discovery that the double, but not single, deficiency in RAD54-dependent homologous recombination and Pol $\eta$ -mediated TLS results in UV sensitivity fits with the observation that XPV cells are sensitive to UV-light only in combination with caffeine, which inhibits among others, the ATM kinase, which has been placed in a pathway with RAD54 [69-72, 80]. A possible explanation for this effect can be a scenario where TLS does not act directly at the fork but rather occurs behind the fork on single-stranded gaps left opposite lesions while the replication fork proceeds. There is ample evidence that UV-induced TLS does indeed occur behind the fork [81]. If Pol $\eta$ -mediated TLS fails, the single-stranded DNA gaps may become prone to breakage. Either these single-stranded DNA gaps or the resulting DSBs can be substrates for a RAD54-dependent mode of homologous recombination. Cellular survival in response to UV irradiation will only be affected when both processes fail.

In conclusion, we have provided evidence showing that homologous recombination is important for the progression of replication forks hindered by UV-induced DNA damage. Our experiments reveal that the cellular response of mammalian stem cells to UV irradiation comprises at least two genetically distinct sub-pathways homologous recombination, one dependent and one independent of RAD54. Furthermore, RAD54-dependent homologous recombination can provide resistance to UV-induced cell killing when the function of TLS Pol $\eta$  is compromised.

## Experimental Procedures

**DNA constructs.** A *Rad54-GFP* knock-in construct was designed to obtain expression of tagged *Rad54* from the endogenous promoter upon homologous integration. This construct was generated by fusing exons 4-18 of the *hRAD54* cDNA, but with the omission of the STOP codon, to a 3'-terminal *GFP* tag, followed by a poly(A) signal and a phosphoglycerate kinase (PGK) promoter driven puromycin selectable marker gene. This fragment was subcloned into exon 4 of a 9-kb *Eco* RI genomic *Rad54* fragment. Using linkers, a downstream *Sfu* I site was introduced. Digestion of this construct with *Sfu* I yielded a fragment containing the 3'-terminal part of the *Rad54-GFP* cDNA spanning exons 4 to 18

and the puromycin gene. This fragment was subcloned into the unique *Sfu* I site in exon 4 of a 9-kb *Eco* RI fragment of the mouse *Rad54* genomic sequence containing exons 4–7 in pBluescript II KS. The construct is schematically depicted in Figure S1A.

**Antibodies.** Mouse anti-GFP was obtained from Roche. The RAD51 protein was detected with rabbit polyclonal anti-RAD51 immunoglobulin [9, 82]. To detect  $\gamma$ -H2AX rabbit polyclonal anti- $\gamma$ -H2AX immunoglobulin (Upstate Biotechnologies) was used. DNA polymerase  $\eta$  was detected by rabbit polyclonal antibody (ab17725) from Abcam. Rabbit anti-hORC2 (#559266) and mouse anti-GRB2 (#610112) were obtained from BD Pharmingen. Rabbit polyclonal anti-53BP1 (#NB100-304) was obtained from Novus Biochemicals. XPA (#FL-273) rabbit polyclonal antibody and the RAD54 (D-18) goat polyclonal antibody were obtained from Santa Cruz Biotechnology.

**Cell culture and gene targeting.** ES cells were cultured on gelatin-coated dishes in a 1:1 mixture of Dulbecco's modified Eagle's medium (DMEM) and buffalo rat liver (BRL) conditioned medium, supplemented with 10% (v/v) FBS (Hyclone), 0.1 mM nonessential amino acids (Biowhittaker), 50 mM  $\beta$ -mercaptoethanol (Sigma) and 500 U ml<sup>-1</sup> leukemia inhibitory factor. U2Os cells were cultured in a 1:1 mixture of DMEM and Ham's F10, supplemented with 10% (v/v) fetal calf serum (HyClone) and streptomycin/penicillin, at 37°C in an atmosphere containing 5% CO<sub>2</sub>. In case of depletion of RAD51, U2Os cells were grown at 3% O<sub>2</sub>.

**SiRNA-mediated down regulation in U2Os cells.** Transfection of siRNA duplexes was carried out using Lipofectamine 2000 (Invitrogen) according to the manufacturer's instructions. U2Os cells were seeded on 60 mm dishes. When their confluency reached 20–30%, cultures were transfected with 200 pmoles of siRNA and 10  $\mu$ l of liposomes per dish. After 48 hrs transfected cells were used for colony survival assays. Sense sequence of the *Xpa*-directed siRNA was (CUGAUGAUAAACACAAGCUUAUU), the sense sequence directed against *Rad51* was (GAGCUUGACAAACUACUUCUU), the sense sequence of *Rad54*-directed siRNAs was (GAACUCCCAUCCAGAAUGAUU) and the sense sequence directed against polymerase  $\eta$  was (UAAACCUUGUGCAGUUGUATT) [73]. The sense sequence of luciferase-directed siRNA was (CGUACGCGGAUACUUCGAdTdT). Whole cells extracts were prepared by lysing cells with SDS sample buffer 48 hrs after transfection. Down regulation was monitored by immunoblotting. Equal loading of proteins was verified by probing for hORC2 or GRB2.

**Colony survival assays.** Sensitivity of ES cells to increasing doses of DNA damaging agents was determined as described previously [64]. Briefly, cells were plated in 6 cm dishes, at various dilutions. After 8–16 hrs, cells were irradiated with a single dose in the range of either 0–6 J/m<sup>2</sup> of UV-C (254 nm) or 0–8 Gy of IR. Subsequently, cells were grown for 7–10

days, fixed, stained and colonies were counted. All experiments were performed in triplicate.

**Immunoblotting.** Cells were directly lysed with SDS sample buffer (2% SDS, 10% glycerol, 60 mM Tris-HCl (pH 6.8)). After the protein concentration was determined by the Lowry protein assay, extracts were supplemented with 0.5%  $\beta$ -mercaptoethanol and 0.02% bromophenol blue. Equal loading of proteins was independently verified by probing with anti-hORC2. After fractionation by SDS-PAGE, proteins were transferred to a nitrocellulose membrane. The blots were blocked with PBS containing 5% skimmed milk and 0.1% Tween 20 and probed with primary antibodies. After washing with PBS containing 0.1% Tween 20, the membranes were probed with the relevant horseradish peroxidase-conjugated secondary antibodies (Jackson ImmunoResearch), and developed with ECL Western blotting detection reagents (AmershamBiosciences).

**Immunofluorescence and confocal microscopy imaging.** Cells were trypsinized and seeded at approximately 25% confluency on glass coverslips coated with 0.1% gelatin. Twenty-four hrs later, the cells were irradiated with 12 Gy of IR or 1 J/m<sup>2</sup> of UV-C (254 nm). Afterwards, cells were washed and incubated in fresh medium at 37°C for 2 hrs and then fixed with 2% *para*-formaldehyde in PBS, pH 7.4, for 15 min. Cells were permeabilized with 0.1% Triton X-100 in PBS. For visualization of the immuno-conjugated proteins, Alexa 594-conjugated goat anti-rabbit immunoglobulin (Molecular Probes) was applied in both cases. All immunoglobulins were diluted in PBS containing 0.15% glycine and 0.5% bovine serum albumin. Nuclear staining patterns were visualized with a Zeiss confocal laser scanning microscope LSM 510 META. Images were recorded with a 488 nm Ar-laser to detect RAD54-GFP and 543 nm HeNe-laser to detect the immunostained proteins.

**Replication labeling and DNA fiber spreads.** To investigate the efficiency of replication fork restart after UV-induced DNA damage the cells were pulsed with 50  $\mu$ M IdU for 15 min. Cells were irradiated with 80 J/m<sup>2</sup> and incubated with medium containing 50  $\mu$ M thymidine which was added for 15 min. The cells were subsequently kept in fresh medium before labeling with 50  $\mu$ M CldU for 15 min after indicated incubation times. The non-treated cells were first pulsed with 50  $\mu$ M IdU for 15 min and subsequently labeled with 50  $\mu$ M CldU for 15 min. For DNA spreads, the cells were trypsinized and resuspended in ice-cold PBS at  $2.5 \times 10^5$  cells/ml. The labeled cells were diluted 1:8 with unlabeled cells, and 2.5  $\mu$ l of cells were mixed with 7.5  $\mu$ l of spreading buffer (0.5% SDS in 200 mM Tris-HCl, pH 7.4, 50 mM EDTA) on a glass slide. After 9 min the slides were tilted at a 15° angle, and the resulting DNA spreads were air-dried, fixed in 3:1 methanol/acetic acid, and refrigerated overnight. The slides were treated with 2.5 M HCl for 1 hr, neutralized with 0.1 M Na<sub>2</sub>B<sub>4</sub>O<sub>7</sub>, pH 8.5 for 7 min, washed in PBS, and were blocked in 1% bovine serum albumin, 0.1% Tween 20 for 20 min. To detect CldU, the slides were incubated for 1 hr at 37°C with rat anti-bromodeoxyuridine antibody (Abcam). Subsequently, after washing with PBS

containing 0.1% Tween 20, the incorporated CldU was identified by Alexafluor 488-conjugated anti-rat antibody (Molecular Probes). Following washing with PBS containing 0.1% Tween 20 and blocking for 20 min, the mouse anti-bromodeoxyuridine antibody to detect IdU (Becton Dickinson) was applied for 1 hr at 37°C. In order to increase discrimination between the two nucleotide analogues using these antibodies, slides were washed with high salt buffer (0.5 M NaCl, 0.3 M Tris-HCl, 0.5 % Tween 20) for 7 min at room temperature. Slides were then rinsed in PBS containing 0.1% Tween 20, and incubated with Cy3-conjugated anti-mouse antibody (Sigma) for 45 min at 37°C. Finally, slides were washed in PBS containing 0.1% Tween 20 and mounted in Vectashield without DAPI. Images were collected using a Zeiss LSM Meta 510 confocal microscope. Experiments were performed in triplicate.

**Pulsed-field gel electrophoresis.** Sub confluent cultures of cycling ES cells were treated with 10 J/m<sup>2</sup> UV-light. After 2 hrs cells were harvested by trypsinization, and agarose plugs of 10<sup>6</sup> cells were prepared with a CHEF disposable plug mold (BioRad). The plugs were incubated in lyses buffer (100 mM EDTA, 1% (w/v) sodium lauryl sarcosine, 0.2% (w/v) sodium deoxycholate, 1 mg ml<sup>-1</sup> proteinase K) at 37 °C for 48 hrs and washed four times in TE buffer (20 mM Tris-HCl (pH 8.0), 50 mM EDTA) before loading them onto an agarose gel. Electrophoresis was performed for 23 hrs at 13 °C in 0.9% (w/v) agarose containing 0.25x TBE (22.5 mM Tris-HCl (pH 8.0), 22.5 mM Boric Acid and 0.5 mM EDTA) using a Biometra Rotaphor apparatus with the following parameters: voltage 180–120 V log; angle from 120° to 110° linear; interval 30 s to 5 s log. Under the electrophoresis conditions used, high-molecular weight genomic DNA (more than several million base pairs (bp)) remains in the well, whereas lower-molecular weight DNA fragments (several Mbp to 500 kbp) migrate into the gel and are compacted into a single band. *S. cerevisiae* chromosomes were run in parallel as molecular size markers. The gel was stained with ethidium bromide and analyzed using a Typhoon 9200 scanner (Amersham). Band intensities were quantified using ImageQuant 5.2 software (GE Healthcare). The amount of broken DNA was calculated as the intensity of DNA in the migrated fraction of the mutated samples compared to that of the non-treated wild-type cells, which was set at 1.

**Analysis of chromosomal aberrations in metaphase chromosomes.** Wild-type (C57Bl/6) and mutant (*Rad54*<sup>-/-</sup>, *Xpa*<sup>-/-</sup> and *Rad54*<sup>-/-</sup> *Xpa*<sup>-/-</sup> clone G2) murine ES cells were exposed to increasing doses of UV-light. Twenty-four hrs after treatment pre-warmed (37°C) Colcemid (10 µg/ml) was added for 15 min. Cells were washed with PBS, trypsinized and centrifuged for 5 min at 1000 rpm. Next, cells were resuspended in pre-warmed hypotonic solution (0.075 M KCl), immediately centrifuged, resuspended once more in hypotonic solution (room temperature), centrifuged again and fixed three times in fresh acetic acid/methanol (3:1, room temperature). Microscope slides were prepared by placing the suspension on a glass slide followed by drying with air and staining with Atrabrine. Chromosomes were visualized using a microscope and structural chromosomal aberrations

were analyzed by eye. The number of aberrations per metaphase was counted, and the aberrations were classified as chromatid or chromosome aberrations. Ten metaphases per cell line were analyzed for the number of chromosomes and 60 for the presence of DNA structural aberrations.

## Acknowledgments

This work was supported by the Netherlands Genomics Initiative/Netherlands Organization for Scientific Research (NWO) and the Dutch Cancer Society (KWF).

## References

1. Flores-Rozas, H. and R.D. Kolodner, *Links between replication, recombination and genome instability in eukaryotes*. Trends Biochem Sci, 2000. **25**(4): p. 196-200.
2. van Gent, D.C., J.H. Hoeijmakers, and R. Kanaar, *Chromosomal stability and the DNA double-stranded break connection*. Nat Rev Genet, 2001. **2**(3): p. 196-206.
3. Lim, D.S. and P. Hasty, *A mutation in mouse rad51 results in an early embryonic lethal that is suppressed by a mutation in p53*. Mol Cell Biol, 1996. **16**(12): p. 7133-43.
4. Tsuzuki, T., et al., *Targeted disruption of the Rad51 gene leads to lethality in embryonic mice*. Proc Natl Acad Sci U S A, 1996. **93**(13): p. 6236-40.
5. Sung, P., et al., *Rad51 recombinase and recombination mediators*. J Biol Chem, 2003. **278**(44): p. 42729-32.
6. Johnson, R.D. and M. Jasin, *Double-strand-break-induced homologous recombination in mammalian cells*. Biochem Soc Trans, 2001. **29**(Pt 2): p. 196-201.
7. Krogh, B.O. and L.S. Symington, *Recombination proteins in yeast*. Annu Rev Genet, 2004. **38**: p. 233-71.
8. Paques, F. and J.E. Haber, *Multiple pathways of recombination induced by double-strand breaks in Saccharomyces cerevisiae*. Microbiol Mol Biol Rev, 1999. **63**(2): p. 349-404.
9. Tan, T.L., et al., *Mouse Rad54 affects DNA conformation and DNA-damage-induced Rad51 foci formation*. Curr Biol, 1999. **9**(6): p. 325-8.
10. Heyer, W.D., et al., *Rad54: the Swiss Army knife of homologous recombination?* Nucleic Acids Res, 2006. **34**(15): p. 4115-25.
11. Clever, B., et al., *Recombinational repair in yeast: functional interactions between Rad51 and Rad54 proteins*. Embo J, 1997. **16**(9): p. 2535-44.
12. Golub, E.I., et al., *Interaction of human recombination proteins Rad51 and Rad54*. Nucleic Acids Res, 1997. **25**(20): p. 4106-10.
13. Van Komen, S., et al., *Superhelicity-driven homologous DNA pairing by yeast recombination factors Rad51 and Rad54*. Mol Cell, 2000. **6**(3): p. 563-72.
14. Amitani, I., R.J. Baskin, and S.C. Kowalczykowski, *Visualization of Rad54, a chromatin remodeling protein, translocating on single DNA molecules*. Mol Cell, 2006. **23**(1): p. 143-8.

15. Bugreev, D.V., O.M. Mazina, and A.V. Mazin, *Rad54 protein promotes branch migration of Holliday junctions*. Nature, 2006. **442**(7102): p. 590-3.
16. Ristic, D., et al., *The architecture of the human Rad54-DNA complex provides evidence for protein translocation along DNA*. Proc Natl Acad Sci U S A, 2001. **98**(15): p. 8454-60.
17. Tan, T.L., R. Kanaar, and C. Wyman, *Rad54, a Jack of all trades in homologous recombination*. DNA Repair (Amst), 2003. **2**(7): p. 787-94.
18. Solinger, J.A., K. Kiianitsa, and W.D. Heyer, *Rad54, a Swi2/Snf2-like recombinational repair protein, disassembles Rad51:dsDNA filaments*. Mol Cell, 2002. **10**(5): p. 1175-88.
19. Alexeev, A., A. Mazin, and S.C. Kowalczykowski, *Rad54 protein possesses chromatin-remodeling activity stimulated by the Rad51-ssDNA nucleoprotein filament*. Nat Struct Biol, 2003. **10**(3): p. 182-6.
20. Alexiadis, V. and J.T. Kadonaga, *Strand pairing by Rad54 and Rad51 is enhanced by chromatin*. Genes Dev, 2002. **16**(21): p. 2767-71.
21. Jaskelioff, M., et al., *Rad54p is a chromatin remodeling enzyme required for heteroduplex DNA joint formation with chromatin*. J Biol Chem, 2003. **278**(11): p. 9212-8.
22. Mazin, A.V., et al., *Rad54 protein is targeted to pairing loci by the Rad51 nucleoprotein filament*. Mol Cell, 2000. **6**(3): p. 583-92.
23. Solinger, J.A., et al., *Rad54 protein stimulates heteroduplex DNA formation in the synaptic phase of DNA strand exchange via specific interactions with the presynaptic Rad51 nucleoprotein filament*. J Mol Biol, 2001. **307**(5): p. 1207-21.
24. Li, X., et al., *PCNA is required for initiation of recombination-associated DNA synthesis by DNA polymerase delta*. Mol Cell, 2009. **36**(4): p. 704-13.
25. Essers, J., et al., *Nuclear dynamics of RAD52 group homologous recombination proteins in response to DNA damage*. Embo J, 2002. **21**(8): p. 2030-7.
26. Tashiro, S., et al., *Rad51 accumulation at sites of DNA damage and in postreplicative chromatin*. J Cell Biol, 2000. **150**(2): p. 283-91.
27. van Veelen, L.R., et al., *Ionizing radiation-induced foci formation of mammalian Rad51 and Rad54 depends on the Rad51 paralogs, but not on Rad52*. Mutat Res, 2005. **574**(1-2): p. 34-49.
28. Hakem, R., *DNA-damage repair; the good, the bad, and the ugly*. Embo J, 2008. **27**(4): p. 589-605.
29. Hoeijmakers, J.H., *Genome maintenance mechanisms for preventing cancer*. Nature, 2001. **411**(6835): p. 366-74.
30. Lehmann, A.R., *Replication of damaged DNA by translesion synthesis in human cells*. FEBS Lett, 2005. **579**(4): p. 873-6.
31. Johnson, R.E., et al., *hRAD30 mutations in the variant form of xeroderma pigmentosum*. Science, 1999. **285**(5425): p. 263-5.
32. Masutani, C., et al., *The XPV (xeroderma pigmentosum variant) gene encodes human DNA polymerase eta*. Nature, 1999. **399**(6737): p. 700-4.

33. Cordonnier, A.M., A.R. Lehmann, and R.P. Fuchs, *Impaired translesion synthesis in xeroderma pigmentosum variant extracts*. Mol Cell Biol, 1999. **19**(3): p. 2206-11.
34. Wyman, C. and R. Kanaar, *DNA double-strand break repair: all's well that ends well*. Annu Rev Genet, 2006. **40**: p. 363-83.
35. Llorente, B., C.E. Smith, and L.S. Symington, *Break-induced replication: what is it and what is it for?* Cell Cycle, 2008. **7**(7): p. 859-64.
36. Cox, M.M., et al., *The importance of repairing stalled replication forks*. Nature, 2000. **404**(6773): p. 37-41.
37. Budzowska, M. and R. Kanaar, *Mechanisms of dealing with DNA damage-induced replication problems*. Cell Biochem Biophys, 2009. **53**(1): p. 17-31.
38. Saleh-Gohari, N. and T. Helleday, *Conservative homologous recombination preferentially repairs DNA double-strand breaks in the S phase of the cell cycle in human cells*. Nucleic Acids Res, 2004. **32**(12): p. 3683-8.
39. Helleday, T., *Pathways for mitotic homologous recombination in mammalian cells*. Mutat Res, 2003. **532**(1-2): p. 103-15.
40. Lundin, C., et al., *RAD51 is involved in repair of damage associated with DNA replication in mammalian cells*. J Mol Biol, 2003. **328**(3): p. 521-35.
41. Mohindra, A., et al., *A tumour-derived mutant allele of XRCC2 preferentially suppresses homologous recombination at DNA replication forks*. Hum Mol Genet, 2004. **13**(2): p. 203-12.
42. Saleh-Gohari, N., et al., *Spontaneous homologous recombination is induced by collapsed replication forks that are caused by endogenous DNA single-strand breaks*. Mol Cell Biol, 2005. **25**(16): p. 7158-69.
43. Lopes, M., M. Foiani, and J.M. Sogo, *Multiple mechanisms control chromosome integrity after replication fork uncoupling and restart at irreparable UV lesions*. Mol Cell, 2006. **21**(1): p. 15-27.
44. Davis, A.P. and L.S. Symington, *RAD51-dependent break-induced replication in yeast*. Mol Cell Biol, 2004. **24**(6): p. 2344-51.
45. Malkova, A., E.L. Ivanov, and J.E. Haber, *Double-strand break repair in the absence of RAD51 in yeast: a possible role for break-induced DNA replication*. Proc Natl Acad Sci U S A, 1996. **93**(14): p. 7131-6.
46. Sonoda, E., et al., *Rad51-deficient vertebrate cells accumulate chromosomal breaks prior to cell death*. Embo J, 1998. **17**(2): p. 598-608.
47. Seigneur, M., S.D. Ehrlich, and B. Michel, *RuvABC-dependent double-strand breaks in dnaBts mutants require recA*. Mol Microbiol, 2000. **38**(3): p. 565-74.
48. Benson, F.E., P. Baumann, and S.C. West, *Synergistic actions of Rad51 and Rad52 in recombination and DNA repair*. Nature, 1998. **391**(6665): p. 401-4.
49. Shinohara, A. and T. Ogawa, *Stimulation by Rad52 of yeast Rad51-mediated recombination*. Nature, 1998. **391**(6665): p. 404-7.
50. New, J.H., et al., *Rad52 protein stimulates DNA strand exchange by Rad51 and replication protein A*. Nature, 1998. **391**(6665): p. 407-10.

51. Sung, P., *Function of yeast Rad52 protein as a mediator between replication protein A and the Rad51 recombinase*. J Biol Chem, 1997. **272**(45): p. 28194-7.
52. Sugawara, N., X. Wang, and J.E. Haber, *In vivo roles of Rad52, Rad54, and Rad55 proteins in Rad51-mediated recombination*. Mol Cell, 2003. **12**(1): p. 209-19.
53. Bravo, R. and H. Macdonald-Bravo, *Changes in the nuclear distribution of cyclin (PCNA) but not its synthesis depend on DNA replication*. Embo J, 1985. **4**(3): p. 655-61.
54. Celis, J.E. and A. Celis, *Cell cycle-dependent variations in the distribution of the nuclear protein cyclin proliferating cell nuclear antigen in cultured cells: subdivision of S phase*. Proc Natl Acad Sci U S A, 1985. **82**(10): p. 3262-6.
55. Essers, J., et al., *Dynamics of relative chromosome position during the cell cycle*. Mol Biol Cell, 2005. **16**(2): p. 769-75.
56. Essers, J., et al., *Nuclear dynamics of PCNA in DNA replication and repair*. Mol Cell Biol, 2005. **25**(21): p. 9350-9.
57. Leonhardt, H., et al., *Dynamics of DNA replication factories in living cells*. J Cell Biol, 2000. **149**(2): p. 271-80.
58. Prelich, G., et al., *The cell-cycle regulated proliferating cell nuclear antigen is required for SV40 DNA replication in vitro*. Nature, 1987. **326**(6112): p. 471-5.
59. Herrick, J. and A. Bensimon, *Single molecule analysis of DNA replication*. Biochimie, 1999. **81**(8-9): p. 859-71.
60. Lebofsky, R. and A. Bensimon, *DNA replication origin plasticity and perturbed fork progression in human inverted repeats*. Mol Cell Biol, 2005. **25**(15): p. 6789-97.
61. Merrick, C.J., D. Jackson, and J.F. Diffley, *Visualization of altered replication dynamics after DNA damage in human cells*. J Biol Chem, 2004. **279**(19): p. 20067-75.
62. Rassool, F.V., et al., *Constitutive DNA damage is linked to DNA replication abnormalities in Bloom's syndrome cells*. Oncogene, 2003. **22**(54): p. 8749-57.
63. Hanada, K., et al., *The structure-specific endonuclease Mus81 contributes to replication restart by generating double-strand DNA breaks*. Nat Struct Mol Biol, 2007. **14**(11): p. 1096-104.
64. Essers, J., et al., *Disruption of mouse RAD54 reduces ionizing radiation resistance and homologous recombination*. Cell, 1997. **89**(2): p. 195-204.
65. de Waard, H., et al., *Cell type-specific hypersensitivity to oxidative damage in CSB and XPA mice*. DNA Repair (Amst), 2003. **2**(1): p. 13-25.
66. Garinis, G.A., et al., *Transcriptome analysis reveals cyclobutane pyrimidine dimers as a major source of UV-induced DNA breaks*. Embo J, 2005. **24**(22): p. 3952-62.
67. Eki, T., et al., *Characterization of chromosome aberrations induced by incubation at a restrictive temperature in the mouse temperature-sensitive mutant tsFT20 strain containing heat-labile DNA polymerase alpha*. Cancer Res, 1987. **47**(19): p. 5162-70.
68. Budzowska, M., et al., *Mutation of the mouse Rad17 gene leads to embryonic lethality and reveals a role in DNA damage-dependent recombination*. Embo J, 2004. **23**(17): p. 3548-58.

69. Broughton, B.C., et al., *Molecular analysis of mutations in DNA polymerase eta in xeroderma pigmentosum-variant patients*. Proc Natl Acad Sci U S A, 2002. **99**(2): p. 815-20.
70. Fujiwara, Y., et al., *A mechanism for relief of replication blocks by activation of unused origins and age-dependent change in the caffeine susceptibility in xeroderma pigmentosum variant*. Mutat Res, 1991. **254**(1): p. 79-87.
71. Lehmann, A.R., et al., *Xeroderma pigmentosum cells with normal levels of excision repair have a defect in DNA synthesis after UV-irradiation*. Proc Natl Acad Sci U S A, 1975. **72**(1): p. 219-23.
72. Cleaver, J.E., *Caffeine toxicity is inversely related to DNA repair in simian virus 40-transformed xeroderma pigmentosum cells irradiated with ultraviolet light*. Teratog Carcinog Mutagen, 1989. **9**(3): p. 147-55.
73. Choi, J.H. and G.P. Pfeifer, *The role of DNA polymerase eta in UV mutational spectra*. DNA Repair (Amst), 2005. **4**(2): p. 211-20.
74. Essers, J., A.B. Houtsmuller, and R. Kanaar, *Analysis of DNA recombination and repair proteins in living cells by photobleaching microscopy*. Methods Enzymol, 2006. **408**: p. 463-85.
75. Thacker, J., *The RAD51 gene family, genetic instability and cancer*. Cancer Lett, 2005. **219**(2): p. 125-35.
76. Pacek, M. and J.C. Walter, *A requirement for MCM7 and Cdc45 in chromosome unwinding during eukaryotic DNA replication*. Embo J, 2004. **23**(18): p. 3667-76.
77. Byun, T.S., et al., *Functional uncoupling of MCM helicase and DNA polymerase activities activates the ATR-dependent checkpoint*. Genes Dev, 2005. **19**(9): p. 1040-52.
78. Walter, J. and J. Newport, *Initiation of eukaryotic DNA replication: origin unwinding and sequential chromatin association of Cdc45, RPA, and DNA polymerase alpha*. Mol Cell, 2000. **5**(4): p. 617-27.
79. Dronkert, M.L., et al., *Mouse RAD54 affects DNA double-strand break repair and sister chromatid exchange*. Mol Cell Biol, 2000. **20**(9): p. 3147-56.
80. Morrison, C., et al., *The controlling role of ATM in homologous recombinational repair of DNA damage*. Embo J, 2000. **19**(3): p. 463-71.
81. Lehmann, A.R. and R.P. Fuchs, *Gaps and forks in DNA replication: Rediscovering old models*. DNA Repair (Amst), 2006. **5**(12): p. 1495-8.
82. Essers, J., et al., *Analysis of mouse Rad54 expression and its implications for homologous recombination*. DNA Repair (Amst), 2002. **1**(10): p. 779-93.

## Supplementary material

### Generation and characterization of cells expressing a GFP-tagged *Rad54* knock-in allele

We designed a knock-in construct for *Rad54* such that a GFP-tagged RAD54 protein would be expressed from its endogenous locus (Supplemental Figure 1A). This construct was homologously integrated into both wild-type and *Xpa*<sup>-/-</sup> ES cells. Cells that contained one wild type *Rad54* allele (*Rad54*<sup>+</sup>) and one knock-in *Rad54* allele (*Rad54*<sup>+/GFP</sup>) were obtained, and will be referred to as *Rad54*<sup>+/GFP</sup> and *Rad54*<sup>+/GFP</sup> *Xpa*<sup>-/-</sup>. Expression of *Rad54* from the knock-in allele, directed by the endogenous *Rad54* promoter, resulted in the production of RAD54-GFP protein at levels similar to that of the untagged protein (Supplemental Figure 1B). Immunoblotting of whole cell extracts using anti-GFP antibodies demonstrated that only the full-length RAD54-GFP protein was present. Degradation or other protein-GFP fusion products as well as free GFP were absent (Supplemental Figure 1B). Subsequent fluorescence activated cell sorting (FACS) analysis of cells containing the RAD54-GFP knock-in allele showed that the distribution of fluorescent positive cells within the *Rad54*<sup>+/GFP</sup> and *Rad54*<sup>+/GFP</sup> *Xpa*<sup>-/-</sup> cell populations was similar confirming that the RAD54-GFP protein expression levels are comparable in both ES cell lines (data not shown). Furthermore, the Gaussian distribution of fluorescence intensity indicated that the tagged protein is homogeneously expressed in both *Rad54*<sup>+/GFP</sup> and *Rad54*<sup>+/GFP</sup> *Xpa*<sup>-/-</sup> cell populations, and therefore a variegated expression pattern can be excluded.

To test whether *Rad54*<sup>GFP</sup> encodes a functional variant of RAD54, we investigated the ability of the fusion protein to protect cells from the lethal effects of ionizing radiation. For that purpose, we generated a *Rad54*<sup>-GFP</sup> ES cell line by targeting the wild type *Rad54* allele in a *Rad54*<sup>+/+</sup> ES cell line with the *Rad54*<sup>GFP</sup> knock-in construct (data not shown). In the cells having undergone homologous recombination at the wild type locus the knock-in allele is consequently the only source of Rad54 protein. Because ES cells lacking functional RAD54 are hypersensitive to ionising radiation [64], the sensitivity of the obtained *Rad54*<sup>-GFP</sup> ES cell line to ionizing radiation was determined. We compared the ionizing radiation sensitivity of *Rad54*<sup>+/+</sup>, *Rad54*<sup>-/-</sup> and *Rad54*<sup>-GFP</sup> ES cells by measuring their efficiency of colony formation as a function of increasing ionizing radiation doses (Supplemental Figure 1C). *Rad54*<sup>+/+</sup> ES cells and *Rad54*<sup>-GFP</sup> ES displayed equal sensitivity to ionizing radiation and were less sensitive than *Rad54*<sup>-/-</sup> control ES cells. We conclude that the RAD54-GFP protein encoded from the knock-in allele is biologically active.

To exclude the possibility that the presence of GFP-tagged RAD54 in *Rad54*<sup>+/GFP</sup> and *Rad54*<sup>+/GFP</sup> *Xpa*<sup>-/-</sup> ES cells interfered with their sensitivity to UV-light we checked the ability of *Rad54*<sup>+/GFP</sup> and *Rad54*<sup>+/GFP</sup> *Xpa*<sup>-/-</sup> cell lines to form colonies after treatment with increasing doses of UV-light. Wild type and *Rad54*<sup>+/GFP</sup> ES cells were only mildly, and equally, sensitive to increasing doses of UV-light. However, the efficiency of colony formation was severely reduced for both *Xpa*<sup>-/-</sup> and *Rad54*<sup>+/GFP</sup> *Xpa*<sup>-/-</sup> cell lines (Supplemental Figure 1D). Therefore, the presence of the *Rad54* knock-in allele has no influence on the resistance of the analyzed cell lines to UV-light.

# Supplementary references

64. Essers, J., et al., *Disruption of mouse RAD54 reduces ionizing radiation resistance and homologous recombination*. Cell, 1997. **89**(2): p. 195-204.

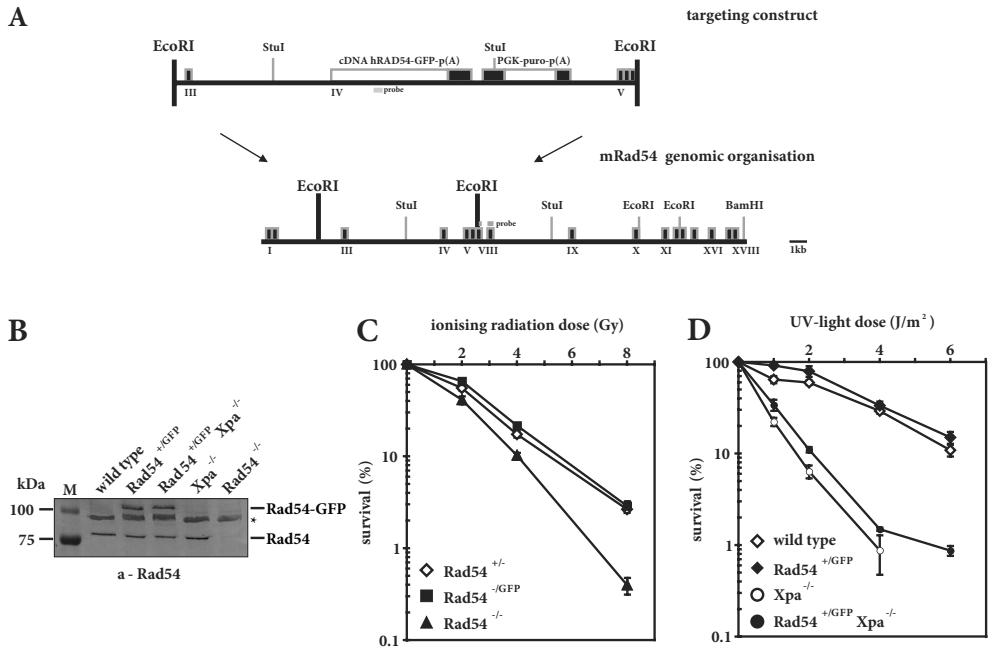


**Figure S1. Generation and characterization of wild-type and *Xpa*<sup>-/-</sup> ES cells expressing RAD54-GFP from the endogenous *Rad54* locus.** (A) *Rad54*-GFP knock-in targeting construct. Structure of the genomic *Rad54* locus and gene targeting construct. The targeting construct (upper line) was generated as described in the Experimental Procedures. The lower line represents the approximately 30 kb mouse *Rad54* genomic locus. All 18 exons of the *Rad54* cDNA are indicated by black boxes. The DNA probe used in blotting experiments to detect correct integration is indicated by grey bars and detects exon 7 and 8. Positions of diagnostic *Stu*I restriction endonuclease sites are indicated. (B) Immunoblot of protein extracts from ES cells used in this study. The expression of RAD54-GFP was confirmed by immunoblot analysis of whole cell extract with anti-RAD54 antibodies. Positions of wild-type and GFP-tagged RAD54 are indicated. Extracts of wild-type, *Rad54*<sup>-/-</sup> and *Xpa*<sup>-/-</sup> cells were used as controls. The nature of the protein cross-reacting with the RAD54 antibody, indicated by an asterisk, is unknown, but serves as a loading control. Clonogenic survival of ES cells treated with (C) IR or (D) UV-light. After treatment with increasing doses of DNA damaging agents cells were grown for 7-10 days, fixed, stained and colonies were counted. The ability to form colonies is plotted as a function of increasing dose of DNA damage. Error bars represent standard error of mean (SEM). Genotypes of analyzed cell lines are indicated.





# Chapter 5

## **ATP-Dependent and ATP-Independent *in Vivo* Roles of the Rad54 Homologous Recombination Protein in Nuclear Foci Kinetics**

**Sheba Agarwal<sup>1</sup>, Wiggert A. van Cappellen<sup>2</sup>, Aude Guénolé<sup>1</sup>, Berina Eppink<sup>1</sup>, Samuel L. Linsen<sup>1</sup>, Eric. Meijering<sup>3</sup>, Adriaan Houtsmuller<sup>4</sup>, Roland Kanaar<sup>1,5</sup>, Jeroen Essers<sup>1,5,6</sup>**

<sup>1</sup>Department of Cell Biology & Genetics, Cancer Genomics Center, <sup>2</sup>Department of Reproduction and Development, <sup>3</sup>Department of Biomedical Imaging group Rotterdam, <sup>4</sup>Department of Pathology, <sup>5</sup>Department of Radiation Oncology, <sup>6</sup>Department of Vascular Surgery, Erasmus Medical Center, Rotterdam, The Netherlands

## Abstract

Homologous recombination is an error free, high fidelity pathway that repairs double stranded breaks (DSBs). Mammalian homologous recombination requires the SWI2/SNF2 ATPase Rad54, which possesses a variety of biochemical activities that can affect Rad51 function in the critical steps of homologous recombination. Rad54's role *in vivo*, however, has not been addressed in great detail. Our *in vivo* study shows that Rad54's ATPase activity is important for DNA repair and recombination, but interestingly, it also affects its cellular behavior. Specifically, we show that it is not necessary for recruitment of the protein into DNA damaged induced structures at sites of DNA damage, known as foci, but rather that it influences Rad54 dissociation from foci. Furthermore, our data show that Rad54 but not its ATPase activity is required for the timely accumulation of Rad51 and Brca2 at sites of DSBs, while RPA and Nbs1 accumulation is not affected, giving a clear indication that the cellular role of Rad54 is downstream DNA break resection. In addition, our data reveal that while the mobility of the vast majority of Rad54 proteins is hardly affected, when it cannot hydrolyze ATP, there is a subset of proteins that is permanently immobilized in a focus. Since Rad54 can only hydrolyze ATP when bound to DNA, our results demonstrate that mutations that attenuate the ATPase activity are separation of functions alleles that reveal that not all Rad54 molecules in a focus are equal. The ATPase activity differentially affects the behavior of the pool of Rad54 in a focus that is bound to DNA versus the pool that is not bound to DNA; the DNA-bound fraction can no longer dissociate, while the unbound fraction that is not actively engaged in DNA repair can still reversibly interact with the focus. Finally, we show that the ATPase activity of Rad54 affects the locations of foci, because after preferential movement to the nuclear periphery, they remain there in the mutant cells.

## Introduction

To preserve the integrity of their genome, cells have evolved a number of pathways to deal with DNA damage that is created by both endogenous sources, such as some byproducts of cellular metabolism like oxygen radicals, and exogenous sources, including ultraviolet and ionizing radiation [1]. Among different kinds of lesions, DNA double-strand breaks (DSBs) present a special challenge to the cells because both strands of the double helix are affected. If misrepaired, DSBs can cause genome rearrangements such as translocations and deletions that can result in development of cancer [2-4]. Thus it is paramount that DSBs are repaired precisely and in a timely fashion.

Homologous recombination is an error free, high fidelity pathway that repairs DSBs by using an undamaged homologous DNA molecule, usually the sister chromatid, as a template to repair the broken molecule [5]. The process is carried out by the Rad52 epistasis group proteins, identified by the genetic analyses of ionizing radiation sensitive *Saccharomyces cerevisiae* mutants [6, 7]. A number of Rad52 group proteins, including Rad51 and Rad54, are conserved in mammals, as is the core mechanism of homologous recombination [8]. The central protein of homologous recombination is Rad51, which mediates the critical step of homologous pairing and DNA strand exchange between the broken DNA molecule and the homologous intact repair template. Once a DSB occurs, it is processed to single-stranded DNA tails with a 3' polarity, onto which Rad51 protomers assemble into a nucleoprotein filament. This nucleoprotein filament is the active molecular entity in recognition of homologous DNA and the subsequent exchange of DNA strands. An extensive number of mediator and/or accessory proteins are implicated in assisting Rad51 at various stages of recombination [9], one of which is Rad54.

*RAD54*, first identified in *S. cerevisiae*, is conserved in vertebrates [10-12]. Rad54 is a member of the SWI2/SNF2 family of double-strand DNA stimulated ATPases that modulate protein-DNA interactions [13]. *Rad54*<sup>-/-</sup> mouse embryonic stem (ES) cells are ionizing radiation sensitive, display reduced level of homologous recombination and exhibit defects in repair of DSBs [11, 14]. A plethora of biochemical activities of Rad54 have been uncovered that have the potential to augment the central function of Rad51 in homologous recombination [15, 16]. First, Rad54 physically interacts with Rad51, both *in vitro* and *in vivo* [17-20]. Interestingly, in mammalian cells the interaction between the proteins can only be detected in cells that have been challenged with DNA damaging agents, suggesting that Rad54 interacts with the Rad51 nucleoprotein filament, rather than Rad51 protomers that are not engaged in recombination [19, 21]. Second, the interaction is not only physical but also functional, as Rad54 stimulates Rad51 mediated D-loop formation, i.e., the generation of a joint between homologous DNA molecules [22]. Third, Rad54 has a potent ATPase activity that is triggered specifically by double-stranded DNA [22, 23]. Fourth, the protein uses energy gained from ATP hydrolysis to translocate along the DNA double helix [24-26]. Fifth, presumably through its DNA translocase activity, Rad54 can affect the interaction of proteins with DNA. Specifically, it can influence the position of histones on DNA and remove Rad51 nucleoprotein filaments from double-stranded DNA [27-32].

Sixth, its translocase activity also allows the protein to perturb DNA structures. Rad54 can promote branch migration thereby affecting the processing of the Holliday junction, which is a 4-way DNA junction that can arise as intermediates at sites where the recombination partners are physically joined [33]. Many of the biochemical activities of Rad54 are affected by abrogating its ATPase activity, hence, the proper functioning of Rad54 depends on its ability to harness the energy from ATP hydrolysis, and this in turn is responsible for augmenting the role of Rad51. However, Rad51 nucleoprotein filament stabilization by Rad54, which is probably required before joint molecule formation occurs, turned out to be independent of its ATPase activity [34].

A striking characteristic of a number of proteins involved in homologous recombination, including Rad51 and Rad54, is their ability to accumulate at a high local concentration into nuclear foci [19, 35, 36]. This occurs spontaneously, that is in the absence of exogenously induced DNA damage, in a low percentage of cells in S phase [37, 38]. Upon the induction of DNA damage to cells, the majority of cells display colocalizing Rad51 and Rad54 foci at sites of DNA damage [19, 38, 39]. While the nature, composition and requirement for foci formation is not apparent from a biochemical point, it is clear that the foci, particularly of Rad51, are biologically relevant because mutant cells that cannot form them are DNA damage sensitive and display spontaneous chromosomal aberrations [40, 41]. The nature of these foci with respect to protein composition is highly dynamic. Photobleaching experiments have shown that Rad51 and Rad54 dissociate and associate with foci, with each protein having a characteristic dwell time [42].

Here, we studied the ATPase function of Rad54 in homologous recombination *in vivo*. To this end we compared knockin mouse embryonic stem (ES) cell lines that express GFP-tagged wild-type Rad54 protein with cell lines expressing ATP hydrolysis defective Rad54 proteins using advanced live-cell confocal microscopy. Time-lapse imaging and fluorescence correlation spectroscopy of individual cells and foci allowed quantitative analysis of the Rad54 in live cells. We discovered protein concentrations and DSB repair foci relocalization to the nuclear periphery upon DNA damage induction. In addition, we used fluorescence photobleaching techniques and show that defective ATPase activity renders a small fraction of the Rad54 molecules in a focus immobile suggesting that only a minority of molecules present in foci is functional in DNA DSB repair and that the ATPase activity of Rad54 is required for the release of protein from DNA damaged induced structures on chromatin.

## Results

To study the effect of the ATPase activity of Rad54 at the cellular level, mouse ES cells were generated that express wild-type and ATPase defective versions of GFP-fused Rad54 from the endogenous *Rad54* locus. A targeting construct, consisting of the human *RAD54* cDNA exons IV – XVIII fused to a GFP coding sequence or containing a point mutation in the Walker A ATPase domain (Figure 1A), was electroporated into ES cells of the genotype *Rad54*<sup>wt-HA/-</sup>, in which one *Rad54* allele is inactivated [19]. Two different mutant constructs

were used, one in which the lysine at position 189 was replaced by arginine, indicated by K189R and one in which the lysine is replaced by alanine, the K189A mutation. The ATPase activity of the purified Rad54<sup>K189R</sup> and Rad54<sup>K189A</sup> proteins was more than 100-fold reduced in comparison to the wild-type protein ([23] and data not shown). Clones carrying a homologously integrated knockin construct were identified by DNA blot analysis. A probe that detects exons VII and VIII was used in combination with genomic DNA digested with StuI, which yielded the expected doublet of bands around 6.5 kb for the *Rad54* knockin allele, while a 6.0-kb band was observed which is diagnostic for the *Rad54* knockout allele (Figure 1B). Proper expression of the full-length wild-type or mutant Rad54-GFP fusion proteins was confirmed by immunoblot analysis (Figure 1C). In the subsequent studies, two independent clones for *Rad54*<sup>K189R-GFP/-</sup> and one for *Rad54*<sup>K189A-GFP/-</sup> were used. As a positive control for all experiments, knockin *Rad54*<sup>WT-GFP/-</sup> ES cells were used; these cells express wild-type Rad54 fused to GFP from the endogenous *Rad54* locus. The function of Rad54 is not affected by its fusion to GFP because *Rad54*<sup>WT-GFP/-</sup> cells are not DNA damage sensitive (This thesis chapter 4).

Genotype	Targeting Efficiency at <i>Rb</i> locus
<i>Rad54</i> <sup>WT-GFP/-</sup>	31.9% (16 out of 46)
<i>Rad54</i> <sup>K189R-GFP/-</sup>	0.95% (1 out of 105)
<i>Rad54</i> <sup>K189A-GFP/-</sup>	1.2% (1 out of 81)
<i>Rad54</i> <sup>-/-</sup>	<1% (0 out of 82)

**Table 1. Efficiency of homologous recombination in Rad54 ATPase defective cells.** ES cells with the indicated genotypes were electroporated with a linearized *Rb-Hyg* construct [43]. Hygromycin resistant clones were expanded, genomic DNA purified, and subjected to DNA blot analysis to distinguish between randomly and homologously integrated events. Values indicate the percentage of clones that contain the homologously integrated targeting construct relative to the total number of clones analyzed. Absolute numbers are indicated in parentheses. The differences in recombination efficiency between *Rad54*<sup>WT-GFP/-</sup> cells and cells of all other genotypes listed are significant ( $p > 0.001$ ), while the difference between the mutant genotypes is not.

Mouse *Rad54*<sup>-/-</sup> ES cells are hypersensitive to ionizing radiation and the interstrand DNA crosslinker mitomycin C [11]. Therefore, we investigated the effect of these DNA damaging agents on *Rad54*<sup>K189R-GFP/-</sup> and *Rad54*<sup>K189A-GFP/-</sup> ES cells. Cells expressing ATPase defective versions of Rad54 were hypersensitive to ionizing radiation and mitomycin C compared to isogenic control cells; this hypersensitivity was similar to that demonstrated by cells lacking Rad54 protein altogether (Figure 1D). Next we tested the effect of Rad54 ATPase activity on homologous recombination. As a measure of homologous recombination efficiency, we determined the efficiency of homologous gene targeting [21,

43]. ES cells of the genotypes indicated in Table 1 were electroporated with a linearized targeting construct for the *Rb* locus that carried a hygromycin selectable marker gene. Genomic DNA was isolated from individual clones and analyzed by DNA-blotting to discriminate between homologous and random integration events. Homologous recombination efficiency was measured as the percentage of clones containing the homologously integrated targeting construct relative to the total number of drug-resistant clones analyzed (Table 1). The homologous targeting efficiency of approximately 32% in *Rad54*<sup>wt-GFP/-</sup> ES cells was reduced to around 1% in *Rad54*<sup>K189R-GFP/-</sup> and *Rad54*<sup>K189A-GFP/-</sup> ES cells. A similar reduction in homologous recombination efficiency was observed in the absence of Rad54. We conclude that the ATPase activity of Rad54 is essential for its DNA repair and recombination functions *in vivo*. In these assays, the physical presence of ATPase defective Rad54 or the complete absence of the protein results in indistinguishable phenotypes.

### ATP hydrolysis by Rad54 affects foci behavior in unchallenged cells

A number of proteins involved in the cellular response to DNA damage and DNA damage repair are known to accumulate in foci at sites of DNA damage [5]. We next analyzed the ATPase defective Rad54 mutant cells for accumulation of Rad54 foci in the absence of exogenously induced DNA damage. Observation of living cells using a confocal microscope revealed a dramatic increase in the amount of foci present in cells containing ATPase deficient *Rad54*<sup>K189R</sup> and *Rad54*<sup>K189A</sup> protein compared to wild-type Rad54 protein (Figure 2A). It should be noted that the increase in spontaneous foci is only observed when all Rad54 molecules in the cell are ATPase defective, since such an increase is absent in *Rad54*<sup>K189R-GFP/+</sup> and *Rad54*<sup>K189A-GFP/+</sup> cells (data not shown).

Rad54 is an accessory protein for Rad51 which performs the core reaction of homologous recombination, homologous DNA pairing and DNA strand exchange [5]. The proteins physically interact and work closely together in a number of biochemical assays [9]. At the cellular level both proteins colocalize in DNA damage induced foci [19]. We analyzed Rad51 foci in the mutant cells to determine whether the ATPase activity of Rad54 impacted the behavior of Rad51 *in vivo*. Unchallenged ES cells were fixed, stained with an antibody against Rad51 and both Rad51 and Rad54-GFP were detected by confocal microscopy (Figure 2B). Compared to cells expressing wild-type Rad54-GFP or lacking Rad54, cells expressing the ATPase defective variants of Rad54-GFP displayed a statistically significant two-fold increase in the number of 'spontaneous' Rad51 foci. Furthermore, almost all Rad54 foci detected (>90%), including those of *Rad54*<sup>K189R-GFP</sup> and *Rad54*<sup>K189A-GFP</sup>, colocalized with Rad51 (Figure 2B). Interestingly, while the number of Rad51 foci per confocal slice was elevated in cells expressing the ATPase defective Rad54 mutants, it was not increased in cells completely lacking Rad54 (Figure 2B).

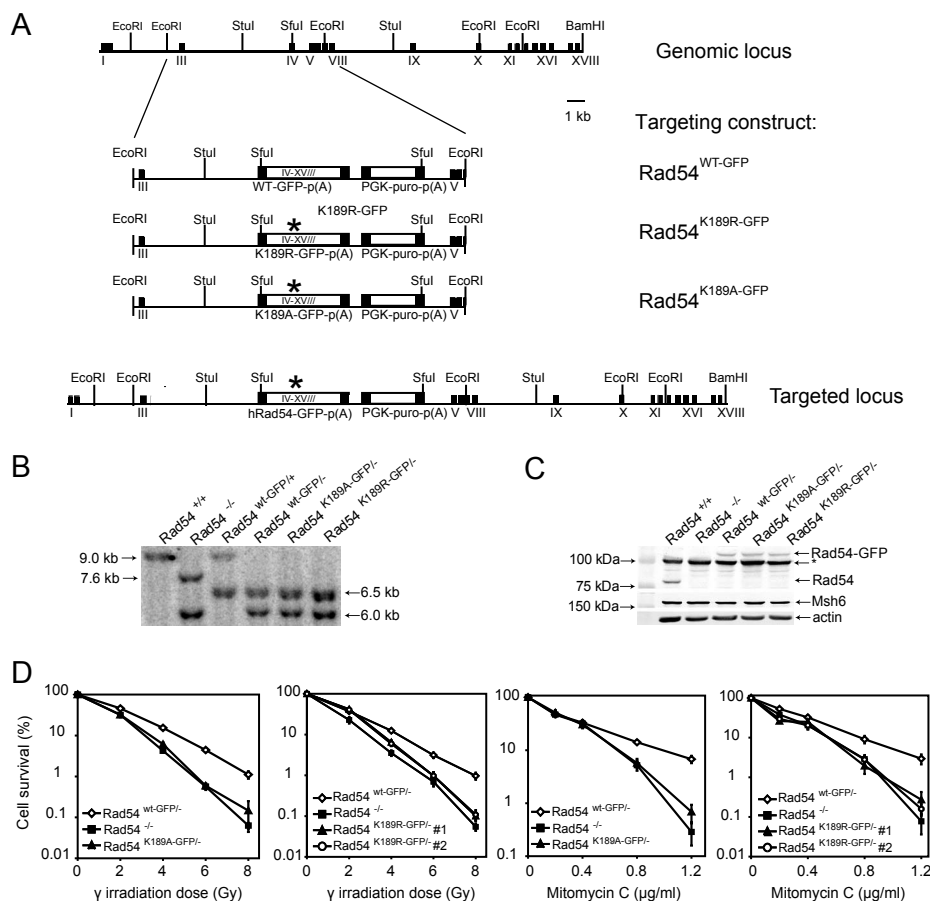


**Figure 1. Characterization of mouse ES cells carrying ATPase defective *Rad54-GFP* alleles.** (A) Schematic representation of the mouse *Rad54* locus and the gene targeting constructs. The top line represent a 30 kb portion of endogenous *Rad54* locus, where black boxes indicate exons I through XVIII. The middle line shows the linearized targeting construct, containing the human *RAD54* cDNA sequence spanning exon IV-XVIII fused to the *GFP* coding sequence. The K189R and K189A mutations in the Walker A ATPase domain are indicated by the asterisk. The construct contains a gene encoding for puromycin resistance as a selectable marker. The targeting construct will replace the regions between exon III and VIII when correctly integrated to generate the targeted allele, as shown in the targeted locus. Homologous integration results in the expression of full length, GFP-tagged Rad54 from its endogenous promoter. (B) DNA blot analysis of ES cells carrying the knockin constructs. DNA blot analysis was carried out using genomic DNA purified from puromycin resistant clones and digested with *StuI*. Detection of bands was carried out using a probe that recognized exon VII/VIII. Restriction of the wild-type allele by *StuI*, (indicated by "+"), yields a 9.0-kb band after hybridization with an exon VII/VIII probe. Diagnostic bands for the neomycin resistant knockout alleles, indicated by "-", are 7.6 kb for a hygromycin resistant allele and 6.0 kb for a neomycin resistant allele. Knockin alleles are characterized by a doublet of bands around 6.5 kb. (C) Immunoblot analysis of proteins produced by the Rad54-GFP knockin and -out alleles. Whole cell extracts of ES cells with

the indicated genotypes were probed with affinity purified anti-human Rad54 antibodies. The position of Rad54 and Rad54-GFP are indicated. The arrowhead indicates a non-specific signal. Probing against Msh6 and actin was used to confirm equal protein loading. (D) Ionizing radiation and mitomycin C survivals. ES cells of the indicated genotypes were tested for their ability to survive treatments with increasing doses of ionizing radiation ( $\gamma$ -irradiation) or mitomycin C using clonogenic survival assays. The assays were performed in triplicate and the error bars indicated the standard error of the mean.

---

### **Increased numbers of spontaneous Rad54 foci do not represent endogenous DNA damage**

Spontaneous foci, including Rad51 and Rad54, that are observed in unchallenged cells are thought to be present at sites of spontaneous DSBs such as those which might occur at impaired DNA replication forks [37, 49, 50]. Therefore, we asked whether the increased number of ‘spontaneous’ foci detected in cells was due to accumulated unrepaired DNA damage in these cells by determining whether the foci colocalized with DNA damage. First, we investigated the levels of  $\gamma$ H2AX, an early marker for DSBs, in whole cell extracts from wild-type and mutant cell lines. Anti- $\gamma$ H2AX antibodies recognize a specific phosphorylation on the histone variant H2AX that is triggered by certain types of DNA damage, including DSBs [50]. However, no increase in the level of H2AX phosphorylation was detected by immunoblotting in populations of unchallenged *Rad54*<sup>K189R-GFP/-</sup> and *Rad54*<sup>K189A-GFP/-</sup> compared to *Rad54*<sup>wt-GFP/-</sup> ES cells (Figure 3A, left panel). The cells expressing ATPase defective Rad54 were able to increase H2AX phosphorylation upon treatment with ionizing radiation (Figure 3A, right panel). In addition, we analyzed H2AX phosphorylation by immunofluorescence experiments (Figure 3B). Untreated *Rad54*<sup>wt-GFP/-</sup> and *Rad54*<sup>K189R-GFP/-</sup> ES cells displayed similar levels of  $\gamma$ H2AX foci, consistent with the immunoblotting results. Furthermore, the immunofluorescence experiments revealed that ES cells contain many more  $\gamma$ H2AX foci than Rad54 foci (Figure 3B). However, most if not all, Rad54 foci (either those made up of wild-type Rad54-GFP or ATPase defective Rad54-GFP) localize at sites of H2AX phosphorylation. In addition to  $\gamma$ H2AX, we also did not observe an increase in the number of foci for the DNA damage marker 53BP1 (Figure 3C). We conclude that the increase in spontaneous Rad54 foci in unchallenged *Rad54*<sup>K189R-GFP/-</sup> and *Rad54*<sup>K189A-GFP/-</sup> ES cells is unlikely to be due to a dramatically increased level of unrepaired DNA damage.

### **Lack of ATPase activity of Rad54 affects dynamic interaction with nuclear foci**

A remarkable feature of DNA damage induced foci is their highly dynamic nature. We previously showed that these accumulations of proteins are not static but that their components dynamically interact with the structures, with residence times ranging from a couple of seconds for Rad54 and several minutes for Rad51 [42]. To determine whether the ATPase activity of Rad54 influences this, we analyzed Rad54 interaction with foci using photobleaching techniques. For this purpose, we used a spot-FRAP protocol in which a

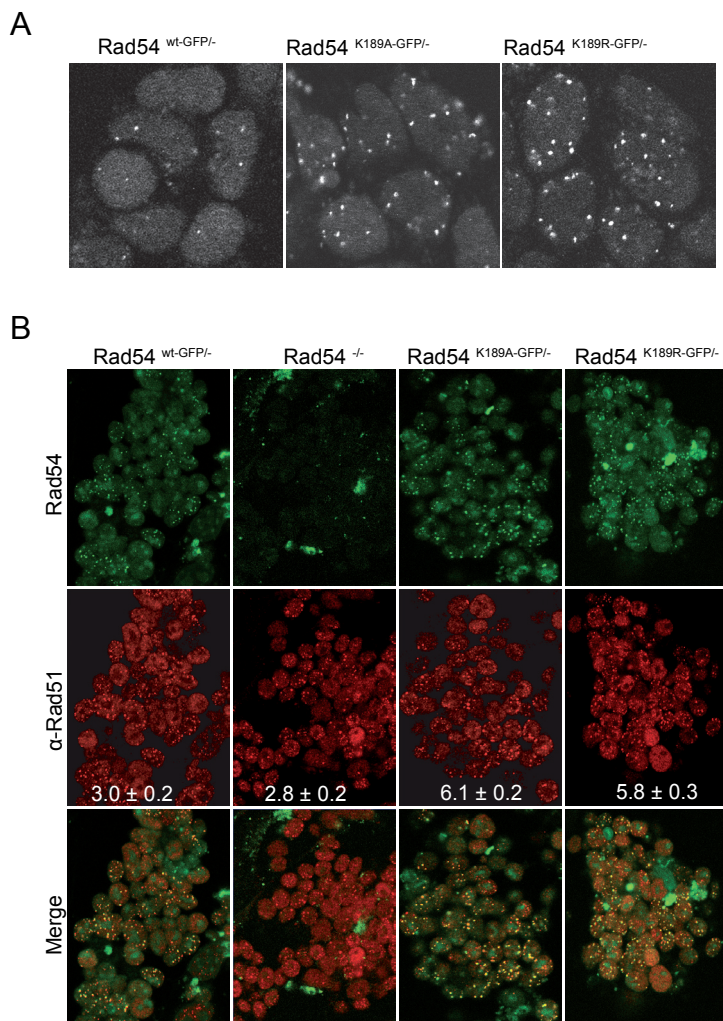


**Figure 2. Effect of Rad54 ATPase activity on focus formation.** (A) Shown are confocal images of untreated living ES cell expressing wild-type or ATPase defective Rad54-GFP. The mean number of spontaneous nuclear foci in cells expressing wild-type Rad54 is significantly greater compared to cells expressing either version of ATPase defective Rad54. (B) Rad51 immunofluorescence in non-treated ES cells of the indicated genotypes. The top panels show confocal images of Rad54 as detected by GFP fluorescence. The middle panels show the Rad51 staining pattern as detected by anti-Rad51 antibody staining. The merged pictures are shown in the bottom panel. The mean number of Rad51 foci per cell is indicated. The difference in number of Rad51 foci per cell between *Rad54*<sup>wt-GFP/-</sup> and *Rad54*<sup>-/-</sup> ES cells and the difference between *Rad54*<sup>K189R-GFP/-</sup> and *Rad54*<sup>K189A-GFP/-</sup> ES cells is not significant, while the difference between these two groups is ( $p < 0.01$ ), as determined by the one way ANOVA and student's t test.

small square encompassing a single Rad54-containing focus was bleached and subsequently monitored. We quantitated and compared the fluorescence recovery of ATPase proficient and defective Rad54 foci (Figure 4A). The bleaching protocol led to the irreversible bleaching of about 20% of the total pool of fluorescent RAD54 in the nucleus. In the experiment shown in Figure 4A the final measured fluorescence intensity was normalized to the pre-bleach pulse fluorescence intensity. The fluorescence in the bleached area recovered to approximately 80% for the wild-type Rad54-GFP protein in the bleached focus. In contrast, ATPase defective Rad54<sup>K189R-GFP</sup> was present in foci in two distinct kinetic pools; a transiently immobile fraction (~90%) similar to wild type Rad54-GFP [52], and a permanently immobilized fraction (~10%), not observed in wild type. The  $t_{1/2}$  of ATPase proficient foci was  $0.9 \pm 0.06$  seconds, which represents a faster recovery as compared to Rad54<sup>K189A-GFP/-</sup> and Rad54<sup>K189R-GFP/-</sup> ( $1.3 \pm 0.10$  seconds)

To obtain independent confirmation of the dynamic behavior of the wild-type Rad54 and Rad54<sup>K189R-GFP</sup> proteins in the DNA damage-induced structures, we examined them using iFRAP [53]. In these experiments the laser pulse used for bleaching fluorescence was aimed to photobleach the fluorescence of a complete nucleus with exception of one individual focus and a region of similar size in which no focus was present. The fluorescence intensity in the two regions (indicated in Figure 4B, blue circle, and red circle, respectively) in the nucleus was measured after the bleach pulse. The observed loss of fluorescence of the unbleached focus was then monitored and compared to the fluorescence level of the unbleached region without a focus. Measurement of the residence time of Rad54 in the nuclear focus revealed a complete exchange of wild-type Rad54 molecules in a focus, but a stably associated fraction for the Rad54<sup>K189R-GFP</sup> mutant, confirming the spot-FRAP measurements (Figure 4C). Thus, while the mobility of the vast majority is hardly affected, a fraction of RAD54 proteins is permanently immobilized if it cannot hydrolyze ATP.

### **The Rad54 protein, but not its ATPase activity, affects Rad51 recruitment to DSBs**

Biochemical experiments have demonstrated that Rad54 stimulates D-loop formation by Rad51 [22]. These and other results have led to the suggestion that Rad54 is important to target the Rad51 nucleoprotein filament to homologous duplex DNA where it will then engage its ATPase activity to promote repair of the DSB [15]. To test whether Rad54 is involved in targeting of Rad51 to the site of DSBs *in vivo*, we subjected a human osteosarcoma cell line (U2Os) to local alpha-particle irradiation using an <sup>241</sup>Am source [39, 44]. Alpha-particle irradiation can be especially useful to analyze the initial response to DNA damage because it can be used to induce DNA damage locally and in a defined pattern, allowing a clear distinction between already existing foci and local protein accumulations due to the induced DNA damage. Straight tracks of DSBs due the interaction of the alpha-particle with chromatin can be visualized using antibodies against  $\gamma$ H2AX [51] or 53BP1 [54]. Rad54 localized to the DSB sites (Figure 5A). Rad54 was depleted from U2Os cells (Figure 5B), and subsequently cells were irradiated with alpha-

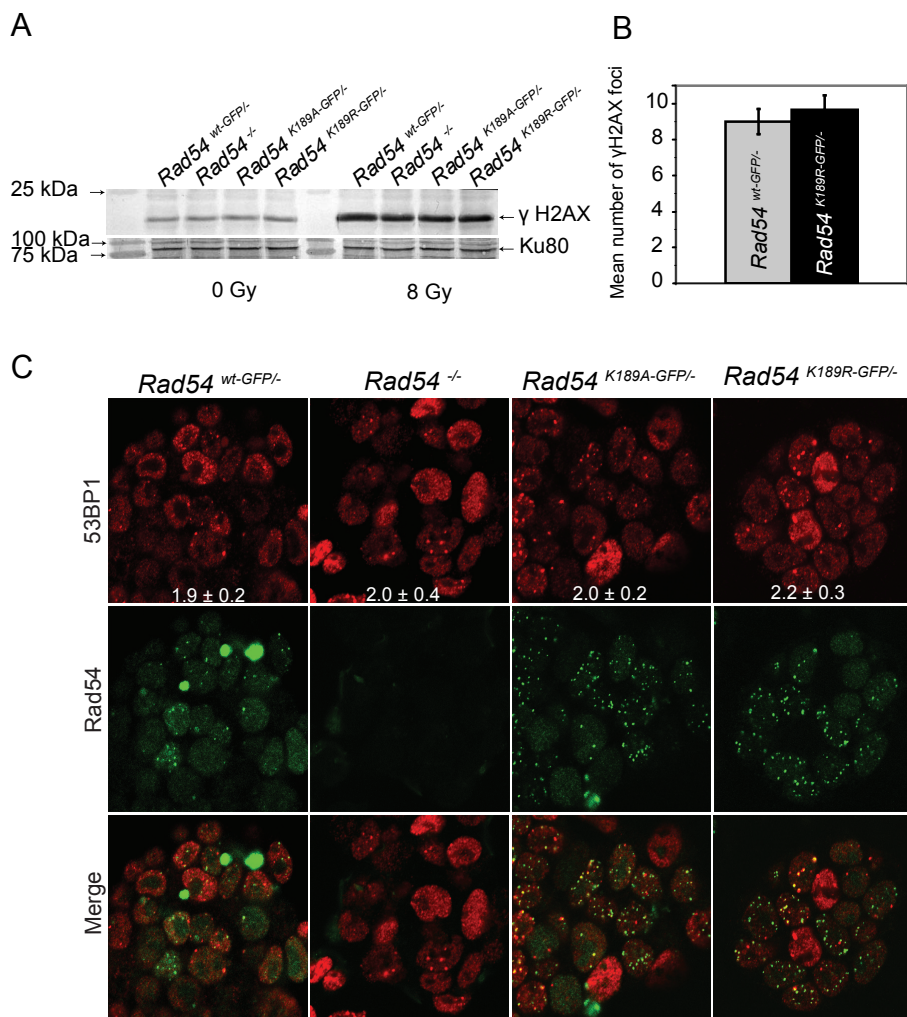


**Figure 3. Analysis of  $\gamma$ H2AX and 53BP1 in Rad54 ATPase defective ES cells.** (A) Whole cell extracts of ES cells with the indicated genotype were either non-treated (left hand panel) or harvested 1 hr after irradiation with 8 Gy (right hand panel) and analyzed by immunoblotting using an anti- $\gamma$ H2AX antibody. Antibodies against Ku80 were used to confirm equal loading (lower panel). (B) Quantification of the average number of  $\gamma$ H2AX foci in untreated *Rad54*<sup>wt-GFP/+</sup> and *Rad54*<sup>K189R-GFP/-</sup> ES cells. (C) Immunofluorescence detection of 53BP1 in untreated ES cells. The top panel shows 53BP1 staining in *Rad54*<sup>wt-GFP/+</sup>, *Rad54*<sup>K189R-GFP/-</sup> and *Rad54*<sup>K189A-GFP/+</sup> ES cells, while the middle shows the GFP staining and the bottom panel shows the merged images.

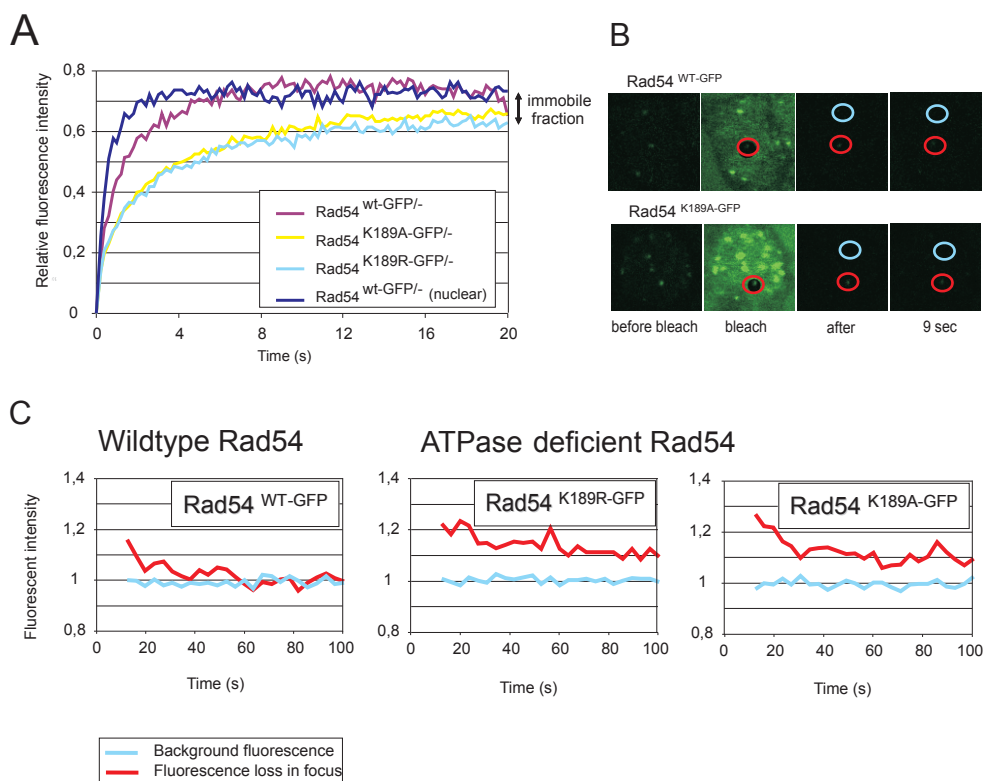


**Figure 4. Photobleaching analysis of Rad54 in foci.** (A) Spot-FRAP analysis of Rad54 in foci. A small square containing an individual Rad54 focus was bleached and monitored for fluorescence recovery for each indicated genotype. As a control the fluorescence recovery of non-foci associated Rad54 was quantitated (dark-blue line). (B) Visualization of i-FRAP analysis of Rad54 in foci. The whole cell was bleached excluding a small square containing an individual Rad54 focus. Fluorescence depletion of the non-bleached focus was monitored for Rad54<sup>wt-GFP</sup> and Rad54<sup>K189A-GFP</sup>. Shown here are 4 frames, before, during, directly after and 9 seconds after bleaching. (C) Quantification of the iFRAP experiment described under (B). Graphs represent the fluorescent depletion over time and are based on 5 individual cells.

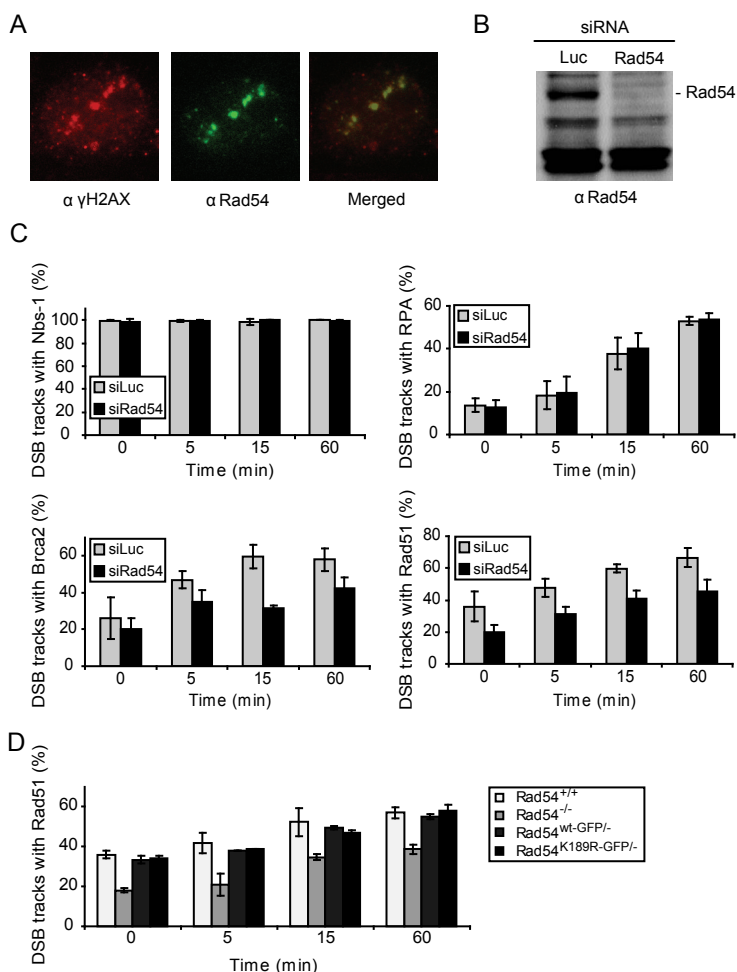


**Figure 5. The Rad54 protein, but not its ATPase activity, affects Rad51 recruitment to sites of DSBs.**

Accumulation of DSB repair proteins at  $\alpha$ -particle-induced DSB tracks. (A) shows the localization of Rad54 to the site of the double stranded break colocalizing with DSB marker  $\gamma$ H2Ax. (B) RAD54 protein levels in U2Os cells transfected with indicated siRNAs. Cell lysates were analyzed by immunoblotting with antibodies against RAD54. Equal sample loading was verified by a non-specific band. (C) Quantification of accumulation of Nbs1, RPA, Rad51 and BRCA2 at  $\alpha$ -particle-induced tracks of DSB 0, 5, 15 and 60 minutes after irradiation in the presence or absence Rad54. U2Os cells were stained for either  $\gamma$ H2Ax (Nbs1 and Rad51) or 53BP1 (RPA and Brca2) as a DSB marker and for one of the indicated repair proteins. Graphs represent average percentage of positive DSB tracks with a repair protein. One hundred cells containing by  $\alpha$ -particle-induced tracks were scored per experiment. Error bars represent the range of percentages obtained from 3 independent experiments. (D) Quantification of accumulation of Rad51 at DSB sites 0, 5, 15 and 60 minutes after irradiation in wild-type (IB10), *Rad54*<sup>-/-</sup> (#10) ES cells, *Rad54*<sup>wt-GFP/-</sup> and *Rad54*<sup>K189R-GFP/-</sup> ES cells. Graphs represent average percentage of Rad51 positive tracks per  $\gamma$ H2Ax track. One hundred cells containing damage induced by  $\alpha$ -particles were scored per experiment. Error bars represent the range of obtained from 2 independent experiments.

particles. Over time there was an increased localization of repair proteins acting early in homologous recombination, including Nbs1 and replication protein A (RPA), as well as Rad51 and BRCA2, to the sites of damage (Figure 5C). Upon Rad54 depletion we observed a transient, but considerable delay in the recruitment of Rad51 and BRCA2 but not of RPA and Nbs1, indicating at the cellular level that Rad54 affects a specific step in the progression of homologous recombination. This delayed accumulation of Rad51 at DSBs was also observed in ES cells deficient in Rad54 (*Rad54*<sup>-/-</sup>) but, remarkably, was independent on the ATPase activity of Rad54 since both *Rad54*<sup>wt-GFP/-</sup> and mutant *Rad54*<sup>K189A-GFP/-</sup> knockin ES cells showed similar kinetics for Rad51 accumulation at sites of DNA damage as wild-type ES cells (Figure 5D). These results show that timely accumulation of Rad51 in foci at sites of DNA damage is dependent on the Rad54 protein but not on its ATPase activity.

### Real-time analysis of Rad54-GFP foci

To investigate whether the ATPase activity of Rad54 influenced the disappearance of Rad54 foci, we employed a global irradiation protocol using a <sup>137</sup>CS source followed by prolonged time-lapse analyses of irradiated cells. To this end time-lapse movies were made of *Rad54*<sup>wt-GFP/-</sup> and *Rad54*<sup>K189R-GFP/-</sup> ES cells starting 45 min after irradiation with 2 Gy (Figure 6A and material and methods). Quantitation of the number of foci per cell over time showed that the appearance of foci containing Rad54<sup>wt-GFP</sup> and Rad54<sup>K189R-GFP</sup> is approximately the same (Figure 6B). In the time interval between 2 and 3 hours after irradiation the maximum number of foci per cell was reached for Rad54<sup>wt-GFP</sup> cells. Interestingly, however, the kinetics of the disappearance of ATPase defective Rad54 foci was reduced compared to wild-type Rad54 foci, as evidenced by comparison of the time required for a two-fold reduction in the number of Rad54 foci from their peak values. This two-fold reduction occurred approximately 9 hours after the irradiation in *Rad54*<sup>wt-GFP/-</sup> cells, while it took at least 25 hours in *Rad54*<sup>K189R-GFP/-</sup> ES cells. This shows that while Rad54 ATPase activity was not necessary for Rad54 recruitment to the sites of damage, it specifically influenced its dissociation from foci.

### Quantification of the number of Rad54-GFP molecules

The knockin ES cells expressing the Rad54-GFP fusion protein from the endogenous *Rad54* locus allow accurate quantitation of the endogenous concentration of Rad54 molecules in an individual cell by fluorescence correlation spectroscopy (FCS) and an estimation of the number of molecules per focus. First, we calibrated the instrument using a dilution series of purified GFP protein in solution (Figure 7A). We then measured fluorescence correlation curves in cells expressing GFP itself, Rad54<sup>wt-GFP</sup>, Rad54<sup>K189A-GFP</sup> and determined actual concentration by curve fitting (Figure 7B). Subsequently, we determined an average ES cell nuclear volume and determined the total number of molecules per cell. Next, we used the time-lapse movies of *Rad54*<sup>wt-GFP/-</sup> and *Rad54*<sup>K189R-GFP/-</sup> ES cells, in which the cells were treated with a dose of 2 Gy and subsequently followed up to 25 hours to analyze the average number of molecules in DNA damage induced foci (Figure 6A). The ratio between free

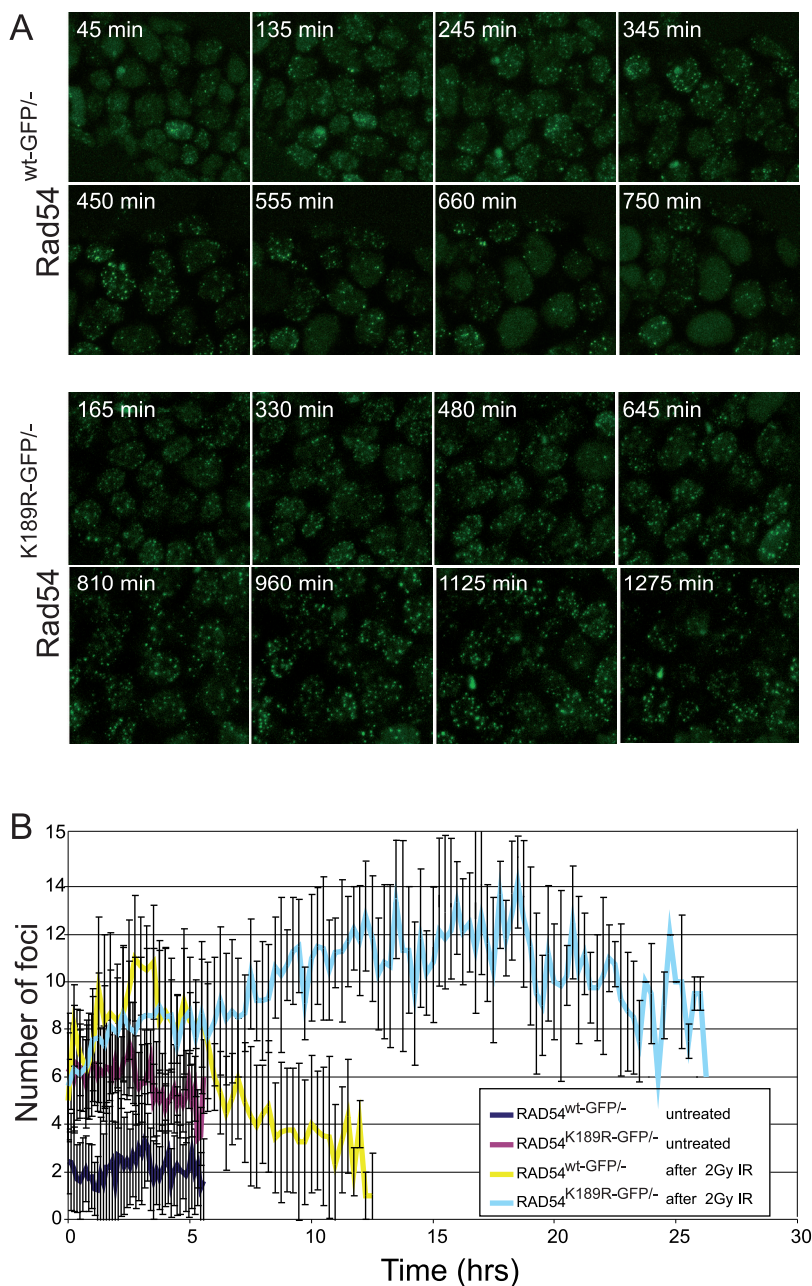


**Figure 6. Quantification of Rad54 foci over time in response to irradiation.** (A) Time-lapse imaging of irradiated *Rad54*<sup>wt-GFP/-</sup> and *Rad54*<sup>K189R-GFP/-</sup> ES cells. Cells were treated with 2 Gy and imaged every 15 min starting 45 minutes post irradiation. Each picture represents a frame in the resulting movie at the indicated time point. (B) Quantification of the number of foci per cell over time based on the movies represented in panel A. Quantification was performed using Image J as described in the Methods.

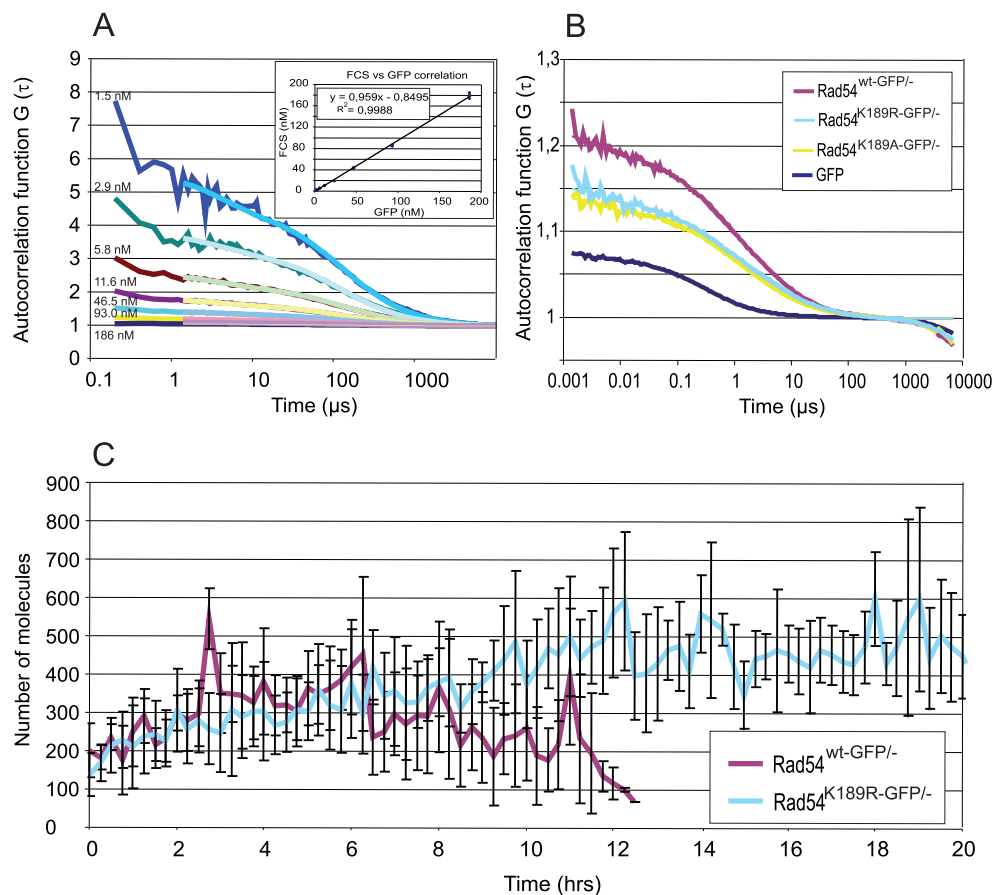


**Figure 7. FCS concentration measurement.** (A) Autocorrelation function  $G(\tau)$  measured by FCS of increasing concentrations of GFP. Inset indicates GFP concentration measurement by FCS of purified GFP in solution plotted as FCS concentration (nM) versus GFP concentration (nM). (B) Autocorrelation function  $G(\tau)$  measured by FCS in wild-type (IB10), *Rad54*<sup>wt-GFP/-</sup> and *Rad54*<sup>K189R-GFP/-</sup> ES cells. As a control cells expressing free untagged GFP were used. (C) Quantification of the number of Rad54-GFP molecules, either wild type of K189R mutant, in a single focus over time.

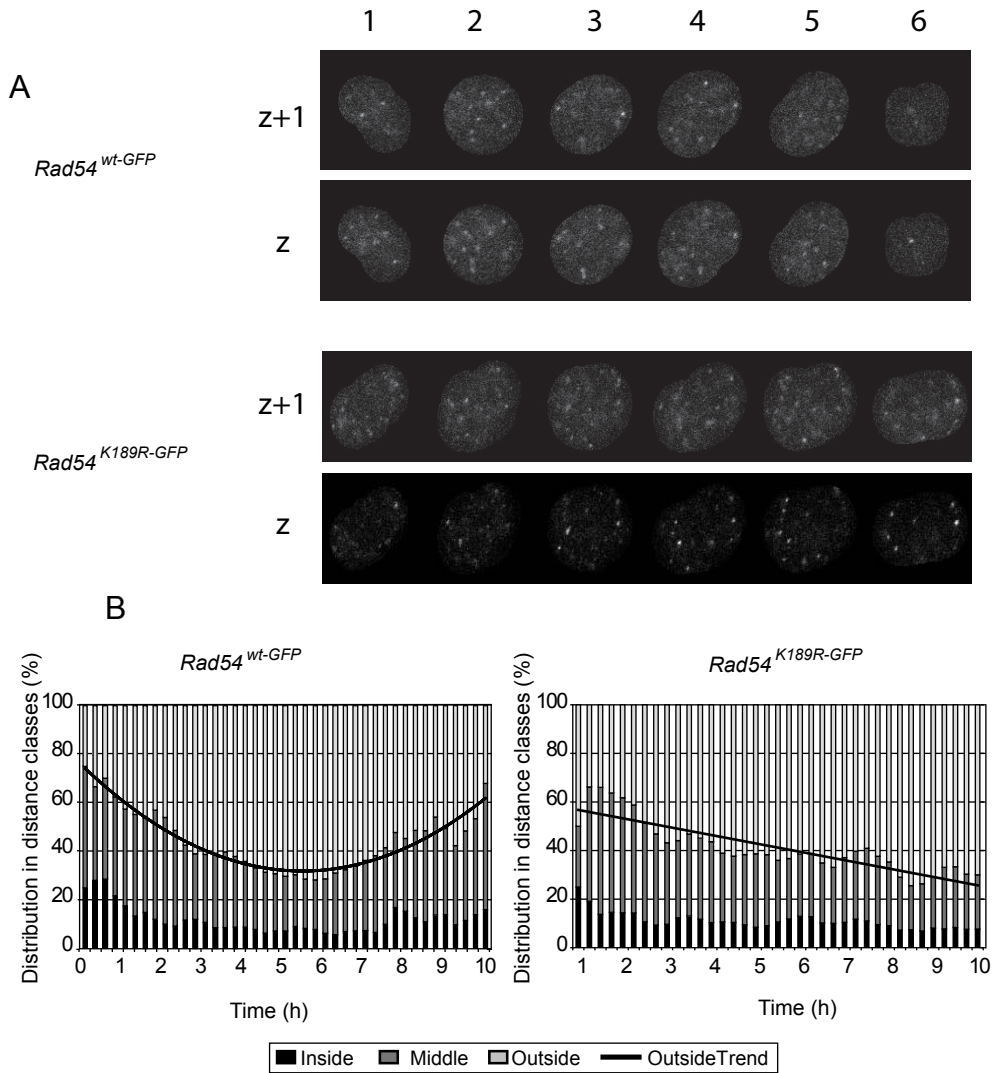


**Figure 8. Nuclear relocation of Rad54-GFP foci in response to DNA damage.** (A) Grayscale representation of a wild-type or ATPase defective Rad54-GFP cell. Shown are a subset of time points in 2 (out of 10) Z-axes of a single cell. (B) Quantification of (A). The relative distribution of foci in distance classes; inside (0-2  $\mu$ m), middle (2-4  $\mu$ m) and outside (> 4  $\mu$ m) followed over time. Graph indicates the average distribution of foci in *Rad54<sup>wt-GFP/-</sup>* and *Rad54<sup>K189R-GFP/-</sup>* cells irradiated with 2 Gy.

molecules and molecules in foci was determined using a calculated thresholding as described in the Materials and Methods section to determine the number of molecules in foci and nucleoplasm. The average number of molecules per focus over time was then plotted against the time period for which the cells could be followed (Figure 7C). This analysis revealed that the average number of molecules in an individual focus varies between 100-600 molecules. In *Rad54*<sup>wt-GFP/-</sup> cells the number of molecules accumulate after damage induction and disappear over time. While in the *Rad54*<sup>K189R-GFP/-</sup> mutant cells the number of molecules also increase but then failed to decrease over time.

### **Rad54 influences relocalization of DSBs to the nuclear periphery**

In yeast, persistent DNA breaks are fixed over time at the nuclear periphery [55-57]. Our targeted knockin approach allowed tracking of the nuclear localization of Rad54 foci over time to determine their cellular localization in mammalian stem cells. In cells followed for at least 15 time points, the relocalization of the DNA damage induced foci was analyzed (Figure 8A). For each focus the center of mass was determined in 2D. Next, the distance of the focus location to the center of mass of the cell was calculated. The foci were then classified in 3 distance classes (see Figure 8B), 'inside', distance less than 2 microns from the center of cell, 'middle', distance between 2 and 4 microns from the center of the cell, 'outside', distance more than 4 microns from the center of the cell. In wild-type cells the outside distance class increases temporarily during the repair process, indicated by the observation that Rad54 foci relocalized to the nuclear periphery and back to their starting positions over time (Figure 8B). In contrast ATPase defective Rad54 foci localized to the nuclear periphery but persisted at this position, indicative of hampered DSB repair.

## **Discussion**

Rad54 is a multifunctional protein that possesses several different activities which promote the progression of homologous recombination, an accurate pathway of repairing DSBs [16]. In addition to a close functional interaction with Rad51, the central protein of homologous recombination, Rad54 also displays potent ATPase activity, which allows it to translocate along DNA. This allows the protein to change the conformation of the template DNA, thereby perturbing DNA structures and influencing protein-DNA interactions [15]. Here, we have investigated the effect of a mutation in the ATPase domain of Rad54 on its cellular behavior.

The primary results of this study are as follows. First, the ATPase activity of Rad54 influences the number of spontaneous Rad54 foci in unchallenged cells, since ATPase defective Rad54 cells contain more of them compared to cells expressing wild-type Rad54. Second, the Rad54 ATPase defective cells also display an increase in spontaneous Rad51 foci. However, the increase of foci containing homologous recombination proteins does not correspond to an increase in DNA damage. Third, the ATPase activity of Rad54 is not required for the formation of foci induced by DNA damaging agents. Fourth, Rad54 but not its ATPase activity is required to timely accumulate Rad51 at sites of DSBs. Fifth, the

occurrence of an immobile fraction of ATPase-defective Rad54 molecules in foci. Sixth, time-lapse studies revealed that the disappearance of DNA damage-induced foci is delayed when Rad54's ATPase activity is attenuated, and these ATPase-defective Rad54 DNA repair foci are stuck at the nuclear periphery.

### **The ATPase activity of Rad54 is essential for its DNA repair function *in vivo***

To address the importance of the ATPase activity of Rad54, we generated mouse embryonic stem (ES) cells that express ATPase defective mutants from the endogenous *Rad54* locus fused to a carboxy-terminal GFP tag (Figure 1), ensuring physiological levels of mutant protein (Figure 1C). The DNA damage sensitivity profiles of the ATPase defective Rad54 mutants are similar to cells lacking Rad54 altogether in terms of hypersensitivity to mitomycin C and ionizing irradiation (Figure 1D). The damage hypersensitivities of the Rad54 ATPase defective cells are probably resulting from defective homologous recombination, because Rad54 ATPase defective and *Rad54*<sup>-/-</sup> ES cells are equally impaired in homologous recombination (Table 1). This indicates that the Rad54 ATPase activity is required for the type of recombination that is used to repair breaks induced by irradiation and mitomycin C, as well to effectively homologously integrate a linear piece of DNA into the genome. Furthermore, this indicates that both binding and hydrolysis of ATP is essential since both ATPase mutants (K189A and K189R) display similar phenotypes. The experiments reveal the essential role of the Rad54 ATPase function in mammalian cells and its *in vivo* importance for DNA repair.

### **Differential cellular behavior of ATPase-proficient and -defective Rad54**

The remarkable feature of *Rad54*<sup>K189R-GFP/-</sup> and *Rad54*<sup>K189A-GFP/-</sup> cells is the presence of an elevated number of spontaneous, 'uninduced' Rad54 foci in their nuclei compared to *Rad54*<sup>wt-GFP/-</sup> cells (Figure 2A). A clear phenotypical difference in the cell biology of cells lacking Rad54 altogether and cells that express ATPase mutants is the corresponding elevated number of Rad51 foci in ATPase mutant cells (Figure 2B). Thus, in addition to causing an increase in its own foci in unchallenged cells, the inability of Rad54 to hydrolyze ATP effectively also causes an increase in the foci of its partner protein, Rad51. Thus it is possible that the ATPase activity of Rad54 is involved in turning over Rad51 in the foci, consistent with biochemical experiments demonstrating that Rad54 can displace Rad51 from double-stranded DNA [30]. Yet, in the absence of Rad54 no increase in Rad51 is detected, although their stability is affected [19, 41]. It is possible that when Rad54 is completely absent, a redundant protein can act at the site of the DSB which might take over Rad54 function with respect to removal of Rad51, but not with respect to DSB repair because this is still impaired in knockout cells. A candidate protein for this function is the Rad54 paralog Rad54B [58]. The presence of the ATPase defective Rad54 protein would then dominantly affect this aspect of Rad54B activity.

The increase in the number of Rad54-GFP foci does not correlate with an increase in spontaneous DNA damage in Rad54 ATPase defective cells, because no increase in the

DNA damage marker  $\gamma$ H2AX can be detected in Rad54 ATPase defective cells versus Rad54 ATPase proficient cells (Figure 3A). Consistently, when analyzed by immuno-fluorescence no increase in the number of 53BP1 and  $\gamma$ H2AX foci can be detected (Figure 3B and C). Thus, within the limitations of these techniques, the level of DNA damage is not significantly different in mutant, wild-type and knockout cells, showing that the elevated number of spontaneous foci is not due to an increased number of unrepaired breaks. However we cannot exclude the possibility that replication associated DSBs, generated due to endogenous damage are efficiently repaired by Rad51, but the complex of Rad54 remains attached after the repair has been completed and therefore Rad54 and Rad51 foci persist. Our data are consistent with the absence of an overt proliferation defect as well as unaffected genomic stability of the cells expressing ATPase defective Rad54 and cells lacking Rad54 (data not shown). In addition, the immunofluorescence experiments show that the ATPase activity of Rad54 is not important for localization of Rad54 and Rad51 to sites of DNA damage. ES cells contain many more  $\gamma$ H2AX foci than Rad54 foci and therefore not all  $\gamma$ H2AX colocalize with Rad54, however most if not all Rad54 foci, also those containing ATPase defective Rad54, are at sites marked by  $\gamma$ H2AX (data not shown).

### **ATPase deficient Rad54 is partially immobilized in nuclear DNA repair foci**

The nature and function of foci is still ambiguous. Many models of the composition of a focus have been postulated. It is possible that, as has been put forth for yeast, the mammalian foci are also a reflection of the so-called “repair centers” [59], but this premise lacks clear cut evidence in mammalian cells. Foci have also been assumed to represent the one or all of the various stages of recombination, and are therefore not a clear method of distinguishing between the different stages of recombination. It is still not clear why such a high local concentration of protein is required at the site of damage, especially since in biochemical studies, the optimal ratios of Rad51 and Rad54 are not necessarily 1 to 1 [17, 18, 20]. However, the presence and quantification of foci have been used as an indication of repair activity, since foci form within a short time in response to DNA damaging agents, and decrease in number over time. A focus is a highly dynamic structure, with active and rapid association and disassociation of proteins, in particular Rad54 [42]. Our FCS analysis revealed that the average number of molecules in an individual focus varies between 100-600 molecules (Figure 7). This number however is higher than expected based on the few Rad54 molecules predicted to be necessary to repair a single DSB. These results implicate that not all molecules present in a foci are necessary to repair the break. Attracting and maintaining Rad54 molecules at the site of the break apparently continues until the break is repaired, as seen by the damage induced increase in the number of molecules over time (Figure 7). These foci might simply continue growing because the signal that locates Rad54 to the site of damage increases and continues to signal. Furthermore our FRAP data show that a small fraction of the molecules in the mutant is stably bound to the chromatin (the immobile fraction) (Figure 4), suggesting that only a minority of molecules present in foci is functional in DNA DSB repair. An interesting question remaining is why are there a ten-

fold more molecules present in foci, then necessary for repair? What role do the excess molecules have? Is it simply a mechanism of trial and error, the higher the local concentration the higher the efficiency of repair or is there an underlying reason that remains to be discovered in the future?

The molecular processes required for the accumulation and disassembly of homologous recombination proteins in foci at sites of DNA damage are not well understood. Cytological studies in yeast, chicken DT-40 cells and mouse ES cells suggest that Rad54 is not necessary for the formation of Rad51 foci [41, 59-62]. We show that the Rad54 but not its ATPase activity is required to timely accumulate Rad51 and BRCA2 into foci (Figure 5), however Rad54 does not influence the accumulation of Nbs1 and RPA. These results furthermore establish the role of Rad54 downstream of break resection and indicate that Rad54 is mainly involved in stages of recombination carried out by Rad51 and BRCA2. These results resemble the biochemical properties of Rad54. We know from biochemical experiments that Rad54 can load Rad51 on the filaments. This activity is independent of Rad54 ATPase activity as shown in yeast experiments [63]. Genetic studies have demonstrated that the ATPase activity is crucial for *in vivo* Rad54 function and we have shown that Rad54 K189R mutants display DNA damage sensitivities equivalent to the deletion mutant (Figure 1). By contrast, the disassembly process is affected by Rad54-mediated hydrolysis of ATP (Figure 7). Clearance of foci induced by DNA damage takes about twice as long in *Rad54<sup>K189R-GFP/-</sup>* cells compared to *Rad54<sup>wt-GFP/-</sup>*. These foci especially persist at the nuclear periphery (Figure 8). This phenomenon has been previously observed for yeast Rad51 [55-57] and indicates persistence of unrepaired DSBs. This behavior of unrepaired breaks, indicates that the prolonged presence of mutant Rad54 at the periphery likely resembles presence of unrepaired breaks. It is not unexpected for a protein in the SWI2/SNF2 family to affect this feature of foci. Just as genuine chromatin remodeling motor proteins affect histone DNA interactions, Rad54's motor activity, in conjunction with its direct interaction with Rad51, might be well suited to deal with accumulations of homologous recombination proteins on chromatin, after the repair process has been completed.

### **Mutations that attenuate the ATPase activity of Rad54 are separation of functions alleles**

The ATPase activity of Rad54 is essential for many of its biochemical activities [16], but its effect on the cellular behavior of the protein is unknown. Using photobleaching experiments in living cells, we determined previously that all of the homogeneously distributed Rad54-GFP in the nucleoplasm is highly mobile [42]. The experiments presented in Figure 4 reveal that while the ATPase activity of Rad54 slightly affects its effective diffusion rate, it renders a fraction of about 10% of molecules immobile in *Rad54<sup>K189A-GFP/-</sup>* and *Rad54<sup>K189R-GFP/-</sup>* cells compared to *Rad54<sup>wt-GFP/-</sup>* cells. The result of this is that it takes about twice as long to repopulate the entire focus. The combination of the time-lapse and photobleaching experiments provides additional insight into foci biology. A DNA

damaged induced Rad54 focus disappears twice as slow and the time it takes to repopulate a focus takes twice as long when Rad54 cannot hydrolyze ATP. The net effect is that on average the same number of Rad54 molecules associated with a single focus over time in wild-type and mutant cells, even though DNA repair is inoperative in the mutant cells.

Our study shows that Rad54's ATPase activity is important for DNA repair and recombination, as expected, but interestingly it is also affecting its cellular behavior. The ATPase activity is required for release of the protein from DNA damaged induced structures on chromatin, not only of itself but also of Rad51. The fact that the ATPase activity of Rad54 affects its cellular behavior is interesting because this activity is only triggered when it is bound to DNA. Likely, mutations that attenuate the ATPase activity of Rad54 are separation of functions alleles that differentially affect the behavior of the pool of Rad54 in a focus that is bound to DNA versus the pool that is not bound to DNA. Rad54 molecules that are not bound to DNA are not hydrolyzing ATP, are therefore not actively engaged in repair, and can still reversibly interact with the focus. On the other hand, the Rad54 molecules bound to DNA, but no longer capable of hydrolyzing ATP appears to have lost the ability to quickly turn-over in the focus. Our observations are of interest in the context of the number of each HR proteins molecule required for DNA repair, which is much less based on biochemical experiments than are present in a focus. Thus, our experiments reveal the need to develop a cellular system that allows the identification and tracking of individual molecules in a crowd. In this way a functional separation can be made of Rad54 molecules that act during repair from those that do not.

## Materials and methods

**Cell culture.** The mouse ES cells used to generate cells expressing ATPase defective Rad54 had the genotype Rad54<sup>wt-HA/-</sup>, where one allele is disrupted, and the other expresses HA-tagged Rad54 from the endogenous Rad54 locus [19]. ES cells were cultured on gelatin-coated dishes in a 1:1 mixture of Dulbecco's modified Eagle's medium (DMEM) and buffalo rat liver (BRL) conditioned medium, supplemented with 10% (v/v) FBS (Hyclone), 0.1 mM nonessential amino acids (Biowhittaker), 50 mM  $\beta$ -mercaptoethanol (Sigma) and 500 U ml<sup>-1</sup> leukemia inhibitory factor. U2Os cells were cultured in a 1:1 mixture of DMEM and Ham's F10, supplemented with 10% (v/v) fetal calf serum (HyClone) and streptomycin/penicillin, at 37°C in an atmosphere containing 5% CO<sub>2</sub>.

**Antibodies.** The primary antibodies used in this study were: anti-Rad51 (rabbit polyclonal, [41]), anti-Rad54 (rabbit polyclonal, [11]), anti- $\gamma$ H2AX (Upstate Biotechnologies), anti-53BP1 (rabbit polyclonal, Novus biochemicals), anti-Rad54 (goat polyclonal (D-18) Santa Cruz Biotechnology), anti-NBS1 (Goat polyclonal (C-19) Santa Cruz Biotechnology), anti-RPA34 (Mouse monoclonal (Ab-2) Oncogene) and anti-BRCA2 (mouse monoclonal (Ab-1) Calbiochem). The secondary antibodies conjugated with alkaline phosphatase were obtained from Roche, the horseradish peroxidase-conjugated antibodies from Jackson

Immunoresearch and relevant Alexa fluor secondary antibodies were obtained from Molecular probes.

**Generation of ES cells carrying knockin alleles expressing ATPase defective Rad54 protein.** Targeting constructs bearing either K189A or K189R mutation (Figure 1) were purified as plasmids and linearized with PvuI, and then purified using electro-elution, phenol extraction and ethanol precipitation. These linearized constructs were then electroporated into Rad54<sup>wt-HA/-</sup> cells, using 2 mm cuvette, at 117 V, 1200  $\mu$ F and for 10 ms in an ECM 830 electroporator (BTX). Replacement of the Rad54<sup>HA</sup> locus would generate ES cells with the genotype Rad54<sup>K189A-GFP/-</sup> or Rad54<sup>K189R-GFP/-</sup>. Twenty four hours after electroporation cells were subjected to puromycin selection (1 $\mu$ g/ml). One hundred puromycin resistant colonies were isolated for each construct and their DNA was analyzed for homologous integration of the knockin constructs in the Rad54<sup>HA</sup> locus by DNA blotting using a probe recognizing exons VII and VIII. Genomic sequence analysis was performed to confirm the correct integration and presence of mutations in the Rad54 locus and protein expression was subsequently analyzed by immunoblotting. DNA damage sensitivities of the cells were assessed by performing clonogenic survival assays as previously described [11]. For ionizing radiation, dishes were treated right away with the indicated dosage. For the rest, cells were allowed to attach for 12 – 16 hours before treatment. Mitomycin C was added for one hour before washing. Finally, as a measure of homologous recombination efficiency, the frequency of homologous versus random integration of gene targeting constructs in the Rb locus was determined as previously described [43].

**Ionizing radiation and immunofluorescence.** ES cells were seeded on a feeder layer of lethally irradiated (70% - 80%) confluent mouse embryonic fibroblasts and left to attach overnight. Cells were irradiated with the indicated doses of ionizing radiation using a <sup>137</sup>Cs source and left to recover for the indicated amount of time. Alpha-particle irradiation was carried out using a <sup>241</sup>Am source as described previously [44]. Shortly, U2Os cells were transfected using Lipofectamine 2000 (Invitrogen) according to the manufacturer's instructions with siRNA against luciferase (CGUACGCGGAAUACUUCGAdTdT) or Rad54 (GAACUCCCAUCCAGAAUGAUU) for 48 hours. After 24 hours cells were plated on a 1.8  $\mu$ m-thick polyester membrane (mylar) and transfection was repeated. In case of embryonic stem cells, mylar dishes were coated with carbon atoms (EMscope SC500 sputter coater) and gelatin, and cells were subsequently plated 24 hours prior to irradiation. Cells were irradiated with  $\alpha$ -particles and subsequently fixed and stained for immunofluorescence at indicated time points as previously described [39]. In case of Rad51 staining pre-extraction for 1 minute with Triton-X-100 buffer (0.5% triton X-100, 20 mM Hepes-KOH (pH 7.9), 50 mM NaCl, 3 mM MgCl<sub>2</sub>, 300 mM Sucrose) was carried out [45]. Alpha-particle tracks were visualized with a Zeiss confocal laser scanning microscope LSM 510 META, consisting of an Axiovert 100 inverted microscope, equipped with an Argon gas

laser (visualizing Alexa 488, green) and a Helium Neon laser (visualizing Alexa 543, red). Images were taken with 63x plan apochromat oil immersion lens, on a single plane of ~ 1  $\mu$ m thickness, through the middle of the cell.

**Immunoblotting.** Whole cell extracts were prepared by lysing cells with SDS sample buffer (2% SDS, 10% glycerol, 60 mM Tris-HCl (pH 6.8)) 48 hours after transfection. After the protein concentration was determined by the Lowry protein assay, extracts were supplemented with 0.5%  $\beta$ -mercaptoethanol and 0.02% bromophenol blue. After fractionation by SDS-PAGE, proteins were transferred to PVDF membrane. The blots were blocked with PBS/ 3% skimmed milk/ 0.1% Tween-20 and probed with primary antibodies. After washing with PBS/ 0.1% Tween-20, the membranes were probed with relevant secondary antibodies, and developed with ECL Western blotting detection reagents (Amersham Biosciences).

**Live cell imaging, semi-automated foci counting and foci tracking.** ES cells were grown on lethally irradiated MEF feeder layer overnight on 24 mm round coverslips. Cells that grew to an approximately 70% confluent monolayer were irradiated with 2 Gy and transferred 45 minutes post irradiation to a specially adapted chamber fitted to the confocal microscope where they could be maintained at 37°C with 5% CO<sub>2</sub>. Using a macro for automated time-lapse imaging, the cells were imaged taking 10 Z slices (covering 9  $\mu$ m in total), every 15 minutes. Movies were analyzed in the AIM image browser (Carl Zeiss, Jena) and exported for detailed analysis using ImageJ software (Rasband, W.S., ImageJ, U. S. National Institutes of Health, Bethesda, Maryland, USA, <http://rsb.info.nih.gov/ij/>, 1997-2009.).

**Time-lapse imaging individual cells.** The low contrast in the images of the *Rad54* knockin cells between green nuclei and background prohibited automated segmentation of the ES cells. A custom made contourJ selection tool was used to select all individual cells by hand. Then, the center of mass (x,y location) for each cell was determined and when the distance of the center of mass in 2 consecutive time points was less than 3  $\mu$ m the cell was regarded as being the same cell. In this way cells could be followed in time. Those cells that could be tracked for at least 15 time points were selected for detailed foci analyses. Each selected cell was then processed to determine the number of foci in the 3D stack. This number per cell was determined as previously described [46]. Briefly, for each cell the mean intensity and standard deviation was determined. Foci were selected based on fluorescence intensity values above mean + 1.5 times the standard deviation (SD) Visual inspection of the images showed that this method detected the majority of the foci. From the resulting image, the number of foci was counted using the particles analysis function of ImageJ. Duplicate foci in different Z-planes were automatically removed from the counting. The data thus obtained was plotted as number of foci per cell against the time during which the cells could be followed.

**Fluorescence correlation spectroscopy experiments.** A Zeiss LSM510 confocor 2 (Carl Zeiss Jena) was used for the fluorescence correlation spectroscopy (FCS) experiments. Data were analyzed with the SSTC data processor (Scientific Software Technologies Center, Minsk, Belarus). Every cell was measured 5 times for 20 seconds. The raw data were autocorrelated and the autocorrelation curves were analyzed as either a one component free diffusion triplet state model (GFP in solution) or a 2 component free diffusion triplet state model (Rad54-GFP) in cells. The models were used to determine the diffusion time, i.e. the time it takes a molecule to move through the confocal laser spot and the total number of molecules in the diffraction limited spot. To be able to estimate the concentration of RAD54 molecules in a cell nucleus, the volume of the diffraction limited spot was determined using standard rhodamine 6G (Invitrogen, California, USA) and GFP solutions with known concentration [47]. We determined an average ES cell nuclear volume by measuring two perpendicular diameters in the confocal plane with the largest size of the nucleus ( $n=37$ ;  $9.5 \pm 1.2$  (mean  $\pm$  sd) micron per cell). The volume of individual cells was estimated by regarding the nucleus as an ellipsoid object of which the volume was determined using the following formula:  $\text{Volume} = (\pi \times d1 \times d2 \times (d1+d2)/2)/6$  in which  $d1$  and  $d2$  are the two perpendicular diameters. The average volume of the nuclei was  $453 \pm 190 \mu\text{m}^3$  (sd,  $N=39$ ) Using the FCS determined concentration and the estimated volume the total number of molecules per nucleus was calculated. From the confocal planes we determined the ratio between the fluorescent signal coming from the foci and the nucleus in total. With the total number of molecules per cell known and the percentage of the signal coming from the foci we then calculated the number of molecules per focus (plotted in Figure 7C).

**Photobleaching experiments.** To determine the mobility of free Rad54 protein we performed fluorescent recovery after photobleaching (FRAP) experiments where we photobleached the fluorescence of individual nuclear foci as described previously [42]. To determine the dynamic interaction of the Rad54 protein with nuclear foci in the ES cells, an area of  $25 \times 25$  pixels containing a focus was bleached at 80% laser intensity, and fluorescence recovery was measured in the area at 0.2 second intervals for 20 seconds. Sixty cells were monitored for each genotype in three independent experiments. Wild-type ES cells stably transfected with pGK-GFP-p(A) were used as a positive control for fluorescence recovery, where cells with comparable fluorescence level as the knockin cells were chosen and treated as detailed above.

Complementary inverted Frap (iFRAP) experiments were performed on a Leica TCS SP5 confocal microscope [48]. All fluorescence in an individual nucleus, with exception of a small region containing a single focus, was bleached and the decrease in fluorescence in the non-bleached focus was recorded. For each time point, the relative intensity was calculated as follows:  $I_{\text{rel},t} = (I_t - \text{BG}) / (I_0 - \text{BG})$ , where  $I_0$  is the average intensity of the region of interest before bleaching, and BG is the background signal.

## Acknowledgements

We thank Nicole van Vliet for expert technical assistance.

## References

1. Friedberg, E.C., L.D. McDaniel, and R.A. Schultz, *The role of endogenous and exogenous DNA damage and mutagenesis*. Curr Opin Genet Dev, 2004. **14**(1): p. 5-10.
2. Agarwal, S., A.A. Tafel, and R. Kanaar, *DNA double-strand break repair and chromosome translocations*. DNA Repair (Amst), 2006. **5**(9-10): p. 1075-81.
3. Bassing, C.H. and F.W. Alt, *The cellular response to general and programmed DNA double strand breaks*. DNA Repair (Amst), 2004. **3**(8-9): p. 781-96.
4. Hoeijmakers, J.H., *Genome maintenance mechanisms for preventing cancer*. Nature, 2001. **411**(6835): p. 366-74.
5. Wyman, C. and R. Kanaar, *DNA double-strand break repair: all's well that ends well*. Annu Rev Genet, 2006. **40**: p. 363-83.
6. Game, J.C. and R.K. Mortimer, *A genetic study of x-ray sensitive mutants in yeast*. Mutat Res, 1974. **24**(3): p. 281-92.
7. Symington, L.S., *Role of RAD52 epistasis group genes in homologous recombination and double-strand break repair*. Microbiol Mol Biol Rev, 2002. **66**(4): p. 630-70, table of contents.
8. Wyman, C. and R. Kanaar, *Homologous recombination: down to the wire*. Curr Biol, 2004. **14**(15): p. R629-31.
9. Sung, P., et al., *Rad51 recombinase and recombination mediators*. J Biol Chem, 2003. **278**(44): p. 42729-32.
10. Bezzubova, O., et al., *Reduced X-ray resistance and homologous recombination frequencies in a RAD54<sup>-/-</sup> mutant of the chicken DT40 cell line*. Cell, 1997. **89**(2): p. 185-93.
11. Essers, J., et al., *Disruption of mouse RAD54 reduces ionizing radiation resistance and homologous recombination*. Cell, 1997. **89**(2): p. 195-204.
12. Kanaar, R., et al., *Human and mouse homologs of the Saccharomyces cerevisiae RAD54 DNA repair gene: evidence for functional conservation*. Curr Biol, 1996. **6**(7): p. 828-38.
13. Pollard, K.J. and C.L. Peterson, *Chromatin remodeling: a marriage between two families?* Bioessays, 1998. **20**(9): p. 771-80.
14. Dronkert, M.L., et al., *Mouse RAD54 affects DNA double-strand break repair and sister chromatid exchange*. Mol Cell Biol, 2000. **20**(9): p. 3147-56.
15. Heyer, W.D., et al., *Rad54: the Swiss Army knife of homologous recombination?* Nucleic Acids Res, 2006. **34**(15): p. 4115-25.
16. Tan, T.L., R. Kanaar, and C. Wyman, *Rad54, a Jack of all trades in homologous recombination*. DNA Repair (Amst), 2003. **2**(7): p. 787-94.

17. Clever, B., et al., *Recombinational repair in yeast: functional interactions between Rad51 and Rad54 proteins*. Embo J, 1997. **16**(9): p. 2535-44.
18. Golub, E.I., et al., *Interaction of human recombination proteins Rad51 and Rad54*. Nucleic Acids Res, 1997. **25**(20): p. 4106-10.
19. Tan, T.L., et al., *Mouse Rad54 affects DNA conformation and DNA-damage-induced Rad51 foci formation*. Curr Biol, 1999. **9**(6): p. 325-8.
20. Jiang, H., et al., *Direct association between the yeast Rad51 and Rad54 recombination proteins*. J Biol Chem, 1996. **271**(52): p. 33181-6.
21. Essers, J., et al., *Analysis of mouse Rad54 expression and its implications for homologous recombination*. DNA Repair (Amst), 2002. **1**(10): p. 779-93.
22. Petukhova, G., S. Stratton, and P. Sung, *Catalysis of homologous DNA pairing by yeast Rad51 and Rad54 proteins*. Nature, 1998. **393**(6680): p. 91-4.
23. Swagemakers, S.M., et al., *The human RAD54 recombinational DNA repair protein is a double-stranded DNA-dependent ATPase*. J Biol Chem, 1998. **273**(43): p. 28292-7.
24. Amitani, I., R.J. Baskin, and S.C. Kowalczykowski, *Visualization of Rad54, a chromatin remodeling protein, translocating on single DNA molecules*. Mol Cell, 2006. **23**(1): p. 143-8.
25. Ristic, D., et al., *The architecture of the human Rad54-DNA complex provides evidence for protein translocation along DNA*. Proc Natl Acad Sci U S A, 2001. **98**(15): p. 8454-60.
26. Van Komen, S., et al., *Superhelicity-driven homologous DNA pairing by yeast recombination factors Rad51 and Rad54*. Mol Cell, 2000. **6**(3): p. 563-72.
27. Alexeev, A., A. Mazin, and S.C. Kowalczykowski, *Rad54 protein possesses chromatin-remodeling activity stimulated by the Rad51-ssDNA nucleoprotein filament*. Nat Struct Biol, 2003. **10**(3): p. 182-6.
28. Alexiadis, V. and J.T. Kadonaga, *Strand pairing by Rad54 and Rad51 is enhanced by chromatin*. Genes Dev, 2002. **16**(21): p. 2767-71.
29. Jaskelioff, M., et al., *Rad54p is a chromatin remodeling enzyme required for heteroduplex DNA joint formation with chromatin*. J Biol Chem, 2003. **278**(11): p. 9212-8.
30. Solinger, J.A., K. Kiianitsa, and W.D. Heyer, *Rad54, a Swi2/Snf2-like recombinational repair protein, disassembles Rad51:dsDNA filaments*. Mol Cell, 2002. **10**(5): p. 1175-88.
31. Li, X. and W.D. Heyer, *RAD54 controls access to the invading 3'-OH end after RAD51-mediated DNA strand invasion in homologous recombination in Saccharomyces cerevisiae*. Nucleic Acids Res, 2009. **37**(2): p. 638-46.
32. Li, X., et al., *PCNA is required for initiation of recombination-associated DNA synthesis by DNA polymerase delta*. Mol Cell, 2009. **36**(4): p. 704-13.
33. Bugreev, D.V., O.M. Mazina, and A.V. Mazin, *Rad54 protein promotes branch migration of Holliday junctions*. Nature, 2006. **442**(7102): p. 590-3.

34. Mazin, A.V., A.A. Alexeev, and S.C. Kowalczykowski, *A novel function of Rad54 protein. Stabilization of the Rad51 nucleoprotein filament*. J Biol Chem, 2003. **278**(16): p. 14029-36.
35. Haaf, T., et al., *Nuclear foci of mammalian Rad51 recombination protein in somatic cells after DNA damage and its localization in synaptonemal complexes*. Proc Natl Acad Sci U S A, 1995. **92**(6): p. 2298-302.
36. Essers, J., A.B. Houtsmuller, and R. Kanaar, *Analysis of DNA recombination and repair proteins in living cells by photobleaching microscopy*. Methods Enzymol, 2006. **408**: p. 463-85.
37. Tarsounas, M., D. Davies, and S.C. West, *BRCA2-dependent and independent formation of RAD51 nuclear foci*. Oncogene, 2003. **22**(8): p. 1115-23.
38. Tashiro, S., et al., *Rad51 accumulation at sites of DNA damage and in postreplicative chromatin*. J Cell Biol, 2000. **150**(2): p. 283-91.
39. Aten, J.A., et al., *Dynamics of DNA double-strand breaks revealed by clustering of damaged chromosome domains*. Science, 2004. **303**(5654): p. 92-5.
40. Thacker, J. and M.Z. Zdzienicka, *The XRCC genes: expanding roles in DNA double-strand break repair*. DNA Repair (Amst), 2004. **3**(8-9): p. 1081-90.
41. van Veelen, L.R., et al., *Ionizing radiation-induced foci formation of mammalian Rad51 and Rad54 depends on the Rad51 paralogs, but not on Rad52*. Mutat Res, 2005. **574**(1-2): p. 34-49.
42. Essers, J., et al., *Nuclear dynamics of RAD52 group homologous recombination proteins in response to DNA damage*. Embo J, 2002. **21**(8): p. 2030-7.
43. Niedernhofer, L.J., et al., *The structure-specific endonuclease Ercc1-Xpf is required for targeted gene replacement in embryonic stem cells*. Embo J, 2001. **20**(22): p. 6540-9.
44. Stap, J., et al., *Induction of linear tracks of DNA double-strand breaks by alpha-particle irradiation of cells*. Nat Methods, 2008. **5**(3): p. 261-6.
45. Petrini, J.H., *The Mre11 complex and ATM: collaborating to navigate S phase*. Curr Opin Cell Biol, 2000. **12**(3): p. 293-6.
46. van Royen, M.E., et al., *Compartmentalization of androgen receptor protein-protein interactions in living cells*. J Cell Biol, 2007. **177**(1): p. 63-72.
47. Weisshart, K., V. Jungel, and S.J. Briddon, *The LSM 510 META - ConfoCor 2 system: an integrated imaging and spectroscopic platform for single-molecule detection*. Curr Pharm Biotechnol, 2004. **5**(2): p. 135-54.
48. Cox, M.M., et al., *The importance of repairing stalled replication forks*. Nature, 2000. **404**(6773): p. 37-41.
49. Budzowska, M. and R. Kanaar, *Mechanisms of dealing with DNA damage-induced replication problems*. Cell Biochem Biophys, 2009. **53**(1): p. 17-31.
50. Rogakou, E.P., et al., *DNA double-stranded breaks induce histone H2AX phosphorylation on serine 139*. J Biol Chem, 1998. **273**(10): p. 5858-68.
51. Misteli, T., *Protein dynamics: implications for nuclear architecture and gene expression*. Science, 2001. **291**(5505): p. 843-7.

52. Houtsmuller, A.B. and W. Vermeulen, *Macromolecular dynamics in living cell nuclei revealed by fluorescence redistribution after photobleaching*. Histochem Cell Biol, 2001. **115**(1): p. 13-21.
53. Bekker-Jensen, S., et al., *Spatial organization of the mammalian genome surveillance machinery in response to DNA strand breaks*. J Cell Biol, 2006. **173**(2): p. 195-206.
54. Oza, P., et al., *Mechanisms that regulate localization of a DNA double-strand break to the nuclear periphery*. Genes Dev, 2009. **23**(8): p. 912-27.
55. Oza, P. and C.L. Peterson, *Opening the DNA repair toolbox: localization of DNA double strand breaks to the nuclear periphery*. Cell Cycle. **9**(1): p. 43-9.
56. Kalocsay, M., N.J. Hiller, and S. Jentsch, *Chromosome-wide Rad51 spreading and SUMO-H2A.Z-dependent chromosome fixation in response to a persistent DNA double-strand break*. Mol Cell, 2009. **33**(3): p. 335-43.
57. Wesoly, J., et al., *Differential contributions of mammalian Rad54 paralogs to recombination. DNA damage repair and meiosis*. In press, 2006.
58. Lisby, M., et al., *Choreography of the DNA damage response: spatiotemporal relationships among checkpoint and repair proteins*. Cell, 2004. **118**(6): p. 699-713.
59. Shinohara, M., et al., *Tid1/Rdh54 promotes colocalization of rad51 and dmc1 during meiotic recombination*. Proc Natl Acad Sci U S A, 2000. **97**(20): p. 10814-9.
60. Miyazaki, T., et al., *In vivo assembly and disassembly of Rad51 and Rad52 complexes during double-strand break repair*. Embo J, 2004. **23**(4): p. 939-49.
61. Takata, M., et al., *The Rad51 paralog Rad51B promotes homologous recombinational repair*. Mol Cell Biol, 2000. **20**(17): p. 6476-82.
62. Wolner, B. and C.L. Peterson, *ATP-dependent and ATP-independent roles for the Rad54 chromatin remodeling enzyme during recombinational repair of a DNA double strand break*. J Biol Chem, 2005. **280**(11): p. 10855-60.



# Chapter 6

## Mild hyperthermia inactivates BRCA2-mediated DNA repair

**Przemek M. Krawczyk<sup>1\*</sup>, Berina Eppink<sup>2\*</sup>, Jeroen Essers<sup>2,3\*</sup>, Jan Stap<sup>1\*</sup>, Hanny Odijk<sup>2</sup>, Alex Zelensky<sup>2</sup>, Nicolaas A. P. Franken<sup>4</sup>, Chris van Bree<sup>4</sup>, Lukas J. Stalpers<sup>5</sup>, Marrije R. Buist<sup>6</sup>, Hence J. M. Verhagen<sup>7</sup>, Roland Kanaar<sup>2,3</sup> and Jacob A. Aten<sup>1</sup>**

<sup>1</sup>Center for Microscopical Research, Department of Cell Biology & Histology, <sup>4</sup>Laboratory for Experimental Oncology and Radiobiology, Center for Experimental and Molecular Medicine and Department of Radiotherapy, <sup>5</sup>Department of Radiation Oncology and <sup>6</sup>Department of Gynecologic Oncology, Academic Medical Center, University of Amsterdam, 1105 AZ, Amsterdam, The Netherlands.

<sup>2</sup>Department of Cell Biology & Genetics, Cancer Genomics Center, <sup>3</sup>Department of Radiation Oncology and <sup>7</sup>Department of Vascular Surgery, Erasmus Medical Center, 3000 DR, Rotterdam, The Netherlands

\*These authors contributed equally to this work

## **Abstract**

Inhibitors of DNA double-strand break (DSB) repair are relevant in anti-cancer therapy because they sensitize cells to various DSB-inducing agents. Elevated temperature (hyperthermia) is one of the oldest clinically applied modalities that is suspected to inhibit DNA repair, but its primary mode of action remains elusive [1, 2]. Here we show that mild (41 - 42.5°C) hyperthermia inhibits the homologous recombination (HR) pathway of DSB repair, induces degradation of BRCA2 and that this effect can be significantly enhanced by the addition of a heat shock protein (HSP) inhibitor. Mammalian tumour cells deficient in HR are sensitive to the inhibition of poly(ADP-ribose)polymerase 1 (PARP-1) [3, 4]. We demonstrate that hyperthermia can be used to sensitize innately HR-proficient tumour cells to PARP-1 inhibition, enabling design of novel therapeutic strategies involving localized induction of HR deficiency.

## Main text

Many anti-cancer strategies are based on cytotoxicity of DSBs induced by ionizing radiation or, indirectly, by chemical agents. However, efficient DSB repair mechanisms protect cells from the genotoxic effects of DSBs, reducing the effectiveness of the therapy. Two major pathways carry out DSB repair in mammalian cells: homologous recombination (HR) and non-homologous end joining (NHEJ). HR utilizes intact homologous DNA sequences – usually the sister chromatid in post-replicative chromatin – to faithfully restore DNA breaks [5]. Major HR factors include the DNA strand exchange protein RAD51 and the recombination mediators BRCA2, XRCC3 and RAD54 [5]. NHEJ operates throughout the entire cell cycle and does not require a DNA template. Core NHEJ functions are performed by the KU70/80 heterodimer, DNA-PK<sub>CS</sub>, DNA LigIV and XRCC4 [6]. Inhibition of DSB repair processes potentiates the cytotoxicity of DSBs in cancer therapy [7], but at the same time it adversely affects normal cells, which need to cope with DSBs arising during metabolic activities [8]. An optimal anti-cancer treatment would thus locally target the tumour cells. Hyperthermia is one anti-cancer agent that can be applied locally and, among other processes, possibly interferes with DSB repair [1, 2]. However, although radiosensitizing properties of hyperthermia have long been used in clinical practice [9], how hyperthermia inhibits DSB repair is unknown [1, 2, 10].

To determine target(s) of mild hyperthermia in mammalian DSB repair pathways, we measured radiosensitization of wild-type, NHEJ (*DNA-PK<sub>CS</sub><sup>-/-</sup>*) and HR (*Rad54<sup>-/-</sup>*) deficient mouse embryonic stem (ES) cells incubated at 41°C for 75 min. We chose temperature below 43°C for two reasons. First, higher temperatures might affect a broader range of metabolic activities and thus hamper explicit interpretation of results. Second, temperatures below 43°C are relevant in clinical practice [11]. Interestingly, we observed that both wild-type and *DNA-PK<sub>CS</sub><sup>-/-</sup>*, but not *Rad54<sup>-/-</sup>* cells incubated at 41°C were more radiosensitive as compared to cells incubated at 37°C (Figure 1A). The inability to further radiosensitize HR deficient cells using hyperthermia was not limited to RAD54 disruption or to mouse ES cells. HeLa cells, in which the HR factor XRCC3 was down-regulated using siRNA, were also refractory to radiosensitization by hyperthermia (Figure 1B). These results suggest that mild hyperthermia sensitizes cells to ionizing radiation by inactivating HR. To directly measure the effect of mild hyperthermia on HR, we quantitated HR-mediated gene targeting in ES cells [12] and found that the efficiency of gene targeting was significantly reduced in cells subjected to hyperthermia (Figure 1C). Similarly, mild hyperthermia reduced the frequency of spontaneous and mitomycin C-induced sister chromatid exchanges (Supplementary Figure 1A), which are to a large extent mediated by HR [13].

The majority of important DSB repair-related proteins accumulate at sites of DSBs, forming so-called ionizing radiation-induced foci (IRIF) [14]. This accumulation is crucial for proper functioning of repair mechanisms as disturbed formation of IRIF is associated with repair deficiencies and genome instability [5]. To pinpoint the defect(s) in the HR pathway caused by hyperthermia, we examined formation of IRIF by a range of DSB repair factors at alpha-particle induced DSBs [15] in U2OS cells incubated at 37°C or 41°C for 60

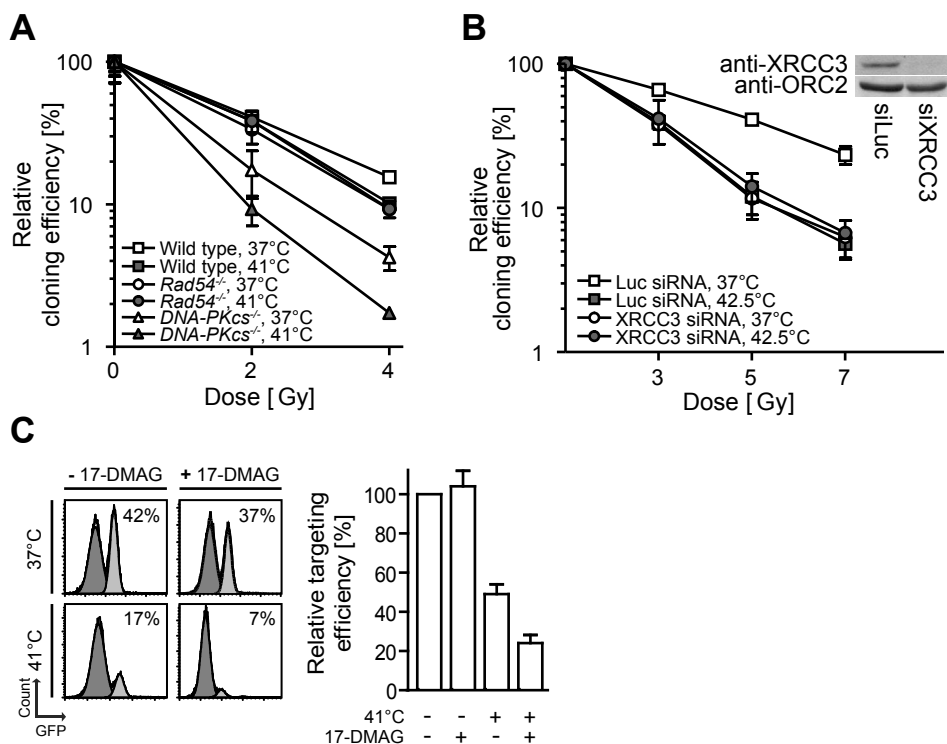


**Figure 1. Mild (<43°C) hyperthermia radiosensitizes HR-proficient, but not HR-deficient cells and inhibits HR repair.** (A) Cloning efficiency of wild-type (squares), *Rad54*<sup>-/-</sup> (circles) and *DNA-PKcs*<sup>-/-</sup> (triangles) mouse ES cells incubated for 75 min at 37°C (open symbols) or 41°C (filled symbols) and subsequently exposed to the indicated dose of γ-rays. (B) Cloning efficiency of HeLa cells transfected with siRNA directed against luciferase (squares) or XRCC3 (circles), incubated for 75 min at 37°C (open symbols) or 42.5°C (filled symbols) and exposed to the indicated dose of γ-rays. Inset shows reduction of XRCC3 protein levels in HeLa cells transfected with siRNA directed against XRCC3. Cell lysates were analyzed by immunoblotting with antibodies against XRCC3. Equal sample loading was verified by probing for ORC2. (C) Efficiency of HR-mediated gene targeting in mouse ES cells. Cells were incubated for 7 h at 37°C or 41°C in the presence or absence of 100 nM 17-DMAG. At 2 h into this incubation period cells were transfected with the *hRad54GFP-puro* knock-in targeting construct. Cells containing integrated construct were then selected in medium containing puromycin and analyzed by FACS. FACS profiles obtained in a single representative experiment (left panel) show the percentage of GFP-positive cells which incorporated the targeting construct into the *mRad54* locus after incubation at indicated conditions. The bar graph (right panel) shows relative average percentage of GFP-positive cells obtained from 3 independent experiments. Error bars represent standard error of the mean.

min prior to irradiation (Figure 2A, 2B and Supplementary Figure. S1). Early in HR, the ends of DSBs are resected in a reaction involving the MRE11/RAD50/NBS1, CtIP and BRCA1 complexes [16, 17] generating single-stranded DNA stretches, which are subsequently coated by RPA [5]. MRE11 and RPA efficiently accumulated at DSB sites,

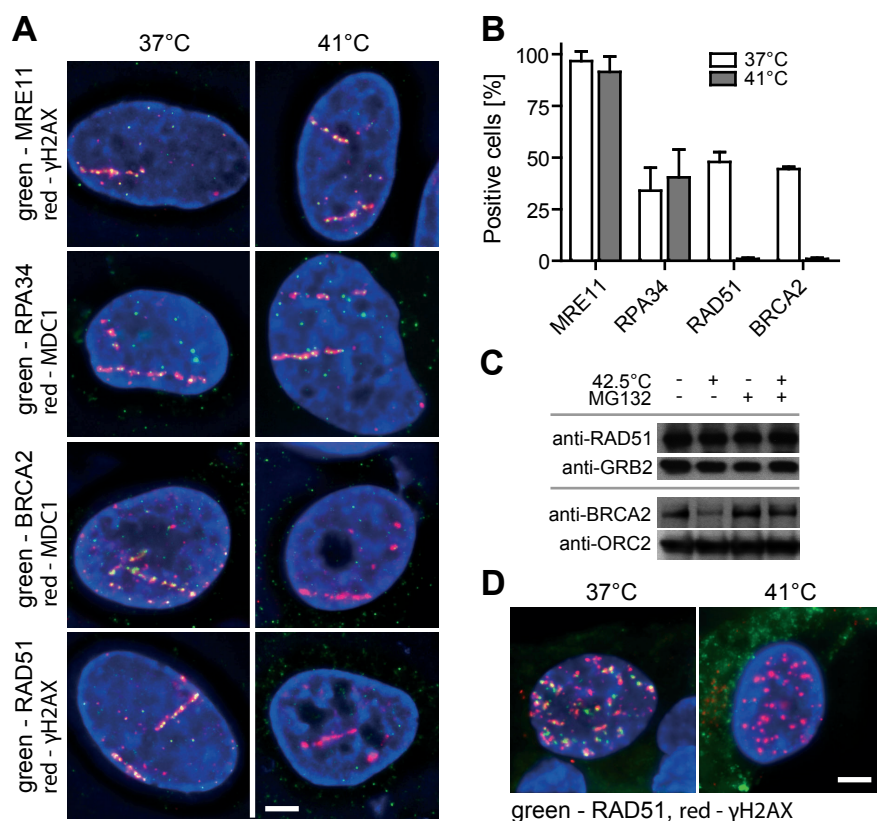


**Figure 2. Mild hyperthermia interferes with functions and stability of HR proteins.** (A) Visualization of accumulation of repair proteins at DSB sites in cells preincubated at 37°C or 41°C. U2OS cells were incubated at 37°C or 41°C for 60 min, then irradiated with  $\alpha$ -particles from a source positioned alongside the cells, resulting in linear arrays of DSBs, incubated for 15 min at 37°C and fixed. Cells were stained for DNA (blue),  $\gamma$ H2AX or MDC1 (red), which were used as markers of the DSBs induced by  $\alpha$ -particles, and either of the following proteins: MRE11, RPA34, BRCA2 or RAD51 (green). Scale bar - 5  $\mu$ m. (B) Quantification of accumulation of repair proteins at DSB sites in cells preincubated at 37°C or 41°C. Cells treated and prepared as in (A) were scored as positive if they contained at least 3 IRIF of indicated repair protein co-localizing with either  $\gamma$ H2AX or MDC1 IRIF. Graphs represent average percentages of positive cells. Error bars represent the range of percentages obtained from 2 independent experiments. At least 50 cells containing damage induced by  $\alpha$ -particles were scored per experiment. (C) Immunoblotting of cells subjected to mild hyperthermia and/or proteasome inhibitor. HeLa cells were incubated at 37°C or 42.5°C for 75 min, in the presence or absence of 10  $\mu$ M MG132. Next, cells were lysed and lysates were analyzed by immunoblotting with antibodies against RAD51 (upper panel) or BRCA2 (lower panel). Equal sample loading was verified by probing for GRB2 or ORC2. (D) Visualization of accumulation of RAD51 at DSB sites in cells isolated from cervix carcinoma biopsies preincubated at 37°C or 41°C for 60 min, then irradiated with  $\alpha$ -particles from a source positioned above the cells, incubated for 30 min at 37°C or 41°C and fixed. Cells were stained for DNA (blue),  $\gamma$ H2AX (red) and RAD51 (green). Scale bar - 5  $\mu$ m.

regardless of whether the cells had been preincubated at 41°C (Figure 2A and 2B), suggesting that DSB end resection is unaffected by hyperthermia. In subsequent steps of HR, the RAD51 recombinase forms nucleoprotein filaments on single-stranded DNA with help of BRCA2 [5, 18]. While RAD51 and BRCA2 IRIF could be detected 15 min post-irradiation in control cells, preincubation at 41°C completely abrogated accumulation of both proteins at DSB sites (Figure 2A and 2B). Similarly, hyperthermia prevented formation of RAD51 IRIF at alpha-particle induced DSBs in HeLa, SW-1573 and RKO cells (data not shown) as well as of RAD54-GFP IRIF at alpha-particle and gamma-ray induced DSBs in mouse ES cells (Supplementary Figure 1B). Moreover, preincubation at 41°C abrogated accumulation of RAD51-GFP in V79 cells [19], but not EGFP-KU80 in XR-V15B cells [20] at laser-induced DNA damage (Supplementary Figure 1C and Supplementary Videos 1-2). These results suggest that hyperthermia inhibits the formation of RAD51 nucleoprotein filaments, a pivotal step of HR [5]. This could be due to defects in RAD51 itself or in BRCA2, which is essential for the loading of RAD51 on the proper DNA substrate [21, 22] and the accumulation of RAD51 in IRIF [23, 24].

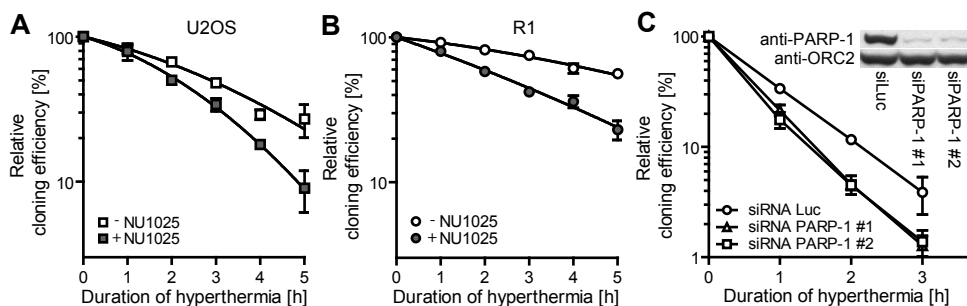


**Figure 3. Mild hyperthermia is toxic to cells lacking PARP-1 functionality.** (A, B) Cloning efficiency of U2OS (A) or R1 (B) cells incubated at 41°C for the indicated period of time in the absence (open symbols) or presence (filled symbols) of 100 μM NU1025. Graphs represent average cloning efficiencies, corrected for the toxicity of NU1025. Error bars represent standard error of the mean from 3 independent experiments. (C) Cloning efficiency of cells with reduced levels of PARP-1 protein subjected to mild hyperthermia. HeLa cells were transfected with siRNA directed against luciferase (circles) or PARP-1 (siRNA #1 – triangles, siRNA #2 – squares) and incubated at 42.5°C for the indicated period of time. Error bars represent standard error of the mean in a single experiment. Figure is representative for 3 independent experiments. Inset shows the efficiency of siRNA-induced reduction of PARP-1 protein levels. Cell lysates were analyzed by immunoblotting with antibodies against PARP-1. Equal sample loading was verified by probing for ORC2.

To establish how these two proteins are affected by mild hyperthermia, we analyzed cell extracts by immunoblotting. Preincubation of HeLa cells at elevated temperature had no detectable effect on RAD51, but did result in considerable reduction of BRCA2 levels (Figure 2C). The latter was also observed in human melanoma cells (BLM) (Supplementary Figure 2A). This reduction can be explained by proteasome-mediated degradation, as we detected no decrease of BRCA2 levels when cells were exposed to 42.5°C in the presence of proteasome inhibitor MG132 [25] (Figure 2C). Importantly, hyperthermia-induced effects on HR proteins were not limited to cultured cells. They were also observed in cells from fresh tumour biopsies and from normal human skin. Mild hyperthermia eliminated accumulation of RAD51 on alpha-particle induced DSBs in biopsies from a cervix carcinoma (Figure 2D). Additionally, reduced levels of BRCA2 were detected by immunoblotting in cells from the part of a skin biopsy incubated at 42.5°C, (Supplementary Figure 2B). Taken together, these results suggest that mild hyperthermia induces degradation of BRCA2 by the proteasome system, resulting in malfunction of HR in human cells, tissues and tumours.

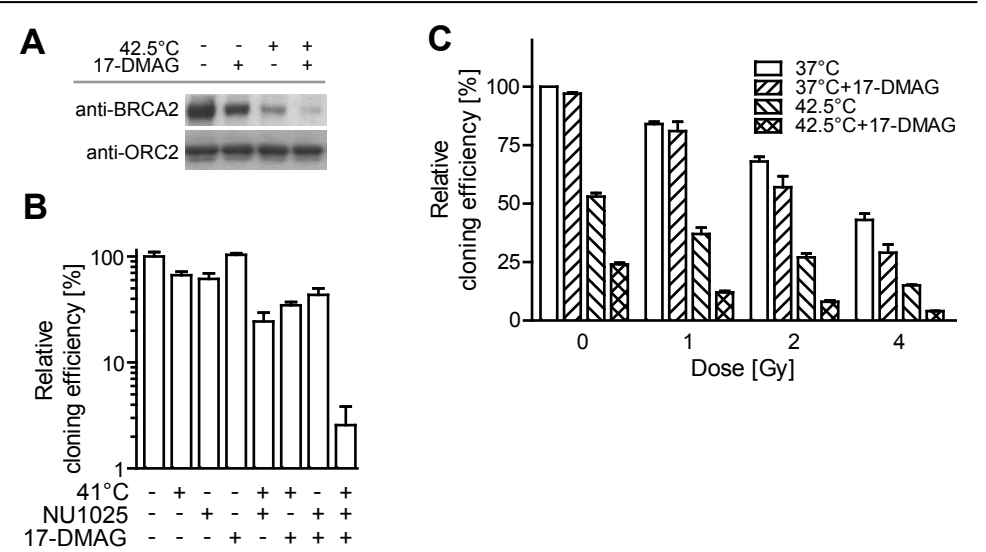


**Figure 4. An HSP90 inhibitor enhances hyperthermia-induced degradation of BRCA2 and sensitivity of hyperthermia-treated cells to PARP-1 inhibitors and to ionizing radiation.** (A) Immunoblotting of cells subjected to mild hyperthermia and/or HSP90 inhibitor. BLM cells have been incubated at 37°C or 42.5°C for 60 min in the presence or absence of 100 nM 17-DMAG. Next, cells were lysed and lysates were analyzed by immunoblotting with antibodies against BRCA2. Equal sample loading was verified by probing for ORC2. (B) Cloning efficiency of R1 cells incubated for the indicated period of time at 41°C in the presence or absence of 100 µM NU1025 and/or 100 nM 17-DMAG. Error bars represent the range of cloning efficiencies obtained in 2 independent experiments. (C) Cloning efficiency of HeLa cells incubated for 75 min at 42.5 or 37°C and subsequently exposed to the indicated dose of γ-rays, in the presence or absence of 100 nM 17-DMAG. Error bars represent standard error of the mean from 3 independent experiments.

HR-deficient cell lines and tumours, particularly those defective in BRCA2, are extremely sensitive to replication-dependent DSBs caused indirectly by PARP-1 inhibitors [3, 4]. Therefore, we hypothesized that inhibition of HR by mild hyperthermia would increase the cytotoxicity of PARP-1 inhibitors in innately HR-proficient cells. As predicted, we observed a decrease in clonogenic survival of human U2OS (Figure 3C) and rat R1 (Figure 3B) cells incubated at 41°C in the presence of the PARP-1 inhibitor NU1025 [26], as compared to cells subjected to hyperthermia alone. To confirm that reduced PARP-1 activity sensitizes cells to hyperthermia, we analyzed cytotoxic effects of hyperthermia on HeLa cells in which PARP-1 was down-regulated by siRNA. Incubation at elevated temperature resulted in diminished survival of these cells, in line with the results obtained with U2OS and R1 cells (Figure 3C).

A battery of HSPs protects proteins from mis- or unfolding induced by heat [27]. BRCA2 is a known client protein of HSP90 and inhibition of HSP90 by the geldanamycin derivative 17-DMAG reduces the level of BRCA2 and down-regulates the DNA damage response [28, 29]. Based on our results, we reasoned that inhibition of HSP90 might enhance the hyperthermia-mediated degradation of BRCA2 and inhibition of HR. As predicted, levels of BRCA2 protein (Figure 4A) and the efficiency of HR-mediated gene targeting (Figure 1C) were further reduced in cells treated with hyperthermia in the presence of 17-DMAG, as compared to those heated in the absence of 17-DMAG or incubated with 17-DMAG at 37°C. These results show that BRCA2 is highly prone to degradation in cells exposed to mild hyperthermia in the absence of the protective activities of HSP90. As a consequence, inhibition of HSP90 should also enhance the cytotoxic effects of PARP-1 inhibition in hyperthermia-treated cells. Indeed, the clonogenic survival of rat R1 cells incubated at 41°C was dramatically (~50 fold) reduced when they were treated in the presence of NU1025 and 17-DMAG (Figure 4B). Moreover, our results suggest that by inhibiting HR, the combination of 17-DMAG and hyperthermia should sensitize cells to ionizing radiation exposure. Indeed, mild hyperthermia applied in the presence of 17-DMAG decreased the clonogenic survival of irradiated HeLa cells by 7- to 10-fold as compared to no treatment and by 3- to 4-fold as compared to hyperthermia treatment alone (Figure 4C).

The results presented here indicate that clinically-relevant, mild hyperthermia targets HR by inducing degradation of BRCA2, a key HR factor. We cannot rule out that higher temperatures or prolonged treatments may affect other components of DSB repair pathways. This could explain reports revealing that heat can radiosensitize cells harboring defects in NHEJ or in both repair pathways [30-35]. We show that impairment of HR by hyperthermia can be enhanced significantly by HSP inhibitor. Importantly, our results suggest that heat exposure alone or in combination with HSP inhibitors can be used to locally introduce BRCA2 deficiency and thereby render HR-proficient tumour cells highly sensitive to PARP-1 inhibitors. Our results might have direct clinical relevance since it has recently been demonstrated in clinical trials that HSP90 and PARP-1 inhibitors are generally safe [36, 37]. Moreover, because our approach is not based on genetic deficiency, as is the case in hereditary BRCA2-deficient tumours, it is not likely to exert selective

pressure, which might lead to development of resistance to the inhibitor [38, 39]. Additionally, we demonstrate that hyperthermia in combination with the HSP90 inhibitor 17-DMAG efficiently sensitizes cells to ionizing radiation. These results provide a rational basis for development of therapies exploiting local induction of HR deficiency in combination with PARP-1 inhibitors, ionizing radiation or other DSB-inducing chemotherapeutic agents.

## Acknowledgements

We would like to thank E. Appeldoorn and P. van Heijningen for experimental support, Dr D. van Gent for providing the EGFP-KU80 expressing cells and Dr T. ten Hagen for providing the BLM cells. This work was supported by the European Commission (Integrated Project 512113 / DNA Repair and STREP ZNIP) and grants from the Netherlands Organization for Scientific Research (NWO), Netherlands Genomics Initiative/NWO, the Maurits and Anna de Kock foundation and the Dutch Cancer Society.

## Materials and methods

**Cell culture.** Embryonic stem (ES) cells were cultured on gelatin-coated dishes in a 1:1 mixture of Dulbecco's modified Eagle's medium (DMEM) and buffalo rat liver conditioned medium, supplemented with 10% FBS (Hyclone), 0.1 mM nonessential amino acids (Biowhittaker), 50 mM  $\beta$ -mercaptoethanol (Sigma) and 500 U ml<sup>-1</sup> leukemia inhibitory factor. Other cells were cultured in following media, supplemented with 10% (v/v) FCS and streptomycin/penicillin: 1:1 mixture of DMEM and Ham's F10 (HeLa), DMEM (human melanoma [40] [BLM], osteosarcoma [U2OS], cervix carcinoma cells), L-15 (human squamous lung carcinoma [SW-1573]), Eagle's MEM (mouse osteosarcoma [MOS], rat rhabdomyosarcoma [R1], V79, XR-V15B), Mc Coy's 5A with 25mM Hepes (human colon cancer [RKO]). Cells were maintained at 37°C in an atmosphere containing 5% (HeLa, BLM), 10% (U2OS, cervix carcinoma cells), 2% (R1, RKO, MOS, V79, XR-V15B) or 0% (SW-1573) CO<sub>2</sub>. Patients with squamous cell carcinoma of the cervix expressed written informed consent to provide fresh biopsies during an investigation under general anesthesia, and use the tumor specimens for this study. This study was approved by the medical ethical committee of the AMC (MEC # 03/137). The biopsies were minced using scalpel, then incubated in Liberase Blendzyme enzyme cocktail (Roche) in DMEM for 60 min at 37°C and plated on glass coverslips in fresh culture medium. Incubations at elevated temperature were performed in a heated waterbath or in an incubator set to required temperature, in an atmosphere containing appropriate CO<sub>2</sub> concentration.

**Antibodies.** Following antibodies were used for western blotting: rabbit (#PC146) and mouse (#OP95) anti-BRCA2 (Ab-1, Calbiochem), rabbit anti-RAD51 [41], rabbit anti-XRCC3 (ab6494, Abcam), rabbit anti-ORC2 (#559266) and mouse anti-GRB2 (#610112) (BD Pharmingen), mouse anti-PARP-1 (C2-10, Alexis Biochemicals) and relevant horseradish peroxidase-conjugated secondary antibodies (Jackson ImmunoResearch).

Following antibodies were used for immunofluorescence: mouse-anti BRCA2 (Ab-1, Calbiochem), mouse-anti RPA34 (Ab-2, Oncogene), mouse anti- $\gamma$ H2AX (05-636, Milipore), rabbit anti-MDC1 (A300-051A, Bethyl Laboratories), rabbit anti-RAD51 [41], rabbit anti-MRE11 [42], goat anti-mouse-Cy3, (115-165-166) and goat anti-rabbit-FITC (111-095-144) (Jackson ImmunoResearch).

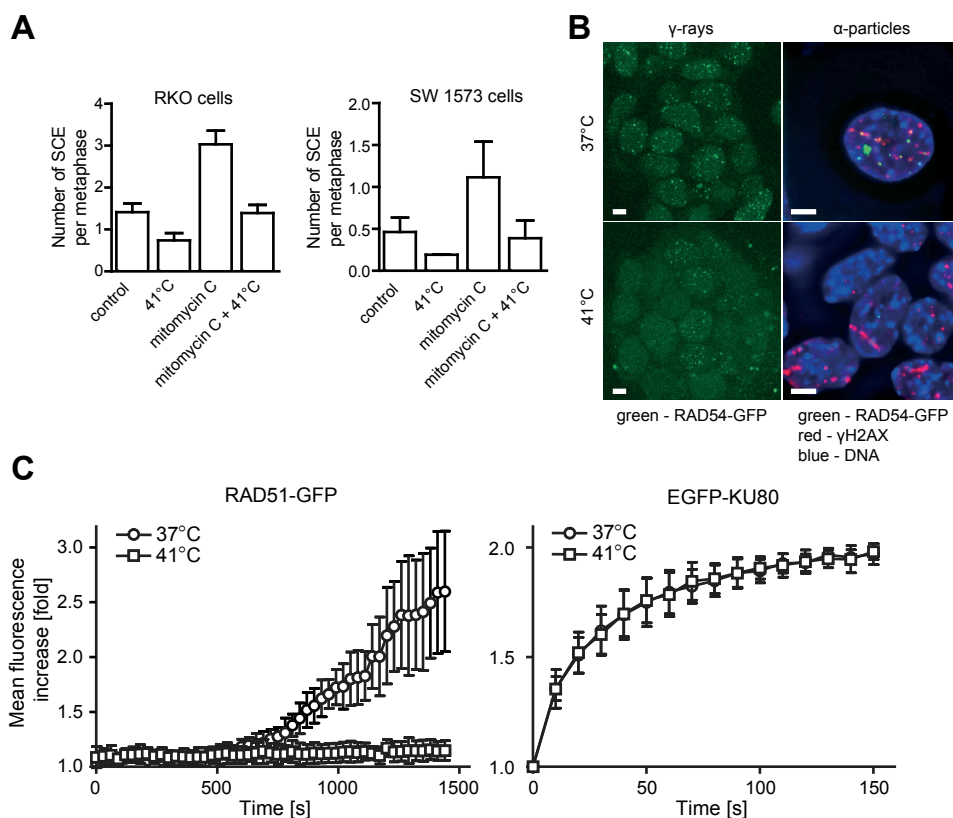
**Chemical agents.** The following chemical agents were used at the indicated final concentrations: 17-DMAG, 100 nM, NU1025, 100  $\mu$ M, mitomycin C, 0.01  $\mu$ g/ml, BrdU, 10  $\mu$ M, colcemid, 0.1  $\mu$ g/ml (all from Sigma-Aldrich), MG-132, 10  $\mu$ M (Calbiochem).

**Tissue/cell lysis and immunoblotting.** Cells were lysed in SDS sample buffer (2% SDS, 10% glycerol, 60 mM Tris-HCl pH 6.8). Skin tissue was lysed in SDS sample buffer, supplemented with protease inhibitor (Roche) and homogenized 2 x 3 min at 30 Hz in Tissue Lyser II (Qiagen) with 5 mm stainless steel beads (Qiagen), on ice. After centrifugation, the supernatant was supplemented with Benzonuclease (Merck), incubated for 10 min at room temperature and 5 min at 95°C. Protein concentration was determined by the Lowry protein assay, extracts were supplemented with 0.5%  $\beta$ -mercaptoethanol and 0.02% bromophenol blue. After fractionation by SDS-PAGE, proteins were transferred to a nitrocellulose membrane and probed with the relevant antibodies. For immunoblotting of BRCA2, a 3-8% Tris-acetate gel system was used. BRCA2 was transferred onto a PVDF membrane.

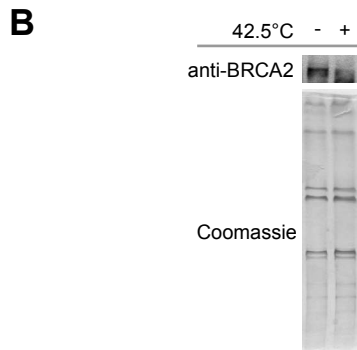
**siRNA treatment.** Transfection of siRNA duplexes was carried out using Lipofectamine 2000 (Invitrogen) according to the manufacturer's instructions. Cells transfected with 200 pmol siRNA per 60-mm culture dish were used for cloning efficiency assays or immunoblotting 48 h after transfection. Sense sequences of siRNA were GAAAGUGUGUCCAACUAAUUUdTdT (#1) and GAAGUCAUCGAUAUCUUUAdTdT (#2) against PARP-1 [43], GGACCUGAAUCCAGAAUUUU against XRCC3 [44] and CGUACGCGGAUACUUCGAdTdT against luciferase.

**Clonogenic assays.** In experiments involving NU1025 or irradiation, cells were trypsinized, counted and plated at appropriate concentrations into 60- or 35 mm dishes. After a 4-6 h attachment period, if required, cells were irradiated, incubated at various temperatures for various periods of time in the presence or absence of the indicated inhibitors. Cells were then incubated for 7-14 days, fixed, stained and colonies exceeding 50 cells were counted. NU1025 was added to the cells 24 h before seeding and remained present during the entire duration of the experiment. In experiments involving a combination of NU1025 and 17-DMAG, cells were first treated as indicated and subsequently trypsinized, counted and plated at various concentrations. 17-DMAG was added to the cells 1 h prior to and removed 30-60 min after the incubation at elevated temperature.

**Gene targeting efficiency and sister-chromatid exchange assays.** The gene targeting assay has been described previously [12, 45]. Cells were incubated at elevated temperature from 2 h prior to transfection until 5 h post transfection. 17-DMAG was added 4 h prior to the hyperthermia treatment and removed 5 h after transfection. The sister-chromatid exchange assay was performed as published before [46].



**Supplementary Figure 1. Mild hyperthermia interferes with HR.** (A) Influence of mild hyperthermia on the frequencies of spontaneous and mitomycin C-induced sister-chromatid exchanges. RKO (left panel) or SW-1573 (right panel) cells were incubated for 2 cell cycles in the presence of BrdU, then for 60 min in the presence or absence of mitomycin C at 37°C or 41°C and processed to obtain metaphase spreads. Graph presents average number of sister-chromatid exchanges (SCE) per scored metaphase. Error bars indicate standard error of the mean obtained from 3 independent experiments. (B) Influence of mild hyperthermia on accumulation of RAD54-GFP at DSB sites. Mouse knock-in ES cells expressing RAD54-GFP were incubated at 37°C or 41°C for 75 min, then irradiated with γ-rays (8Gy, left column) or α-particles (right column) and fixed 30 min after irradiation. Cells were then either directly imaged using a confocal microscope, (left column) or stained for γH2AX and DNA and imaged using a wide-field fluorescence microscope (right column). Scale bar - 5 μm. (C) Quantification of accumulation of GFP-RAD51 and EGFP-KU80 at sites of DNA damage induced by UVA laser microirradiation in living cells preincubated at 37°C or 41°C. V79 cells expressing GFP-RAD51 (left panel) and XR-V15B cells expressing EGFP-KU80 (right panel)



1. Kampinga, H.H. and E. Dikomey, *Hyperthermic radiosensitization: mode of action and clinical relevance*. Int J Radiat Biol, 2001. **77**(4): p. 399-408.
2. Iliakis, G., W. Wu, and M. Wang, *DNA double strand break repair inhibition as a cause of heat radiosensitization: re-evaluation considering backup pathways of NHEJ*. Int J Hyperthermia, 2008. **24**(1): p. 17-29.
3. Farmer, H., et al., *Targeting the DNA repair defect in BRCA mutant cells as a therapeutic strategy*. Nature, 2005. **434**(7035): p. 917-21.
4. Bryant, H.E., et al., *Specific killing of BRCA2-deficient tumours with inhibitors of poly(ADP-ribose) polymerase*. Nature, 2005. **434**(7035): p. 913-7.
5. San Filippo, J., P. Sung, and H. Klein, *Mechanism of eukaryotic homologous recombination*. Annu Rev Biochem, 2008. **77**: p. 229-57.
6. Weterings, E. and D.J. Chen, *The endless tale of non-homologous end-joining*. Cell Res, 2008. **18**(1): p. 114-24.
7. O'Connor, M.J., N.M. Martin, and G.C. Smith, *Targeted cancer therapies based on the inhibition of DNA strand break repair*. Oncogene, 2007. **26**(56): p. 7816-24.
8. Hoeijmakers, J.H., *Genome maintenance mechanisms for preventing cancer*. Nature,

2001. **411**(6835): p. 366-74.
9. Moyer, H.R. and K.A. Delman, *The role of hyperthermia in optimizing tumor response to regional therapy*. Int J Hyperthermia, 2008. **24**(3): p. 251-61.
10. Kampinga, H.H., J.R. Dynlacht, and E. Dikomey, *Mechanism of radiosensitization by hyperthermia (> or = 43 degrees C) as derived from studies with DNA repair defective mutant cell lines*. Int J Hyperthermia, 2004. **20**(2): p. 131-9.
11. Myerson, R.J., et al., *Modelling heat-induced radiosensitization: clinical implications*. Int J Hyperthermia, 2004. **20**(2): p. 201-12.
12. Budzowska, M., et al., *Mutation of the mouse Rad17 gene leads to embryonic lethality and reveals a role in DNA damage-dependent recombination*. Embo J, 2004. **23**(17): p. 3548-58.
13. Sonoda, E., et al., *Sister chromatid exchanges are mediated by homologous recombination in vertebrate cells*. Mol Cell Biol, 1999. **19**(7): p. 5166-9.
14. Bekker-Jensen, S., et al., *Spatial organization of the mammalian genome surveillance machinery in response to DNA strand breaks*. J Cell Biol, 2006. **173**(2): p. 195-206.
15. Stap, J., et al., *Induction of linear tracks of DNA double-strand breaks by alpha-particle irradiation of cells*. Nat Methods, 2008. **5**(3): p. 261-6.
16. D'Amours, D. and S.P. Jackson, *The Mre11 complex: at the crossroads of dna repair and checkpoint signalling*. Nat Rev Mol Cell Biol, 2002. **3**(5): p. 317-27.
17. Sartori, A.A., et al., *Human CtIP promotes DNA end resection*. Nature, 2007. **450**(7169): p. 509-14.
18. Thorslund, T. and S.C. West, *BRCA2: a universal recombinase regulator*. Oncogene, 2007. **26**(56): p. 7720-30.
19. Essers, J., et al., *Nuclear dynamics of RAD52 group homologous recombination proteins in response to DNA damage*. Embo J, 2002. **21**(8): p. 2030-7.
20. Mari, P.O., et al., *Dynamic assembly of end-joining complexes requires interaction between Ku70/80 and XRCC4*. Proc Natl Acad Sci U S A, 2006. **103**(49): p. 18597-602.
21. Chen, Z., H. Yang, and N.P. Pavletich, *Mechanism of homologous recombination from the RecA-ssDNA/dsDNA structures*. Nature, 2008. **453**(7194): p. 489-4.
22. San Filippo, J., et al., *Recombination mediator and Rad51 targeting activities of a human BRCA2 polypeptide*. J Biol Chem, 2006. **281**(17): p. 11649-57.
23. Jasin, M., *Homologous repair of DNA damage and tumorigenesis: the BRCA connection*. Oncogene, 2002. **21**(58): p. 8981-93.
24. Yuan, S.S., et al., *BRCA2 is required for ionizing radiation-induced assembly of Rad51 complex in vivo*. Cancer Res, 1999. **59**(15): p. 3547-51.
25. Lee, D.H. and A.L. Goldberg, *Proteasome inhibitors: valuable new tools for cell biologists*. Trends Cell Biol, 1998. **8**(10): p. 397-403.
26. Bowman, K.J., et al., *Differential effects of the poly (ADP-ribose) polymerase (PARP) inhibitor NU1025 on topoisomerase I and II inhibitor cytotoxicity in L1210 cells in vitro*. Br J Cancer, 2001. **84**(1): p. 106-12.
27. Riezman, H., *Why do cells require heat shock proteins to survive heat stress?* Cell Cycle,

2004. **3**(1): p. 61-3.
28. Noguchi, M., et al., *Inhibition of homologous recombination repair in irradiated tumor cells pretreated with Hsp90 inhibitor 17-allylamino-17-demethoxygeldanamycin*. Biochem Biophys Res Commun, 2006. **351**(3): p. 658-63.
29. Dote, H., et al., *Inhibition of hsp90 compromises the DNA damage response to radiation*. Cancer Res, 2006. **66**(18): p. 9211-20.
30. Raaphorst, G.P., M. Thakar, and C.E. Ng, *Thermal radiosensitization in two pairs of CHO wild-type and radiation-sensitive mutant cell lines*. Int J Hyperthermia, 1993. **9**(3): p. 383-91.
31. Kampinga, H.H., et al., *Thermal radiosensitization in heat- and radiation-sensitive mutants of CHO cells*. Int J Radiat Biol, 1993. **64**(2): p. 225-30.
32. Dynlacht, J.R., et al., *The non-homologous end-joining pathway is not involved in the radiosensitization of mammalian cells by heat shock*. J Cell Physiol, 2003. **196**(3): p. 557-64.
33. Yin, H.L., et al., *Radiosensitization by hyperthermia in the chicken B-lymphocyte cell line DT40 and its derivatives lacking nonhomologous end joining and/or homologous recombination pathways of DNA double-strand break repair*. Radiat Res, 2004. **162**(4): p. 433-41.
34. Raaphorst, G.P., J. Maude-Leblanc, and L. Li, *Evaluation of recombination repair pathways in thermal radiosensitization*. Radiat Res, 2004. **161**(2): p. 215-8.
35. Iliakis, G. and R. Seamer, *A DNA double-strand break repair-deficient mutant of CHO cells shows reduced radiosensitization after exposure to hyperthermic temperatures in the plateau phase of growth*. Int J Hyperthermia, 1990. **6**(4): p. 801-12.
36. Plummer, R., et al., *Phase I study of the poly(ADP-ribose) polymerase inhibitor, AG014699, in combination with temozolomide in patients with advanced solid tumors*. Clin Cancer Res, 2008. **14**(23): p. 7917-23.
37. Modi, S., et al., *Combination of trastuzumab and tanespimycin (17-AAG, KOS-953) is safe and active in trastuzumab-refractory HER-2 overexpressing breast cancer: a phase I dose-escalation study*. J Clin Oncol, 2007. **25**(34): p. 5410-7.
38. Sakai, W., et al., *Secondary mutations as a mechanism of cisplatin resistance in BRCA2-mutated cancers*. Nature, 2008. **451**(7182): p. 1116-20.
39. Edwards, S.L., et al., *Resistance to therapy caused by intragenic deletion in BRCA2*. Nature, 2008. **451**(7182): p. 1111-5.
40. Quax, P.H., et al., *Metastatic behavior of human melanoma cell lines in nude mice correlates with urokinase-type plasminogen activator, its type-1 inhibitor, and urokinase-mediated matrix degradation*. J Cell Biol, 1991. **115**(1): p. 191-9.
41. Essers, J., et al., *Analysis of mouse Rad54 expression and its implications for homologous recombination*. DNA Repair (Amst), 2002. **1**(10): p. 779-93.
42. de Jager, M., et al., *DNA-binding and strand-annealing activities of human Mre11: implications for its roles in DNA double-strand break repair pathways*. Nucleic Acids Res, 2001. **29**(6): p. 1317-25.

43. Mathieu, J., et al., *A PARP-1/JNK1 cascade participates in the synergistic apoptotic effect of TNFalpha and all-trans retinoic acid in APL cells*. *Oncogene*, 2008. **27**(24): p. 3361-70.
44. Modesti, M., et al., *RAD51AP1 is a structure-specific DNA binding protein that stimulates joint molecule formation during RAD51-mediated homologous recombination*. *Mol Cell*, 2007. **28**(3): p. 468-81.
45. Essers, J., et al., *Disruption of mouse RAD54 reduces ionizing radiation resistance and homologous recombination*. *Cell*, 1997. **89**(2): p. 195-204.
46. Lin, M.S. and O.S. Alf, *Detection of sister chromatid exchanges by 4'-6-diamidino-2-phenylindole fluorescence*. *Chromosoma*, 1976. **57**(3): p. 219-25.



# **Chapter 7**

## **Prevention of thermotolerance after repetitive hyperthermia**

**Berina Eppink, Hanny Odijk, Alex Zelensky, Jeroen Essers and Roland Kanaar**

## **Abstract**

Mild hyperthermia is an anti-cancer therapy that can be applied locally and interferes with homologous recombination repair via degradation of BRCA2. One major limitation for the efficacy of hyperthermia is thermotolerance. Thermotolerance is being defined as the ability of a cell or organism to become resistant to heat stress after a prior sub lethal heat exposure. In this study the relationship between the level of BRCA2 and thermotolerance is investigated. For this purpose the BRCA2 protein level is followed over time and after repeated hyperthermia treatments. We show that while the first application of hyperthermia results in the degradation of BRCA2, a second application does not lead to the same extent of degradation. Concomitantly, the second hyperthermia treatment does not inhibit homologous recombination nor induce radiosensitization. Finally, we show that the HSP90 inhibitor 17-DMAG mitigates the stabilizing effect of the second hyperthermia application on BRCA2 and can be used to prevent thermotolerance with regard to radiosensitization. We suggest that the level of BRCA2 is indicative of the effectiveness of hyperthermia treatment and provides a simple assay, as well as a rational basis for development of strategies to circumvent thermotolerance.

## Introduction

Many anti-cancer strategies are based on cytotoxicity of DNA double-strand breaks (DSBs) induced by ionizing radiation or, indirectly, by radiomimetic drugs. However, efficient DSB repair mechanisms protect cells from the genotoxic effects of DSBs, reducing the effectiveness of the therapy. Inhibition of DSB repair processes potentiates the cytotoxicity of DSBs in cancer therapy [1], but at the same time adversely affects normal cells, which need to cope with DSBs arising during normal metabolic activities [2]. Thus, the effectiveness of anti-cancer treatments can be enhanced by preferentially targeting the tumor cells. Hyperthermia is one anti-cancer modality that can be applied locally and, among other processes, interferes with DSB repair (This thesis chapter 6).

Protein damage and denaturation are the main molecular events underlying the biological effects of hyperthermia in the clinically relevant temperature range of 39°C to 45°C [3]. Previously we have shown that mild hyperthermia induces radiosensitization through the proteasome-mediated degradation of BRCA2, a key DSB repair protein (This thesis chapter 6). BRCA2 functions in homologous recombination, a DNA repair pathway that, utilizes intact homologous DNA sequences – usually the sister chromatid in post-replicative chromatin – to faithfully restore DNA damage, including DSBs [4]. The core homologous recombination protein in mammalian cells is RAD51 which is essential for cell viability [5, 6] and mediates strand exchange between the damaged DNA and the repair template. During homologous recombination numerous accessory proteins, or mediators, influence and control the action of RAD51, one of them being BRCA2 [7]. BRCA2 targets RAD51 filament formation to the single-stranded DNA- double-stranded DNA junction on single-stranded DNA [8-10], a critical step during homologous recombination.

Mammalian cells, when exposed to a sub-lethal heat shock, have the ability to acquire a transient resistance to subsequent exposures to elevated temperatures, a phenomenon termed thermotolerance [11]. Thermotolerance occurs within several hrs, lasts 3-5 days and is dependent on time and temperature. During this tolerant state cells are much more heat resistant than cells that have never been exposed to elevated temperatures. Thermotolerance negatively influences the efficacy of hyperthermia, since it results in loss of radiosensitization. The mechanisms underlying thermotolerance are not clear. However, heat shock proteins play important roles in modulating cellular responses to heat shock and their actions are implicated in the development of thermotolerance [12]. The levels of heat shock proteins, especially HSP70 and HSP90, rise and fall following heating [13].

Here we investigate the relationship between BRCA2 protein levels and thermotolerance. We measured relative levels of the BRCA2 protein over time after repeated hyperthermia treatments. We show that once recovered from the first hyperthermia treatment, BRCA2 levels are no longer reduced by a second treatment. The heat resistant BRCA2 protein is functional in homologous recombination and its level provides an indication for the efficiency of radiosensitization and whether or not thermotolerance will occur. Finally, we demonstrate that thermotolerance can be circumvented by treating cells with the HSP inhibitor 17-DMAG. Treatment of cells with

this compound results in degradation of BRCA2 even by the second hyperthermia treatment and thereby alleviates the inability of a second round of hyperthermia to induce radiosensitization.

## Results

### **Levels of BRCA2 correspond to effectiveness of hyperthermia with regard to radiosensitization**

Upon application of hyperthermia (42.5°C) BRCA2 undergoes proteasome-mediated degradation (This thesis chapter 6). To get insight in the temperature and time dependence of BRCA2 degradation we compared hyperthermia mediated BRCA2 degradation at 41°C for four hours (Figure 1A) with 42.5°C for 75 minutes. At 42.5°C more BRCA2 was degraded in less time than at 41°C, indicating that the extent of BRCA2 degradation is dependent on temperature. Furthermore, we monitored the recovery of BRCA2 protein levels over a time period of 24 hrs, to get insight in the duration of the suppression of BRCA2 protein levels. BRCA2 levels recovered within 24 hrs and even reached a higher level than before hyperthermia treatment (Figure 1B). Upon an additional application of hyperthermia the BRCA2 level dropped again (Figure 1C). However, since the second application of hyperthermia is to cells that already have a higher BRCA2 level, the resulting lower level after the second application of hyperthermia is similar to that of untreated cells (Figure 1C). These levels suggest that directly after the repeated hyperthermia treatment cells should display normal levels of homologous recombination and no radiosensitization. To test this hypothesis, we first measured the effect of the second round of hyperthermia on the efficiency of homologous recombination. We quantified homologous recombination-mediated gene targeting in mouse embryonic stem (mES) cells. Cells treated only once with hyperthermia, which reduces gene targeting efficiency, were used as a control (This thesis chapter 6). Indeed, gene targeting was reduced in efficiency when measured directly after hyperthermia treatment (Figure 1D). However, the efficiency of gene targeting measured in cells 24 hrs after a single hyperthermia treatment was higher compared to non-treated cells, correlating with the increased BRCA2 level. Next, we subjected cells to two rounds of hyperthermia, spaced by 24 hrs. Targeting efficiency, measured directly after the second treatment, decreased compared to 24 hrs after a single treatment, but only to an efficiency comparable to that of non-treated cells (Figure 1D). We conclude that immediately after a second hyperthermia treatment homologous recombination is operational, indicating that the degradation-resistant BRCA2 protein is functional. Furthermore, these results show that the repressive effect of hyperthermia on homologous recombination correlates with the level of BRCA2.

After repeated hyperthermia treatment cells adapt to the temperature up-shift and acquire a state of thermotolerance. The efficiency of radiosensitization is affected by thermotolerance and can be used as a measure to monitor the effectiveness of hyperthermia after repetitive treatments.

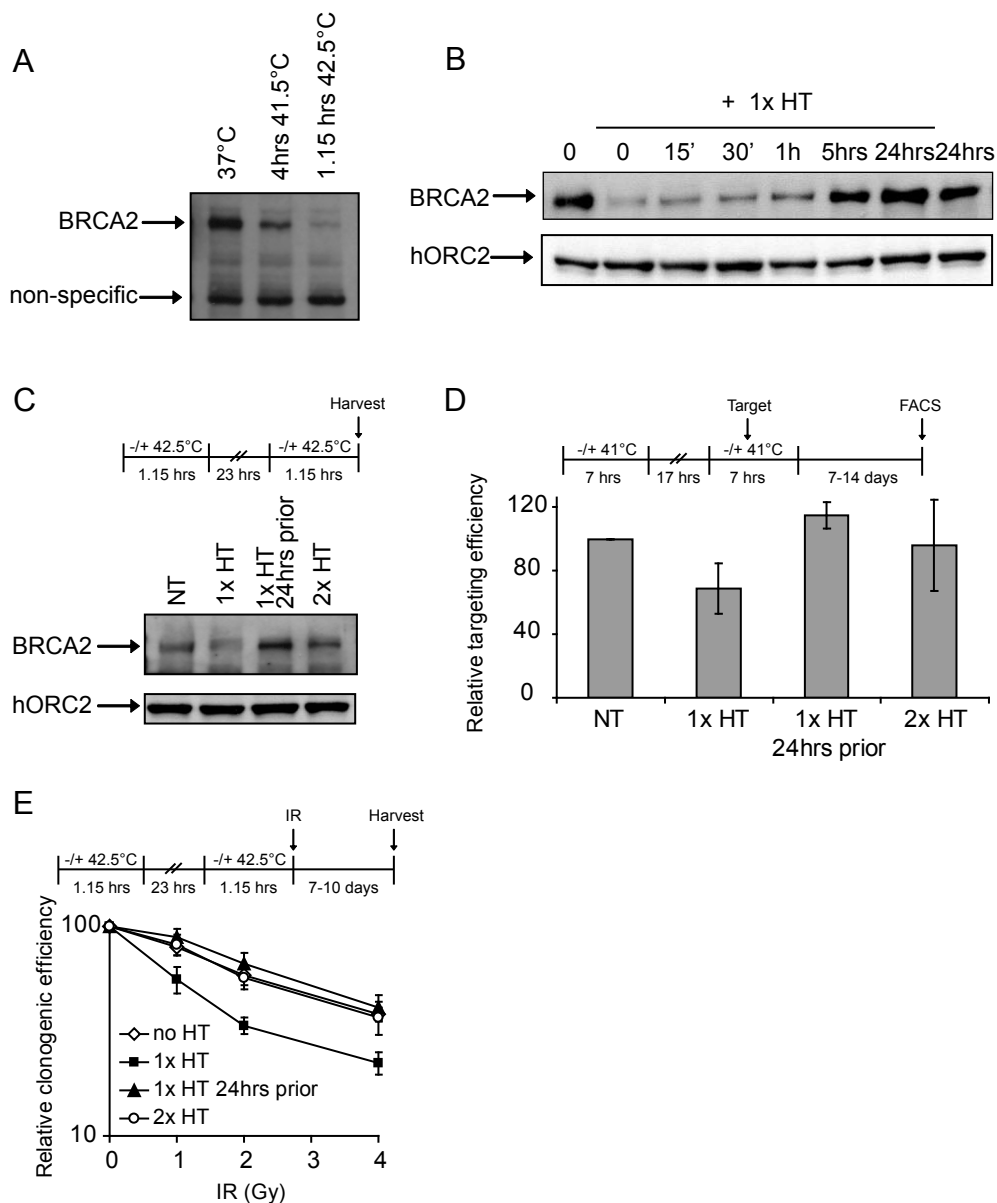


**Figure 1. The level of BRCA2 corresponds to effectiveness of hyperthermia in response to radiosensitization.** Mild hyperthermia induces degradation of BRCA2. **(A)** Immunoblotting of cells subjected to mild hyperthermia. Extracts from BLM cells incubated at 37°C, 41.5°C for 4 hrs or 42.5°C for 75 minutes were blotted and probed with an anti-BRCA2 antibody. Equal sample loading is indicated by a non-specific band. **(B)** Immunoblotting of cells subjected to mild hyperthermia. BLM cells were incubated at 37°C or 42.5°C for 75 min. Next, cells were incubated at 37°C for the indicated period of time (0, 15', 30', 1 hrs, 5 hrs or 24 hrs) and lysed. Lysates were analyzed by immunoblotting and probed with antibodies against BRCA2 (upper panel). Equal sample loading was verified by

probing for ORC2 (lower panel). (C) Immunoblotting of extracts from cells subjected to mild hyperthermia and corresponding to the cells used the clonogenic irradiation survival experiment depicted in panel E. HeLa cells were incubated at 37°C (NT) or 42.5°C for 75 min either once 24 hrs prior irradiation (1x HT 24 hrs prior), once just before irradiation (1x HT) or twice at both time points (2x HT). Next, cells were lysed and lysates were analyzed by immunoblotting with antibodies against BRCA2. In case of two treatments lysates were made directly after the second treatment. Equal sample loading was verified by probing for ORC2 (lower panel). (D) Efficiency of homologous recombination-mediated gene targeting in mouse ES cells as measured by transfection. Cells were incubated for 7 hrs at 37°C (NT) or at 41°C either once 24 hrs prior transfection (1x HT 24 hrs prior), once during transfection (1x HT), or twice, 24 hrs prior and during transfection (2x HT). Two hrs into this first or second incubation period, respectively, cells were transfected with the *hRad54GFP-puro* knock-in targeting construct (Target). Cells containing the integrated construct were then selected in medium containing puromycin and analyzed by FACS for homologous integration. The bar graph shows the relative targeting efficiency under the indicated conditions, obtained from 3 independent experiments. Error bars represent standard error of the mean. (E) Cloning efficiency of HeLa cells incubated at 37°C (open rhombus; NT) or for 75 min at 42.5°C either once 24 hrs prior irradiation (filled triangles; 1x HT 24 hrs prior), once just before irradiation (filled squares; 1x HT) or twice, 24 hrs prior and just before irradiation (open circles; 2x HT) and subsequently exposed to increasing doses (0, 1, 2 and 4 Gy) of  $\gamma$ -rays. Error bars represent standard error of the mean.

---

To investigate whether the level of BRCA2 and the proficiency in recombination are indicative for the effectiveness of radiosensitization we performed clonogenic survival experiments. Cells were treated with hyperthermia and increasing doses of ionizing radiation (IR). Hyperthermia treatment was not given at all (37°C), or once directly before IR treatment or 24 hrs prior to IR treatment. Finally, hyperthermia was applied twice, once 24 hrs prior and once directly before IR treatment (Figure 1E). When hyperthermia was given prior to irradiation, cells were sensitized to IR. When the hyperthermia treatment was given 24 hrs prior to irradiation, no radiosensitization occurred, which is consistent with the level of BRCA2 under those conditions. Furthermore, two subsequent applications of hyperthermia, conditions that should trigger thermotolerance and do not lead to degradation of BRCA2, also did not sensitize cells to irradiation. In conclusion, our results indicate that the level of BRCA2 can be taken as an easy read-out as to whether conditions under which hyperthermia is applied will lead to radiosensitization.

### **Prevention of thermotolerance after repeated hyperthermia**

To get better insight in the duration of the thermotolerant state we followed the level of BRCA2 over time. We monitored BRCA2 after hyperthermia application and tested the impact of a second application of hyperthermia. We applied a second round of hyperthermia 24 or 48 hrs after the first round (Figure 2A and B). To assess this we followed two distinct protocols. In the first approach the cells were grown on plates which were splitted and reseeded every day (Figure 2A). In the second approach, we first generated colonies by starting with single cells which were first grown for five consecutive days into a colony and subsequently treated and harvested on indicated time points (Figure

2B). The reason for these two protocols was that the duration of the procedure made it impossible to maintain an exponentially growing population of cells without replating. Replating might influence the exponentially status of a population of cells for a short period of time. BRCA2 protein levels are highly dependent on an exponentially growing population of cells, since BRCA2 is mostly expressed in S-phase [14, 15], and levels might vary due to replating. For this reason variation in non-treated BRCA2 levels needed to be minimized. In the first approach the culture is maintained exponentially by replating every day at structured time points, minimizing the influence of replating. The second approach resembles tumor formation; a dense population in the middle and an exponentially growing population on the outside. This approach resulted in a balanced population of cells circumventing replating during the experiment and therefore minimizing variation.

Upon treatment the cells grown on plates showed that 48 hrs after hyperthermia BRCA2 levels were not below non-treated levels indicating that the state of thermotolerance persisted for at least 48 hrs (Figure 2A). However the colonies showed that BRCA2 levels were lower than non-treated levels already after 24 hrs (Figure 2B) indicating lack of thermotolerance. This shows a different view compared to the plates, possible due to the influence of the growing procedures, but gives us a useful tool to circumvent BRCA2 levels. In order to test whether these BRCA2 levels in the colonies correlated to the degree of radiosensitization we monitored survival. These colonies were treated with hyperthermia and increasing doses of ionizing radiation. Hyperthermia treatment was not given at all (37°C), or once directly before IR treatment or was applied twice, once 24 hrs prior and once directly before IR treatment (Figure 2C). Repetitive hyperthermia treatment sensitized cells for IR, correlating with the levels of BRCA2 (Figure 2C), further acknowledging that BRCA2 protein levels are indicative for the effectiveness of hyperthermia.

BRCA2 is a known client protein of HSP90 and inhibition of HSP90 by the geldanamycin derivative 17-DMAG reduces the level of BRCA2 and down-regulates the DNA damage response (28, 29). We previously showed that impairment of homologous recombination by hyperthermia is enhanced significantly by the HSP inhibitor (This thesis chapter 6). Therefore, we used 17-DMAG in combination with hyperthermia to test whether we could reduce the level of BRCA2 below that of non-treated cells and whether this would prevent thermotolerance. After a single treatment with either 100 nM 17-DMAG or hyperthermia the level of BRCA2 was reduced (Figure 2D). The combination of 17-DMAG and hyperthermia resulted in a further reduction. Subsequently, hyperthermia was repeated 24 hrs after its first application. No reduction of BRCA2 was observed after the second hyperthermia treatment compared to non-treated cells (Figure 2D). Hyperthermia was also repeated, either in the absence or presence of 17-DMAG, on cells that had between treated with 17-DMAG during the first application of hyperthermia. In this case, the 17-DMAG treatment, either once or twice, resulted in lowering of the BRCA2 level compared to the first combination treatment (Figure 2D).

Next, we tested whether the application of 17-DMAG after the second round of hyperthermia would be able to further decrease cell survival, and in this way circumvent the stage of thermo-tolerance. To this end we performed clonogenic survival assays on samples



of the cells used in the protocol described above. Indeed, we found that while 17-DMAG alone and two rounds of hyperthermia did not reduce the number of colonies, the combination of both further reduced cellular survival, thereby circumventing thermotolerance. These results further demonstrate that BRCA2 protein levels are a good indicator for potential radiosensitization and indirect for thermotolerance.

## **Discussion/ conclusion**

In this study we show that the level of BRCA2 protein is highly regulated upon hyperthermia treatment. The BRCA2 protein level corresponds to a functional protein, and is an indication for the efficiency of radiosensitization and indirect for whether cells will be thermotolerant to irradiation. Furthermore, we describe conditions that circumvent this thermotolerance effect and show that when the level of BRCA2 can be reduced under conditions that normally would trigger thermotolerance, then hyperthermia-induced radiosensitization is again effective.

BRCA2 is a very large protein involved in homologous recombination-mediated DSB repair and in Fanconi anemia-mediated interstrand crosslink repair [16-18]. Previously, we have shown that upon treatment with hyperthermia BRCA2 undergoes proteasomal-mediated degradation (This thesis chapter 6). Here, we show that the extent of BRCA2 degradation is dependent on time and temperature (Figure 1A), correlating with the general idea in the hyperthermia field of the concept of “thermal dose”, which is the effective dose of hyperthermia being a combination of time and temperature [19]. Our results further indicate that the cellular level of BRCA2 correlates with the efficiency of radiosensitization. Of course hyperthermia will affect many cellular processes and we cannot rule out that higher temperatures or prolonged treatments may affect other components of DSB repair pathways, but the correlative regulation of BRCA2 suggests some specificity. After a single hyperthermia treatment over time the level of BRCA2 recovers (Figure 1B), as does homologous recombination efficiency. Thus, the newly expressed BRCA2 protein is functional (Figure 1D). Our findings with regard to regulation of the BRCA2 level by hyperthermia correspond to the finding that the creation of thermotolerance in relationship to radiosensitization is dependent on protein synthesis after the first hyperthermia treatment [20]. This furthermore shows that levels of BRCA2 are under tight regulation, as is the case during the cell cycle. The potential of the cell to regulate its BRCA2 level in response to an external stimulus is not unlike the regulation of BRCA2 during the normal cell cycle [14, 15].

A second hyperthermia treatment does change the level of BRCA2 level, however not to the same extent as after the first application (Figure 1C). By applying hyperthermia twice cells adapt to, and no radiosensitization occurs (Figure 1E), indicating a stage of thermotolerance. During this tolerant state cells are much more heat resistant than cells that have never been exposed to elevated temperatures [11]. In our current experiments thermotolerance is only monitored in correlation with radiosensitization and we cannot rule out the possibility that changes in other proteins affect survival. Our data indicate that

the level of BRCA2 is an indication whether radiosensitization can occur and therefore whether a stage of thermotolerance is created. Hyperthermia treatment renders cells deficient in homologous recombination, which sensitizes them for radiation. However, repeated hyperthermia renders cells homologous recombination proficient resulting in lack of radiosensitization (Figure 1). These results can be a molecular explanation for the effects observed in the clinic, in the effectiveness of hyperthermia.

Thermotolerance is a major problem for the efficacy of hyperthermia applied in the clinic [12]. Understanding the underlying mechanism provides possibilities to circumvent thermotolerance. 17-DMAG may be a very promising tool to prevent thermotolerance (Figure 2 D, E), since we show that 17-DMAG itself causes a reduction in the level of BRCA2, irrespectively of the presence of hyperthermia. In addition, it creates a synergic effect when applied in combination with hyperthermia. Our results reveal that the addition of 17-DMAG in combination with repeated hyperthermia reduces the level of BRCA2 below that of cells treated with hyperthermia alone and these conditions significantly enhance cell killing. Since 17-DMAG is an inhibitor one of the HSP90 heat shock proteins, one of the possible explanations for the effect observed of both 17-DMAG and hyperthermia is that 17-DMAG inhibits the primary heat shock response and prevents binding from HSP90 to BRCA2, rendering BRCA2 instable. Overall our results might have direct clinical relevance since it has recently been demonstrated in clinical trials that HSP90 inhibitors are generally safe [21]. Finally, our results show that the level of BRCA2 is indicative of the effectiveness of hyperthermia treatment and provides a simple assay, as well as a rational basis for development of strategies to circumvent thermotolerance.

## Materials and methods

**Cell culture.** Cells were cultured in a 1:1 mixture of DMEM and Ham's F10 (HeLa) or DMEM (human melanoma [22] [BLM]), both supplemented with 10% (v/v) FCS and streptomycin/penicillin. Cells were maintained at 37°C in an atmosphere containing 5% CO<sub>2</sub>. Incubations at elevated temperature were performed in an incubator set to the required temperature.

**Antibodies.** The following antibodies were used for immuno-blotting: rabbit (#PC146) and mouse (#OP95) anti-BRCA2 (Ab-1, Calbiochem), rabbit anti-ORC2 (#559266) and relevant horseradish peroxidase-conjugated secondary antibodies (Jackson ImmunoResearch).

**Tissue/cell lysis and immunoblotting.** Cells were lysed in SDS sample buffer (2% SDS, 10% glycerol, 60 mM Tris-HCl pH 6.8) and incubated for 5 min at 95°C. Protein concentration was determined by the Lowry protein assay, extracts were supplemented with 0.5%  $\beta$ -mercaptoethanol and 0.02% bromophenol blue. After fractionation by SDS-PAGE, proteins were transferred to a PVDF membrane and probed with the relevant antibodies.

**Survival assays.** For clonogenic survival assays, cells were trypsinized, counted and 150 cells were plated into 60 mm dishes. After a 6 hrs, if cells were required to attach, cells were incubated at various temperatures for various periods of time in the presence or absence of 17-DMAG (Sigma) and subsequently irradiated. Cells were then incubated for 7-14 days, fixed, stained and colonies exceeding 30 cells were counted. 100 nM 17-DMAG was added to the cells 1 hr prior to and removed 1 hr after the incubation at elevated temperature. Cells were irradiated directly after incubation at elevated temperature, by  $\gamma$ -rays from a Cesium source ( $^{137}\text{Cs}$ , 0.70 Gy/min) as described previously [23]. For the experiment done on clones, 500 cells were grown on 10 cm dishes for 5 days before treatment, treated, and subsequently grown for another 7 days before cells were counted (Coulter automated cell counter).

**Gene targeting efficiency.** The gene targeting assay has been described previously [24, 25]. Cells were incubated at elevated temperature from 2 hrs prior to transfection until 5 hrs post transfection.

## References

1. O'Connor, M.J., N.M. Martin, and G.C. Smith, *Targeted cancer therapies based on the inhibition of DNA strand break repair*. *Oncogene*, 2007. **26**(56): p. 7816-24.
2. Hoeijmakers, J.H., *Genome maintenance mechanisms for preventing cancer*. *Nature*, 2001. **411**(6835): p. 366-74.
3. Lepock, J.R., *Role of nuclear protein denaturation and aggregation in thermal radiosensitization*. *Int J Hyperthermia*, 2004. **20**(2): p. 115-30.
4. San Filippo, J., P. Sung, and H. Klein, *Mechanism of eukaryotic homologous recombination*. *Annu Rev Biochem*, 2008. **77**: p. 229-57.
5. Lim, D.S. and P. Hasty, *A mutation in mouse rad51 results in an early embryonic lethal that is suppressed by a mutation in p53*. *Mol Cell Biol*, 1996. **16**(12): p. 7133-43.
6. Tsuzuki, T., et al., *Targeted disruption of the Rad51 gene leads to lethality in embryonic mice*. *Proc Natl Acad Sci U S A*, 1996. **93**(13): p. 6236-40.
7. Sung, P., et al., *Rad51 recombinase and recombination mediators*. *J Biol Chem*, 2003. **278**(44): p. 42729-32.
8. Yang, H., et al., *The BRCA2 homologue Brh2 nucleates RAD51 filament formation at a dsDNA-ssDNA junction*. *Nature*, 2005. **433**(7026): p. 653-7.
9. San Filippo, J., et al., *Recombination mediator and Rad51 targeting activities of a human BRCA2 polypeptide*. *J Biol Chem*, 2006. **281**(17): p. 11649-57.
10. Yang, H., et al., *BRCA2 function in DNA binding and recombination from a BRCA2-DSS1-ssDNA structure*. *Science*, 2002. **297**(5588): p. 1837-48.
11. Henle, K.J. and L.A. Dethlefsen, *Heat fractionation and thermotolerance: a review*. *Cancer Res*, 1978. **38**(7): p. 1843-51.
12. Li, G.C., N.F. Mivechi, and G. Weitzel, *Heat shock proteins, thermotolerance, and their relevance to clinical hyperthermia*. *Int J Hyperthermia*, 1995. **11**(4): p. 459-88.

13. Landry, J., et al., *Synthesis and degradation of heat shock proteins during development and decay of thermotolerance*. Cancer Res, 1982. **42**(6): p. 2457-61.
14. Su, L.K., et al., *Characterization of BRCA2: temperature sensitivity of detection and cell-cycle regulated expression*. Oncogene, 1998. **17**(18): p. 2377-81.
15. Vaughn, J.P., et al., *Cell cycle control of BRCA2*. Cancer Res, 1996. **56**(20): p. 4590-4.
16. Thorslund, T. and S.C. West, *BRCA2: a universal recombinase regulator*. Oncogene, 2007. **26**(56): p. 7720-30.
17. Li, X. and W.D. Heyer, *Homologous recombination in DNA repair and DNA damage tolerance*. Cell Res, 2008. **18**(1): p. 99-113.
18. Thompson, L.H. and J.M. Hinz, *Cellular and molecular consequences of defective Fanconi anemia proteins in replication-coupled DNA repair: mechanistic insights*. Mutat Res, 2009. **668**(1-2): p. 54-72.
19. Roti Roti, J.L., *Cellular responses to hyperthermia (40-46 degrees C): cell killing and molecular events*. Int J Hyperthermia, 2008. **24**(1): p. 3-15.
20. Armour, E., et al., *Thermotolerance and radiation sensitizing effects of long duration, mild temperature hyperthermia*. Int J Hyperthermia, 1994. **10**(3): p. 315-24.
21. Plummer, R., et al., *Phase I study of the poly(ADP-ribose) polymerase inhibitor, AG014699, in combination with temozolomide in patients with advanced solid tumors*. Clin Cancer Res, 2008. **14**(23): p. 7917-23.
22. Quax, P.H., et al., *Metastatic behavior of human melanoma cell lines in nude mice correlates with urokinase-type plasminogen activator, its type-1 inhibitor, and urokinase-mediated matrix degradation*. J Cell Biol, 1991. **115**(1): p. 191-9.
23. Stap, J., et al., *Induction of linear tracks of DNA double-strand breaks by alpha-particle irradiation of cells*. Nat Methods, 2008. **5**(3): p. 261-6.
24. Budzowska, M., et al., *Mutation of the mouse Rad17 gene leads to embryonic lethality and reveals a role in DNA damage-dependent recombination*. Embo J, 2004. **23**(17): p. 3548-58.
25. Essers, J., et al., *Disruption of mouse RAD54 reduces ionizing radiation resistance and homologous recombination*. Cell, 1997. **89**(2): p. 195-204.





## List of abbreviations

AP site	Apurinic or apyrimidinic site	NER	Nucleotide excision repair
ATM	Ataxia–telangiectasia mutated	NHEJ	Non-homologous end-joining
BER	Base excision repair	PAR	ADP-ribose polymer
BrdU	Bromodeoxyuridine	PARP-1	Poly-ADP-ribose polymerase-1
CldU	Chlorodeoxyuridine	PCNA	Proliferating cell nuclear antigen
CPD	Cyclobutyl pyrimidine dimers	PFGE	Pulsed field gel electrophoresis
CS	Cockayne syndrome	PI	Propidium iodide
DDR	DNA damage response	PIKKs	Phosphoinositide 3-kinase-like kinases
D-Loop	Displacement loop	PTM	Post translational modification
DNA	Deoxyribonucleic acid	RFC	Replication factor C
DSBs	DNA double-strand breaks	RNF	Ring finger protein
FACS	Fluorescence-activated cell sorting	RPA	Replication protein A
FCS	Fluorescence correlation spectroscopy	SDSA	Synthesis dependent strand annealing
FEN1	Flap endonuclease 1	SSBs	Single-stranded breaks
FRAP	Fluorescent recovery after photobleaching	TC-NER	Transcription coupled nucleotide excision repair
GC	Gene conversion	TLS	DNA translesion synthesis
GG-NER	Global-genome nucleotide excision repair	TTD	Trichothiodystrophy
GFP	Green fluorescent protein	UV	Ultraviolet
HR	Homologous recombination	XP	Xeroderma pigmentosum
HSP	Heat shock protein	$\gamma$ H2AX	Phosphorylated H2AX
HT	Hyperthermia	6-4PP	Pyrimidine (6-4) pyrimidone photoproduct
ICL	DNA interstrand crosslink		
IdU	Iododeoxyuridine		
IR	Ionizing radiation		
IRIF	Ionizing radiation-induced foci		
mES or ES	Mouse embryonic stem cells		
MMR	Mismatch repair		
MRN	<u>M</u> RE11, <u>R</u> AD50 and <u>N</u> BS1		
mUbH2B	Mono-ubiquitination of human histone H2B		



## Nederlandse samenvatting

DNA is de drager van de erfelijke eigenschappen van cellen, de bouwstenen van het lichaam. DNA bestaat uit twee lange strengen van aaneengesloten nucleotiden, die zich samen buigen tot een dubbele helix. De totale lengte van de DNA strengen, in een menselijke cel is ongeveer twee meter. In het DNA liggen de instructies opgeslagen, die zorg dragen voor het correct functioneren van de lichaamscellen. De integriteit van de DNA keten wordt voortdurend bedreigd door een variëteit aan DNA schade inducerende agentia, welke potentieel schadelijk zijn voor de integriteit van de DNA structuur en de genetische code. Hierbij moet men niet alleen denken aan toxische stoffen en stralingbronnen uit het milieu (bijvoorbeeld röntgen, zonlicht, uitlaatgassen, sigarettenrook of andere chemische middelen) maar ook aan stoffen die vrij komen bij chemische processen in ons eigen lichaam (zoals vrije zuurstofradicalen). Eenvoudige DNA beschadigingen, kunnen vaak gemakkelijk worden gerepareerd. Echter, wanneer deze eenvoudige beschadigingen worden aangetroffen tijdens cellulaire processen zoals transcriptie of replicatie kunnen meer complexe breuken ontstaan zoals enkelstrengs- of dubbelstrengsbreuken. Dubbelstrengsbreuken zijn een van de meest gevaarlijke vormen van DNA beschadigingen, want niet of onnauwkeurig gerepareerde dubbelstrengsbreuken kunnen leiden tot mutaties, wat resulteert in onvolledig replicatie, chromosomale afwijkingen en vervolgens het verlies van de celfunctie en celdood. De herstelcapaciteit van cellen heeft dus een grote invloed op het uiteindelijke effect van de DNA schades. Deze schades worden gerepareerd door verschillende DNA herstel mechanismes, die gecoördineerd worden om de stabiliteit en integriteit van het genoom te handhaven. Het belang van nauwkeurige reparatie van DNA schade wordt weerspiegeld in het feit dat afwijkingen in DNA herstel mechanismes worden geassocieerd met erfelijke aanleg voor de ontwikkeling van kanker. Deze reparatie mechanismes worden besproken in **hoofdstuk 1**.

Er zijn gespecialiseerde DNA reparatie mechanismes voor het herstel van dubbelstrengsbreuken, een daarvan is homologe recombinatie. Homologe recombinatie is de focus van dit proefschrift. Homologe recombinatie is erg belangrijk voor het instant houden van de genetische code, het gebruikt namelijk een homologe DNA streng om de informatie te kopiëren, en voorkomt hierdoor mutaties in de DNA sequentie. Homologe recombinatie gebeurt in drie stappen, eerst wordt de dubbelstrengsbreuk herkend en worden er enkelstrengs uiteinden gevormd. Vervolgens moet er paring plaatsvinden tussen de gebroken streng en zijn intacte zuster streng, dit wordt een “joint” molecuul formatie genoemd. Vanuit deze joint molecuul kan er langs de breuk gekopieerd worden wat vervolgens resulteert in een gerepareerde dubbelstrengsbreuk. RAD51 is het centrale eiwit

in homologe recombinatie, en zorgt voor herkenning van de homologe DNA streng en voor het uitwisselen van deze streng. Een uitgebreid aantal helper eiwitten is betrokken bij de ondersteuning van RAD51 tijdens de verschillende stadia van recombinatie, onder wie BRCA2 en RAD54. Een specifieke cellulair kenmerk van homologe recombinatie-geassocieerde eiwitten is de accumulatie in hoge lokale concentraties op de plekken van DNA schade in subnucleaire structuren ook wel 'foci' genoemd. Homologe recombinatie beperkt zich meestal tot de synthese (S)-fase van de celcyclus, wanneer het DNA wordt gedupliceerd, dit heeft als voordeel dat er een perfect tweede exemplaar aanwezig is (zusterchromatide) voor het kopiëren langs de breuk. Tijdens de S-fase voert de cel replicatie uit en kopieert de cel haar hele genoom. DNA-replicatie is een kwetsbaar proces, omdat onvermijdelijke laesies in het DNA de oorzaak zijn dat de replicatieve polymerase tot stilstand komt. Deze laesies vormen een ernstige bedreiging voor de integriteit van het genoom. Homologe recombinatie en andere processen zoals translesie DNA-synthese (TLS) en de novo herstart van de DNA-replicatie zorgen voor robuuste replicatie doordat ze voorbij beschadigd DNA kunnen navigeren. In **hoofdstuk 2** wordt de relatie tussen deze drie processen beschreven.

Chromatine is het complex van DNA en histonen, welke samen de chromosomen vormen. De histonen in het chromatine hebben diverse functies: ze helpen het DNA te verpakken in zeer compacte structuren en ze spelen een belangrijke rol in de regulatie van veel nucleaire processen door middel van modificaties. Optimale verwerking en reparatie van dubbelstrengsbreuken eist chromatine reorganisatie rondom de beschadigde DNA sites. In **hoofdstuk 3** richten we ons op de histon H2B mono-ubiquitinatie, een zeer dynamische chromatine modificatie uitgevoerd door de E3 ubiquitine ligase RNF20. We laten zien dat bij het ontbreken van RNF20 de tijdige accumulatie van homologe recombinatie-eiwitten in gebieden van dubbelstrengsbreuken wordt beïnvloed, hierbij wordt de homologe recombinatie activiteit functioneel onderdrukt. Deze gegevens duiden op een rol voorafgaand aan homologe recombinatie voor RNF20 mogelijk via de chromatine modificatie mono-ubiquitinatie van H2B.

Homologe recombinatie is tevens betrokken bij DNA-schade herstel ten gevolge van UV-licht. Specifiek zorgt homologe recombinatie ervoor dat DNA-replicatie door kan gaan na UV-schades door deze te repareren of voorbij beschadigd DNA te navigeren. In **hoofdstuk 4** zoomen we verder in op de rol van homologe recombinatie tijdens het herstel van UV-geïnduceerde replicatie problemen. We tonen aan dat in de afwezigheid van een functionele nucleotide excisie herstel, de samenwerkende homologe recombinatie eiwitten RAD54 en RAD51 herlokalisieren in foci op plaatsen van UV-licht geïnduceerde DNA schade, dit gebeurt specifiek op plekken van DNA replicatie. Deze lokalisatie is functioneel,

omdat op de individuele replicatie vork, RAD54 deficiënte cellen replicatie minder effectief is na UV bestraling. Verder, resulteert dit in meer dubbelstrengsbreken, zowel als meer chromosoom afwijkingen. Als laatste laten onze experimenten zien dat er RAD54 afhankelijke en onafhankelijke bijdragen zijn voor homologe recombinatie in de cellulaire UV-gevoeligheid en dat de problemen ten gevolge van de afwezigheid van TLS polymerase  $\eta$  kunnen worden verholpen door de rol van RAD54. Deze resultaten laten zien dat een afwezigheid van gevoeligheid van polymerase  $\eta$  veroorzaakt wordt door RAD54 afhankelijk homologe recombinatie.

RAD54 bezit verschillende biochemische activiteiten die de activiteit van RAD51 beïnvloeden tijdens belangrijke stappen van homologe recombinatie. In **hoofdstuk 5** wordt de RAD54 ATPase functie in homologe recombinatie *in vivo* verder onderzocht. We laten zien dat de ATPase activiteit van RAD54 belangrijk is voor dubbelstrengsbreuk herstel doormiddel van homologe recombinatie. Verder laten we zien dat de ATPase activiteit van RAD54 niet nodig is voor het tijdig ophopen van het belangrijkste homologe recombinatie eiwit RAD51 op plekken van dubbelstrengsbreuk geïnduceerde foci. Echter is de ATPase activiteit wel nodig voor ontmanteling van de foci. Deze data demonstreren een essentiële rol voor RAD54 en zijn ATPase activiteit in homologe recombinatie.

Remmers van dubbelstrengsbreuk reparatie zijn relevante antikanker therapieën doordat ze cellen gevoelig maken voor verschillende dubbelstrengsbreuk-inducerende stoffen. Verhoogde temperatuur (hyperthermie) is een van de oudste klinisch toegepast modaliteiten waarvan wordt vermoed dat het DNA herstelmechanismes remt, maar zijn primaire werkingsmechanisme blijft ongrijpbaar. In **hoofdstuk 6** laten we zien dat een milde hyperthermie behandeling homologe recombinatie remt, en dat dit effect aanzienlijk versterkt kan worden door de toevoeging van een heat shock eiwit remmers. Tumorcellen met verminderde homologe recombinatie activiteit zijn gevoelig voor de remming van poly (ADP-ribose) polymerase-1 (PARP-1). We laten zien dat hyperthermie kan worden gebruikt om tumorcellen met functionele homologe recombinatie gevoelig te maken voor PARP-1 remming, hierdoor kunnen nieuwe therapeutische strategieën worden ontworpen met betrekking tot lokale inductie van homologe recombinatie deficiëntie. Een grote tegenvaller tijdens de behandeling met hyperthermie is thermotolerantie. In **hoofdstuk 7** wordt de relatie tussen homologe recombinatie en thermotolerantie onderzocht. Thermotolerantie vermindert de werking van hyperthermie en correleert met een functionele homologe recombinatie status.

Deze resultaten geven verder inzicht in het cellulaire proces van homologe recombinatie. Dit inzicht kan verder worden vertaald naar toepassingen in de kliniek, voor een betere en specifiekere behandeling van kanker.



## Curriculum Vitae

### Personal details

Name: Berina Eppink  
Date of Birth: 28<sup>th</sup> September 1982  
Place of Birth: Winterswijk, The Netherlands

### Education

2003-2005 Master of Science, specialization biological chemistry,  
Wageningen University and Research centre, The Netherlands

2001-2002 Entrepreneurship, Saxion hogeschool Deventer, The Netherlands

1999-2003 Bachelor in biochemistry, Saxion hogeschool Deventer, The  
Netherlands

1994-1999 HAVO, Schaersvoorde, Aalten, The Netherlands

### Scientific background

2005-present PhD research in the Department of Cell biology and Genetics,  
ErasmusMC, Rotterdam, The Netherlands. Promotors: Prof Dr  
R. Kanaar and Prof Dr J. Hoeijmakers.

2005 Internship, Institute of Molecular Cancer Research, University of  
Zurich.

2004-2005 Msc thesis, Department of Biochemistry, Wageningen University  
and Research centre, The Netherlands.

2003-2005 Laboratory assistant at ROC A12, Ede, The Netherlands.

2002-2003 Bsc thesis at Numico Research BV, The Netherlands.

## Publication list

**Eppink B**, Wyman C & Kanaar R (2006) Multiple interlinked mechanisms to circumvent DNA replication roadblocks. *Exp. cell res.* 312: 2660-2665.

Muñoz IM, Hain K, Déclais AC, Gardiner M, Toh GW, Sanchez-Pulido L, Heuckmann JM, Toth R, Macartney T, **Eppink B**, Kanaar R, Ponting CP, Lilley DM & Rouse J. (2009) Coordination of structure-specific nucleases by human SLX4/BTBD12 is required for DNA repair. *Mol Cell.* 35(1):116-27.

Moyal L, Gana-Weisz M, Lerenthal Y, Mass G, So S., Wang S, **Eppink B**, Chung Y, Shalev G, Shema E, Shkedy D, Smorodinsky N, Vliet van N, Kuster B, Mann M, Ciechanover A, Kanaar R, Hu M, Chen D, Oren M & Shiloh Y. ATM-dependent monoubiquitination of histone H2B at DNA double strand breaks is required for timely damage repair (Manuscript submitted).

Krawczyk PM\*, **Eppink B\***, Essers J\*, Stap J\*, Odijk H, Zelensky A, Franken NAP, Bree van C, Stalpers LJ, Buist MR, Verhagen HJM, Kanaar R & Aten JA. Mild hyperthermia inactivates BRCA2-mediated DNA repair (Manuscript in preparation).

**Eppink B\***, Tafel AA\*, Hanada K, Drunen van E, Hickson ID, Essers J & Kanaar R. Repair of UV-induced DNA damage during S-phase involves multiple DNA repair pathways (Manuscript in preparation).

Agarwal S, Cappellen van WA, Guénolé A, **Eppink B**, Linsen SL, Meijering E, Houtsmuller A, Kanaar R & Essers J. ATP-Dependent and ATP-Independent *in Vivo* Roles of the Rad54 Homologous Recombination Protein in Nuclear Foci Kinetics (Manuscript in preparation).

**Eppink B**, Essers J & Kanaar R. Interplay and quality control of DNA damage repair mechanisms (Manuscript submitted for Wiley-VCH book "Genome organization & function in the cell nucleus").

\*These authors contributed equally to this work.

## Portfolio

Name PhD student: B. Eppink  
PhD period: Dec 2005 - Jun 2010  
ErasmusMC department: Cell Biology and Genetics  
Promoters: Prof. dr. R. Kanaar and Prof. dr. J.H.J Hoeijmakers  
Supervisor: Dr. J. Essers  
Research School: MGC

### General academic skills

Laboratory animal science

### Research skills

Working in the C-lab  
Confocal microscopy course

### In-depth courses (e.g. Research school, medical training)

Experimental approach to Molecular and Cell Biology  
Genome maintenance and cancer  
Reading and discussing literature

### Presentations

18<sup>th</sup> MGC symposium

### International conferences

Summer school on DNA and chromosomes, Physical and Biological approaches, 2006  
Cargese Corsica, France (Poster contribution).  
Conference on Genetic Recombination and Genomic rearrangements, 2009, FASEB  
summer research conference, Snowmass Village, Colorado, USA (poster contribution).

### Seminars and workshops

MGC Promovendi workshop	2006-2009
2008 organising committee	

### Teaching

Junior science program	2006-2009
Supervision of 3 bachelor students	



## Dankwoord

Zo... eindelijk bij het belangrijkste gedeelte van mijn proefschrift aangekomen. De mensen bedanken zonder wie dit eindresultaat niet tot stand zou zijn gekomen. Eigenlijk zijn deze paar bladzijdes toch echt te kort om iedereen te bedanken die een rol heeft gespeeld de afgelopen vier en een half jaar, of beter gezegd de afgelopen (bijna) 28 jaar. Dus bij dezen voor iedereen die ik alvast vergeet te noemen maar toch een rol heeft gespeeld in het tot stand komen van dit boekje **BEDANKT**.

Allereerst wil ik mijn (co) promotoren bedanken. Roland, dank je wel voor de afgelopen jaren. Door jouw toedoen heb je een plek gecreëerd waar bijna ongelimiteerd onderzoek gedaan kan worden, een ongekende luxe in het onderzoek. Daarnaast haal je het onderste uit de kan voor jezelf en voor de mensen om je heen strevend naar het ultieme resultaat. Dank je wel voor de energie die je in mijn onderzoek hebt willen steken en voor de kans die je mij hebt geboden voor de aankomende jaren.

Jeroen, als copromotor en dagelijks begeleider heb je mijn beste en slechtste kanten gezien. Mijn goede kanten heb je altijd aangemoedigd en van mijn slechte kanten heb je me bewust gemaakt en helpen te verbeteren. Dank je wel voor je begeleiding, en de moeite die je erin hebt gestoken om van mij een goede onderzoeker te maken.

Jan jij bent diegene die mij een jaar of zeven geleden hebt geïntroduceerd met het onderwerp DNA reparatie, tijdens een gastcollege aan Wageningen universiteit. Hier is mijn interesse geprikkeld om onderzoek te gaan doen naar het ontstaan van kanker, waardoor ik eerst in Zwitserland een stage en vervolgens hier een promotieonderzoek ben gaan doen. Dank je voor je kritische kijk op onderzoek en je gave om fundamentele wetenschap om te zetten naar toepassingen.

Mijn speciale dank gaat uit naar mijn commissie die de dappere taak op zich hebben genomen om zich door mijn boekje heen te worstelen. Ellen, Timo, Nora, Titia, Jacob en Claire bedankt.

Paula en Hanny weet waar jullie aan begonnen zijn, als ik flauwval tijdens mijn promotie moeten jullie de vragen beantwoorden, maar ik beschouw het als een grote eer dat jullie dat willen doen. Paula het was een verademing de dag dat je bij ons binnengelopen kwam. Je "Rotterdams" gepraat en gelach schalde vaak door gang, wat een hoop gezelligheid met zich mee bracht. Hanny zonder jouw gouden handjes zou onderzoek doen een stuk lastiger worden. Ik heb veel kunnen leren van je technische vaardigheden in het lab, daarnaast ben je een uniek persoon in het lab en sta je altijd voor iedereen klaar.

Thanks to all my colleagues at the sixth Floor in the past and in the present. Daniel het was leuk om gelijktijdig met iemand hetzelfde traject van promoveren door te lopen. Succes met het afronden van je eigen promotie en met je postdoc in San Francisco. Cecile, onze

regelneef, wat zouden we toch zonder jouw in het lab moeten beginnen, dank je voor alle goede zorgen de afgelopen jaren. Tommy, it is very nice having you around in the lab, your always joyful making jokes most of us don't get. Linda het was jammer de ik je maar zo kort in het lab heb mogen meemaken, ik mis onze koffie-uurtjes nog steeds. Ilaria good luck with your own PhD, make something nice out of the hyperthermia project. Alex thank you for reminding me more than once, that treating cancer just needs to work, irrespectively of its rational or mechanistic insights. Joyce en Claire, er zouden meer vrouwen zoals jullie in de wetenschap moeten zitten, gewoon laten zien hoe het moet. Koos en Dik dank jullie wel voor die ongelofelijke feitenkennis die jullie hebben en die jullie graag delen met ons "beginners".

Natuurlijk wil ik de mensen van de 7<sup>e</sup> verdieping celkweek bedanken. De keukendames, Jan, Arjan, Niels, Jurgen, Petra, Anja, Nienke en iedereen die ik door de jaren heen ben tegengekomen in de celkweek en wie er aan bijgedragen hebben dat de celkweek een leuke en gezellige plek is om te werken.

Tallose keren hebben zij mij uit de brand geholpen, wat zou ik zonder de jongens van de computers en de dames van het secretariaat hebben moeten doen. Bedankt!

Mijn boekje er kaal uitzien zonder de bijzondere samenwerking met de mensen in Amsterdam. Przemek, Jan en Jacob wat een gave hebben jullie om met nieuwe creatieve ideeën te komen welke tot een heel bijzonder project hebben geleid. Nu alleen nog even duimen voor de laatste grote hobbel en dan kan de kroon worden gezet.

Jasper bedankt dat je al je creativiteit hebt willen botvieren op mijn werk en voor deze bijzondere voorkant. Christel het was heerlijk om af te toe even weg te kunnen lopen en even te komen buurten. Niet alleen hier maar ook tijdens onze tallose etentjes. Maureen, Petra en Leon dank jullie wel voor jullie vriendschap en het delen van lief en leed deze afgelopen jaren. Veel succes met jullie eindsprint. Hilbert and Liat, Thank you for such a beautiful holiday destination, good to have you back in Europe. Peter, Marietta en Linda bedankt voor de eindeloze discussies over de belangrijke dingen van het leven. Harry, Brigitta en de rest van de fam, dank jullie wel voor het warme welkom dat ik altijd bij jullie heb gehad, en de eindeloze interesse hoe het nou met studeren ging en wanneer ik nou eens echt ging werken, vanaf nu dus!

Pap, mam en Hanneke wat zou ik toch zonder jullie hebben gedaan. Dan was ik waarschijnlijk al gestrand bij het middelbare school Engels haha. En nu ligt er een heel boek geschreven in dit zelfde Engels. Dank jullie wel voor het vertrouwen en de steun die jullie mij de afgelopen jaren hebben gegeven en de interesse die jullie altijd hebben getoond, ook al snaptten jullie er niet altijd wat van.

Natuurlijk last but not least Maurice, zonder jouw was er niets terecht gekomen van dit proefschrift. Het eindeloze geduld dat je hebt gehad met me de afgelopen jaren, als de proeven niet wilden lukken, en zeker deze laatste maanden tijdens het schrijven. Mijn geduld was hier toch echt op, maar die van jouw gelukkig niet. Nu is mijn proefschrift klaar en kunnen we op naar jouw eindstreep. Je weet het hè “words are meaningless”, dank je wel voor alles, jij maakt het allemaal de moeite waard.

Dit was alweer het einde, ik ben blij dat het erop zit ik heb een hele leuke tijd gehad hier in Rotterdam, veel leuke mensen ontmoet, op naar de volgende uitdaging!

Berina

